Image credit: *The Garden of Words* from Makoto Shinkai

The Delicacy of “Imperfection”: Thermodynamics, Transport, and Spectroscopy as Lenses

在不完美中窥见精微：热力学、输运与光谱的三重视角

Quantum Measurement Group @MIT

Chu-Liang Fu

2025/07/21

材料科学是什么？

- Science for…… ?

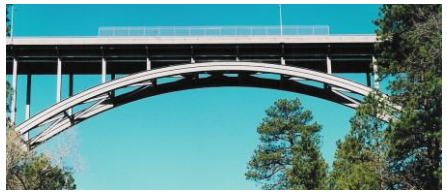

Canyon Bridge, Los Alamos, NM

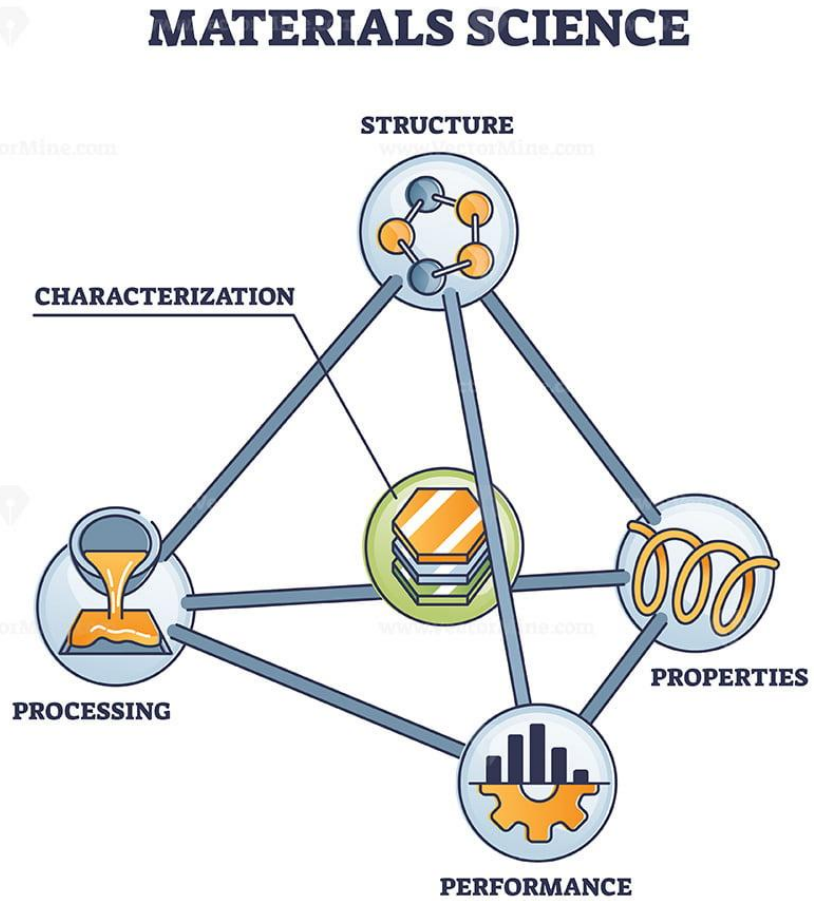

美国部分大学博士核心课程

- Stanford：

Courses

Core Courses[1]

MATSCI 211 ↗ : Thermodynamics and Phase Equilibria

MATSCI 212 ↗ : Rate Processes in Materials

MATSCI 213 ↗ : Defects and Disorder in Materials

MATSCI 214 ↗ : Structure and Symmetry

MATSCI 215 ↗ : Quantum Mechanics for Materials Science

- NWU:

First Year Core Courses

Fall Quarter

- 401 Chemical and Statistical Thermodynamics of Materials
- 402 Structure of Crystalline and Noncrystalline Materials

Winter Quarter

- 404 Imperfections in Materials
- 408 Phase Transformations in Materials

Spring Quarter

- 405 Physics of Solids
- 406 Symmetry and Mechanical Properties of Materials

- MIT:

Program Requirements

Required Seminars		
3.201	Introduction to DMSE	3
3.202	Essential Research Skills	3
Core Curriculum [1]		
3.20	Materials at Equilibrium	15
3.21	Kinetic Processes in Materials	15
3.22	Structure and Mechanics of Materials	12
3.23	Electrical, Optical, and Magnetic Properties of Materials	12
Electives [2]		**27-36**
Minor [3]		**18-33**

跟物理学的对应关系？

- 热力学　统计力学

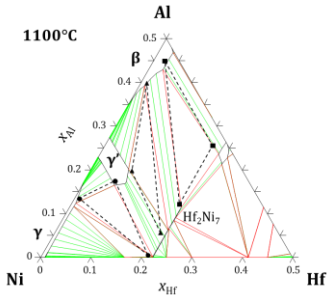

- 晶体结构　固体物理

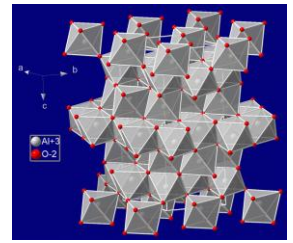

- 第一组对偶：平衡/含时演化
- 第二组对偶：对称/破缺
- 动力学　输运/扩散/BTE

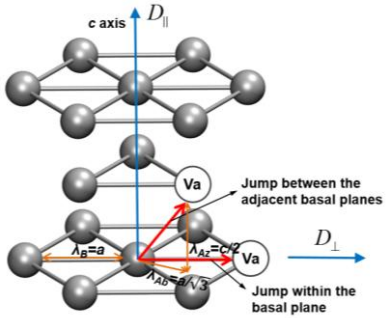

- 缺陷　X

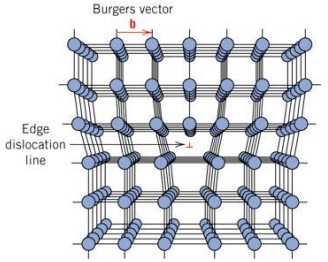

Various “Imperfection”, various space to optimize & engineering!

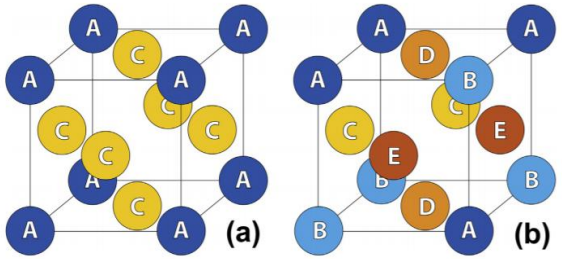

High Entropy Alloy: Combinatorial Disorder

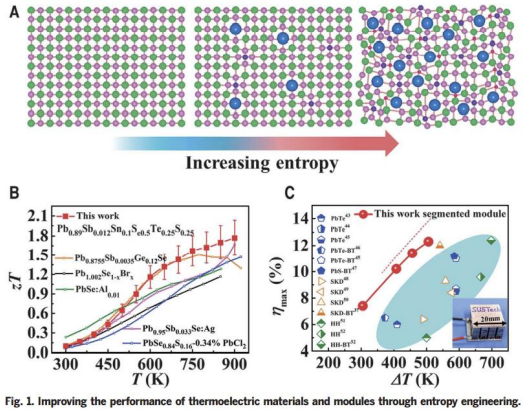

Fig. 1. Improving the performance of thermoelectric materials and modules through entropy engineering.

Jiang, Binbin, et al. "High-entropy-stabilized chalcogenides with high thermoelectric performance." *Science* 371.6531 (2021): 830-834.

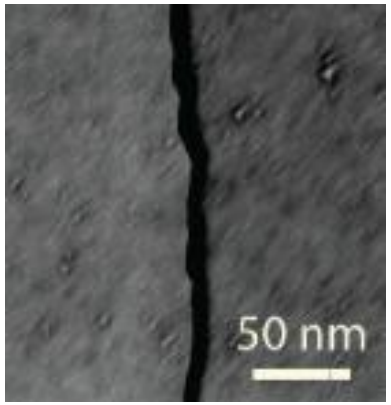

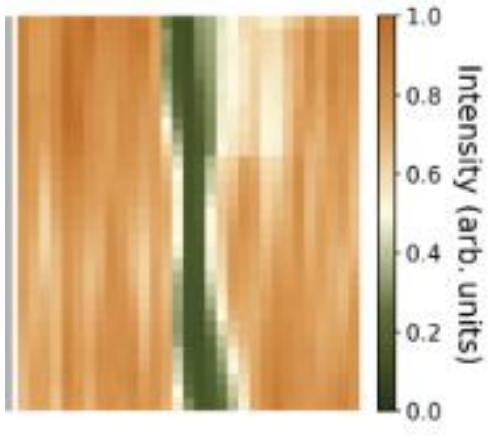

Wrinkle in semiconductor device

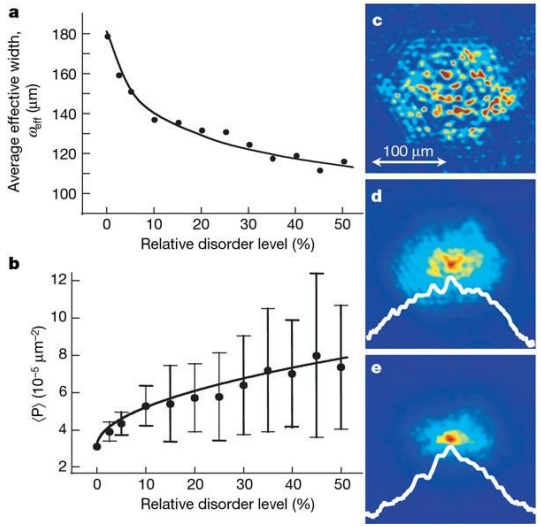

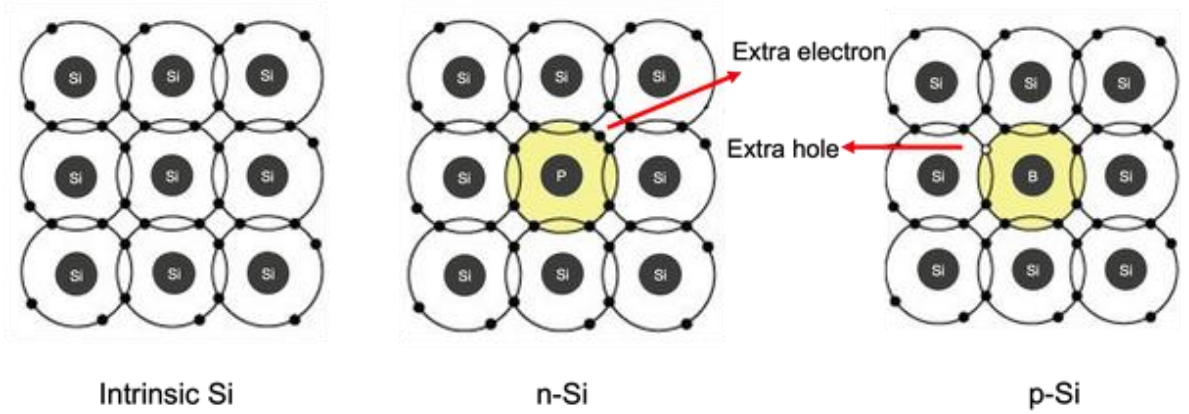

Doping to adjust semiconductor properties

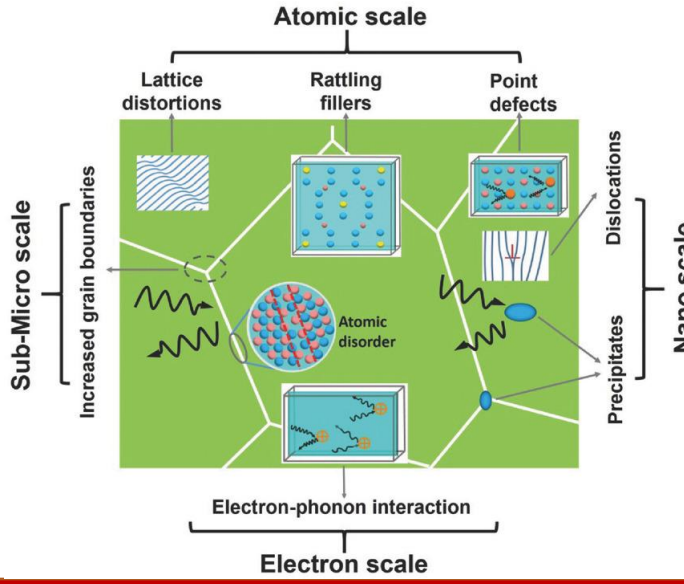

Schwartz, Tal, et al. "Transport and Anderson localization in disordered two-dimensional photonic lattices." *Nature* 446.7131 (2007): 52-55.

材料科学几千年了，我来干什么？

工作经历

- **麻省理工学院** 剑桥，麻萨诸塞州，美国
  博士后，量子测量组（*quantum measurement group*），导师：李明达，核科学与工程系 *2023.09-*
  - 主要承担组内理论小组和参与计算小组的相关科研工作，了解实验小组的相关实验。
  - 材料表征，尤其是依赖于大装置（*X* 射线，中子散射）的谱学理论与实验设计，主要的两个结果应用于中子核磁相干散射的理论和 *X* 射线光子相关光谱的量子理论。
  - 基于线性响应理论的光谱学测量的理论计算，已应用于 2 维材料和量子点嵌入的复合材料的实验结果分析。
  - 基于光谱学测量数据的反问题的计算研究，应用于对于材料的热传导和动力学的数学建模。
  - 其他完成和在尝试中的材料的结构与现象的理论分析与建模包括：参与光分子效应的理论构建，材料点缺陷表征的机器学习算法，基于实验数据的晶界动力学的数学建模等。

教育经历

- **弗吉尼亚大学** 夏洛茨维尔，弗吉尼亚州，美国
  材料科学，博士 *2023.08*

  导师：周必成 博士论文：*A Novel Computational Thermodynamics Framework with Intrinsic Chemical Short-Range Order* 博士研究参与美国 *NSF Career Award 2042284(A Novel Computational Thermodynamics Framework with Intrinsic Chemical Short-Range Order)* 项目的项目计划写作并接受资助，承担组内计算热力学和动力学的理论计算模型的研究，将刻画化学短程序的团簇变分法的热力学模型引入相图计算方法 *(CALPHAD)*，将构型尤其是化学短程序，振动，弹性，电子等物理自由度系统地融入计算热力学的自由能框架，促进材料尤其是高熵合金的设计。相关结果获 *CALPHAD* 年度会议最佳学生海报奖，并陆续发表中。
- **云南大学** 中国昆明
  数学与应用数学，本科 *2017.07*

  本科毕业论文指导老师：魏舟 & 支元洪. 毕业论文：椭圆偏微分方程-*Calderón-Zygmund* 引理在 *Hölder* 估计中的应用

- 应用数学：
  - 把实际问题的复杂性转化为数学问题处理
  - 用数学搭建框架
- 材料科学：
  - 手段：理论 & 计算 对材料做观察
  - 目标：材料的设计与优化

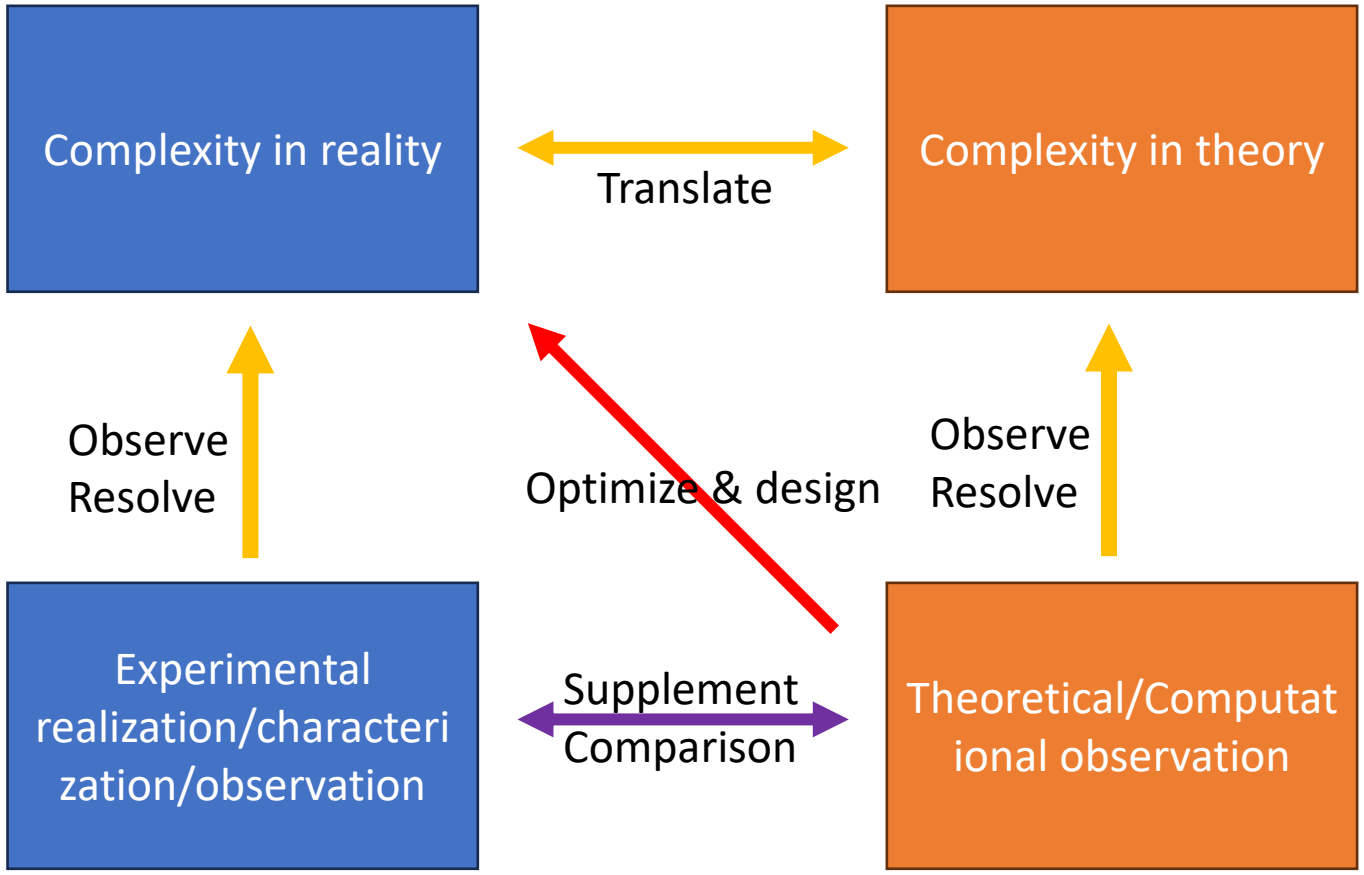
Complexity in reality
Translate
Complexity in theory
Observe
Resolve
Optimize & design
Observe
Resolve
Experimental realization/characterization/observation
Supplement
Comparison
Theoretical/Computational observation

理解材料复杂性的实验表征手段

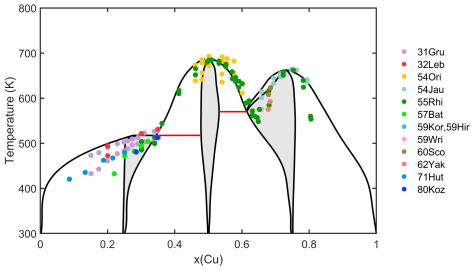

7.1 Crash course in modern experimental techniques

7.1.1 Basic concepts

Crudely speaking, experimental condensed matter physics can be subdivided into three[1] broad categories of analytical technique:

- ▷ experiments probing thermodynamic coefficients;
- ▷ transport experiments;
- ▷ spectroscopy.

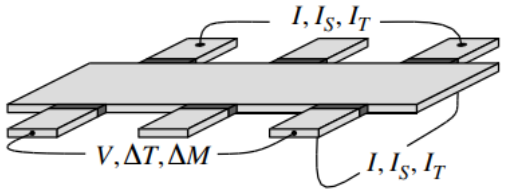

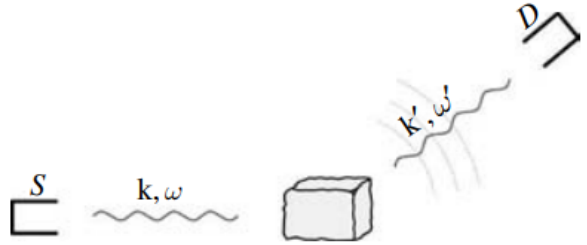

- Mechanical experiments, EIS, synthesis, cold atom…

Altland, Alexander, and Ben D. Simons. Condensed matter field theory. Cambridge university press, 2010.

Outline:

- Thermodynamics: High entropy alloy, combinatorial disorder
- Cluster based thermodynamics modeling

- Transport: Measuring in-plane thermal transport with wrinkle
- Modified conduction equation

- Spectroscopy: electron-phonon coupling
- Anomalous Neutron Nuclear-Magnetic Interference Spectroscopy

Outline:

- High entropy alloy, combinatorial disorder
- Cluster based thermodynamics modeling

- Measuring in-plane thermal transport with wrinkle
- Modified conduction equation

- electron-phonon coupling within localized state, interplay between disorder and the electron-phonon interaction
- Anomalous Neutron Nuclear-Magnetic Interference Spectroscopy

Solid solution, a platform with more configuration “Disorder”

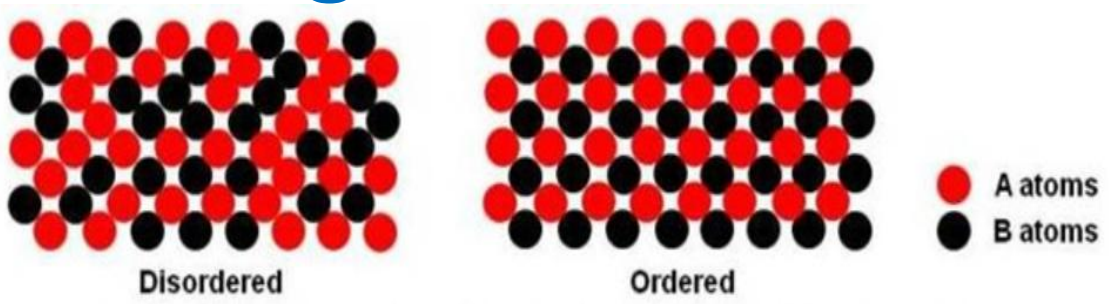

Introduce more disorder!

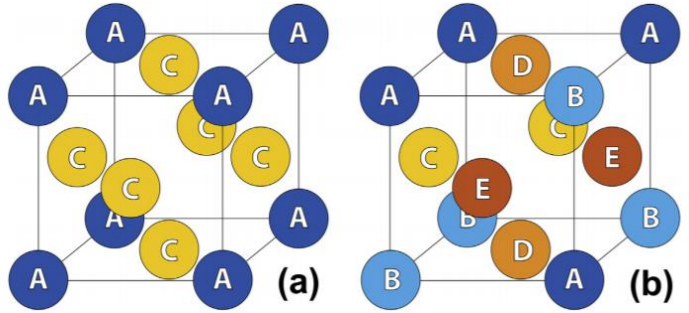

High Entropy Alloy

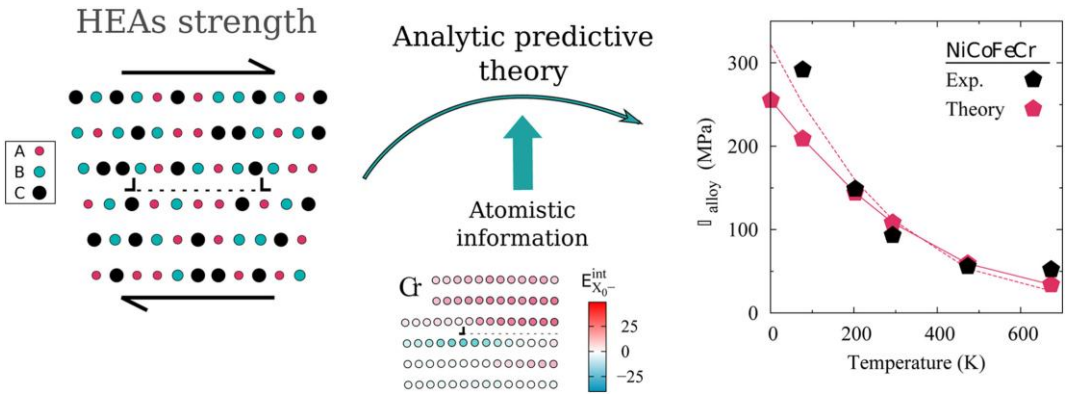

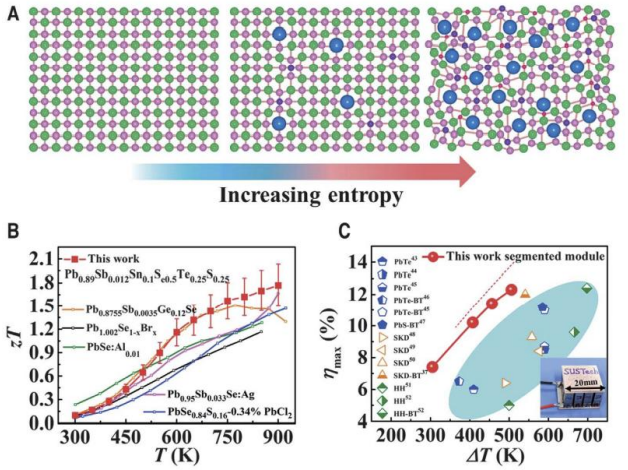

Fig. 1. Improving the performance of thermoelectric materials and modules through entropy engineering.

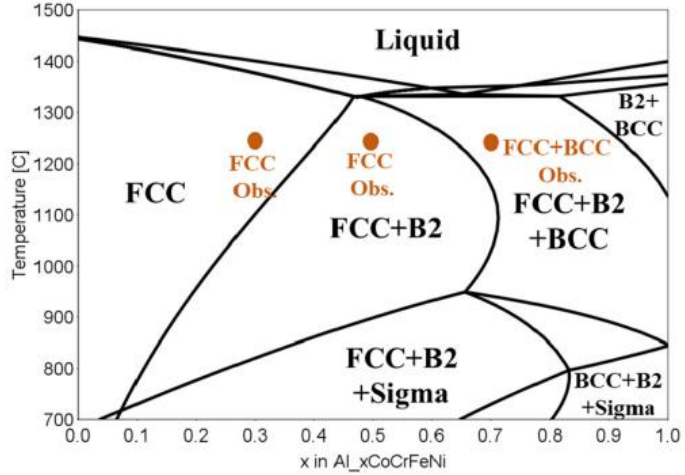

Varvenne, Céline, Aitor Luque, and William A. Curtin. "Theory of strengthening in fcc high entropy alloys." *Acta Materialia* 118 (2016): 164-176.

Jiang, Binbin, et al. "High-entropy-stabilized chalcogenides with high thermoelectric performance." *Science* 371.6531 (2021): 830-834.

Saal, James E., et al. "Equilibrium high entropy alloy phase stability from experiments and thermodynamic modeling." *Scripta Materialia* 146 (2018): 5-8.

Thermodynamic stability of solid solutions: first-principles-based or data-based?

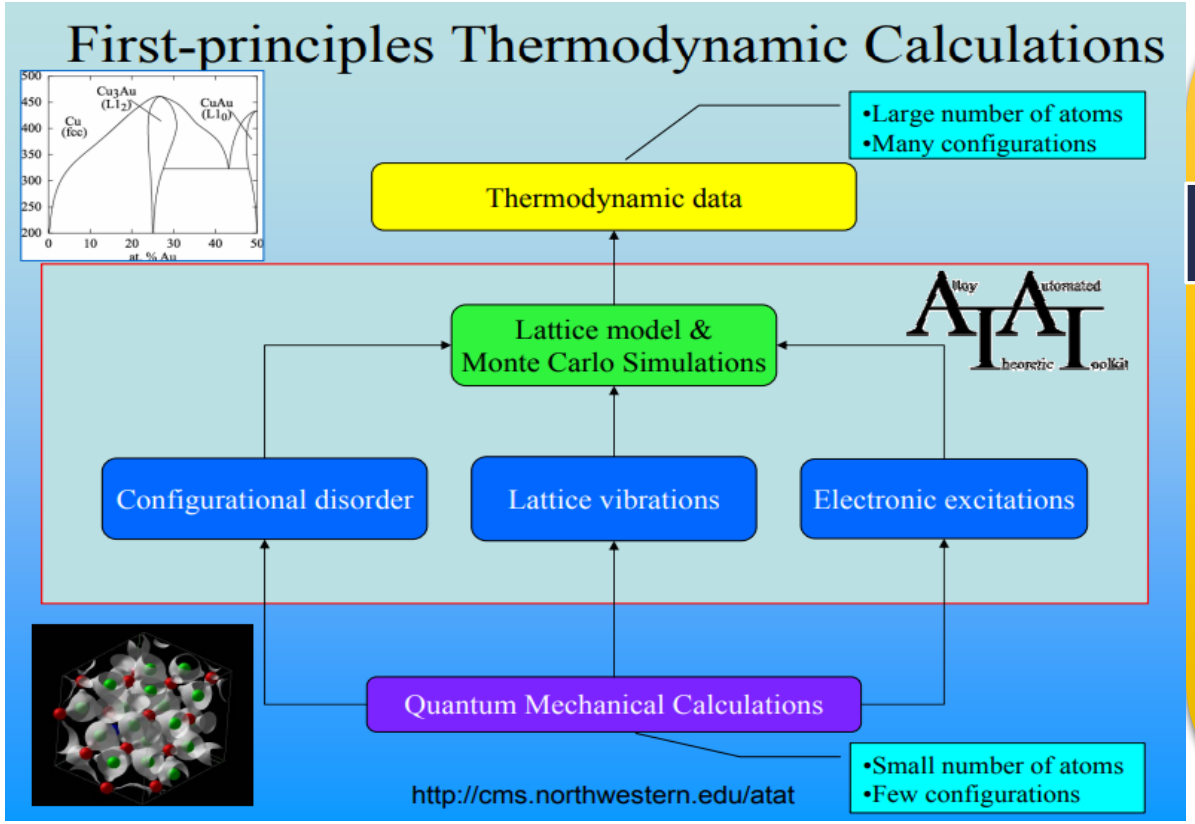

Thermodynamic databases by the CALPHAD (*CAL*culation of *PHA*se *Dia*gram) method

Good for first-principles

Thermochemical data
enthalpy, entropy, heat capacity, activity

Good for experiments

Phase equilibrium data
phase boundary, phase fraction and composition

Gibbs energy of individual phases

$$G_m\,(T,P,x_i) = {}^{\circ}G_m + \Delta^{id}G_m + \Delta^{xs}G_m + {}^{phys}G_m$$

Databases
Pure elements → Binary → Ternary → Multicomponent

Applications

However, for fully first-principles based method, accuracy matters

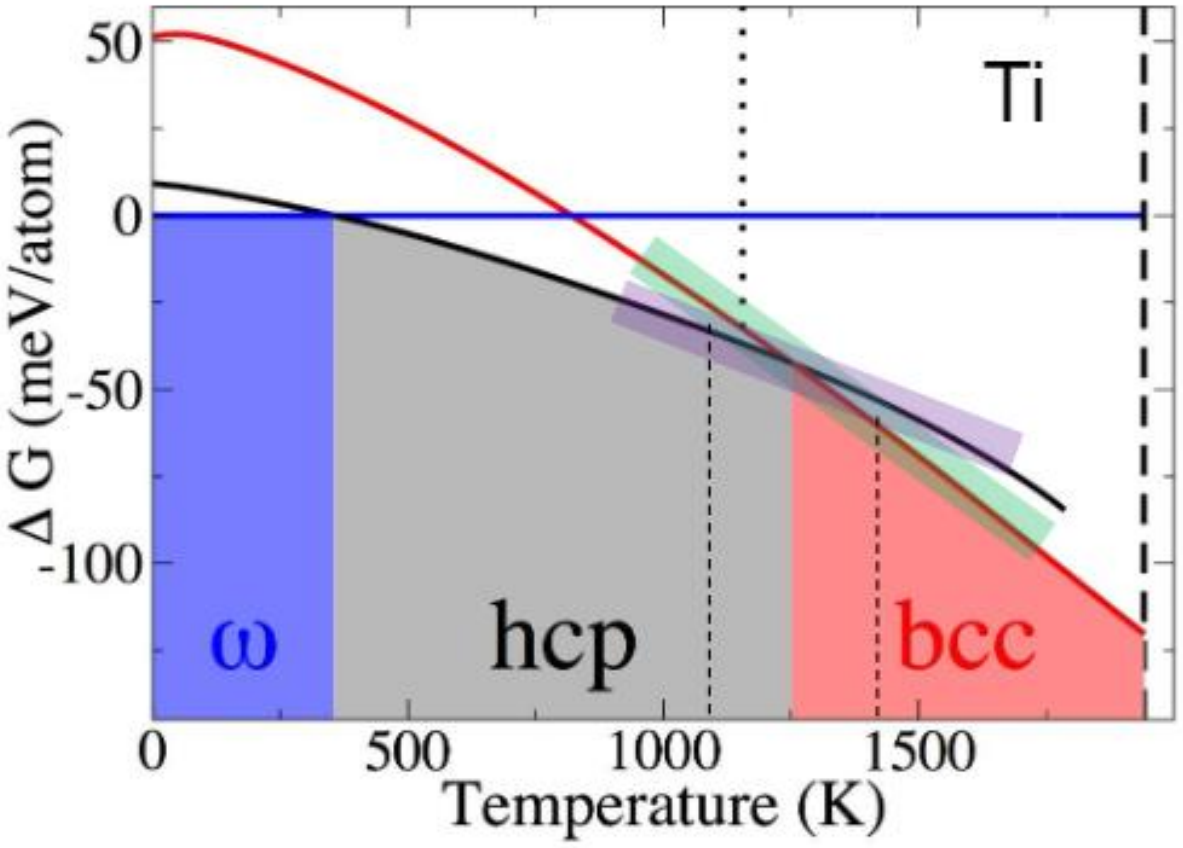

- Typical DFT chemical accuracy: >10 meV/atom. It is challenging to use DFT alone to get the correct phase boundary.
- Experimental data also has the “noise” with defects, but still very valuable in actual world.
- Multicomponent case requires large computational cost.

Data-based Computational thermodynamics: CALculation of PHAse Diagram(CALPHAD) (1970)

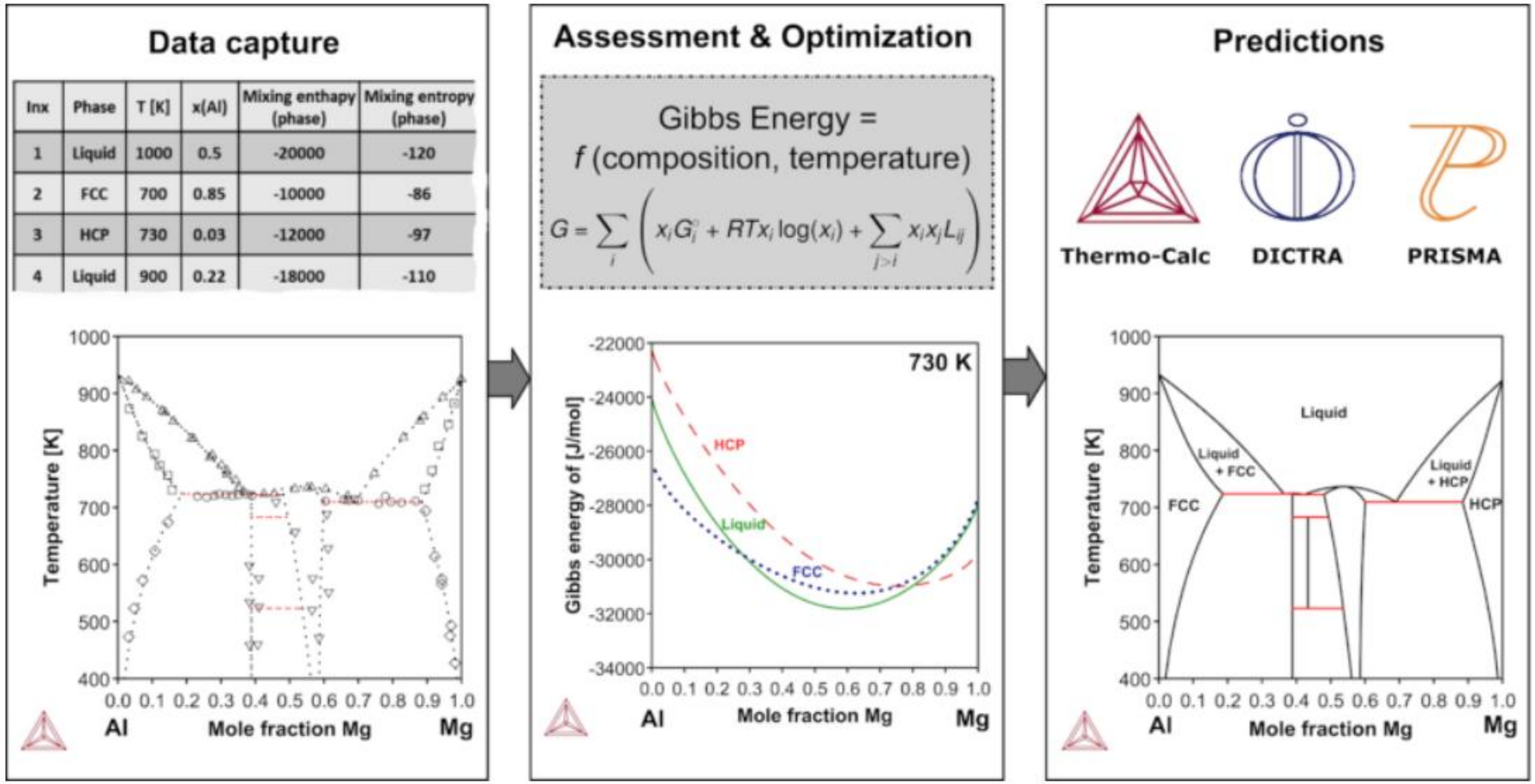

Combine two paths?

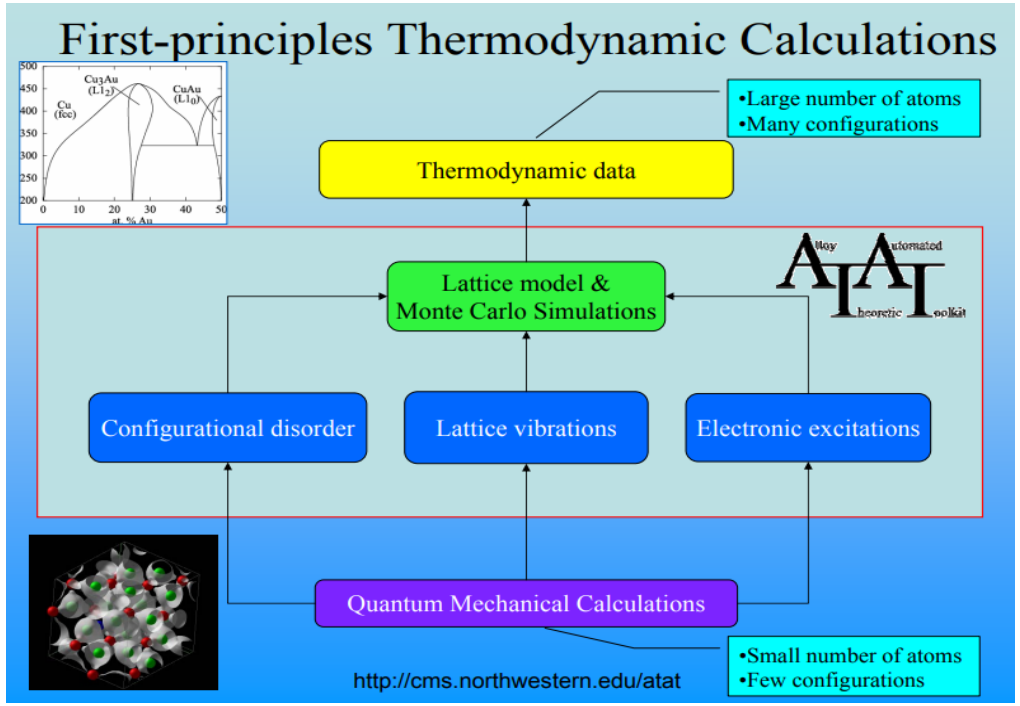

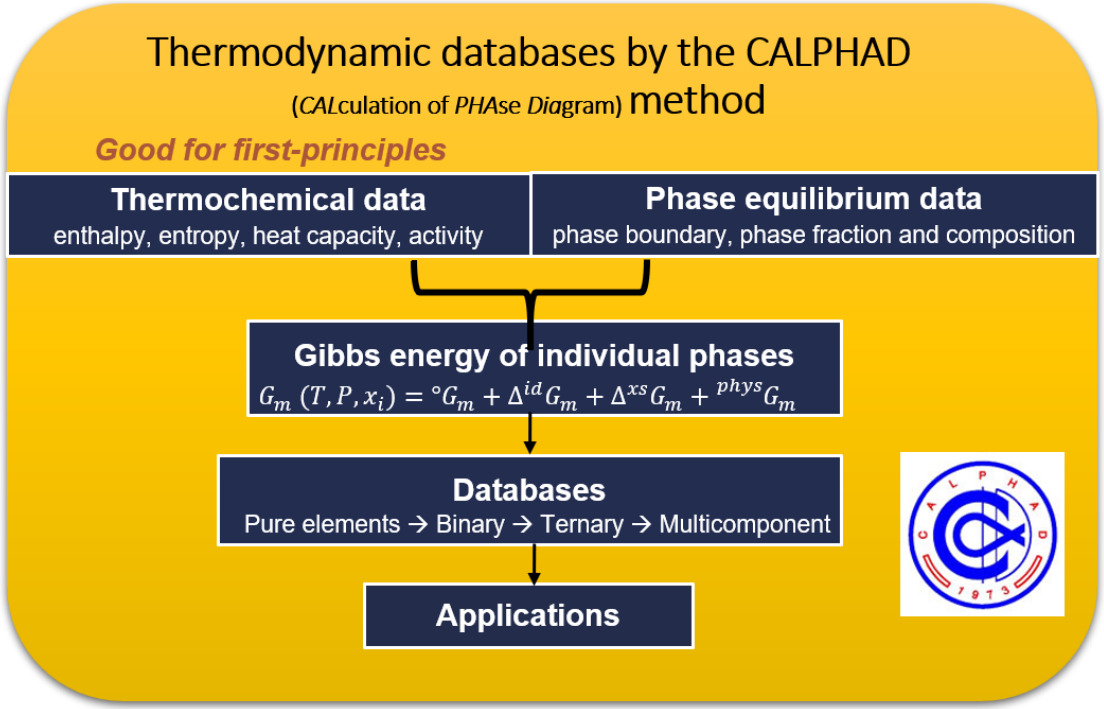

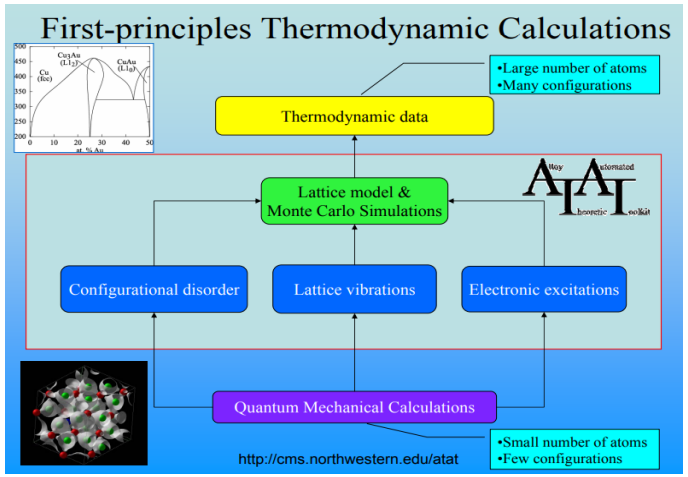

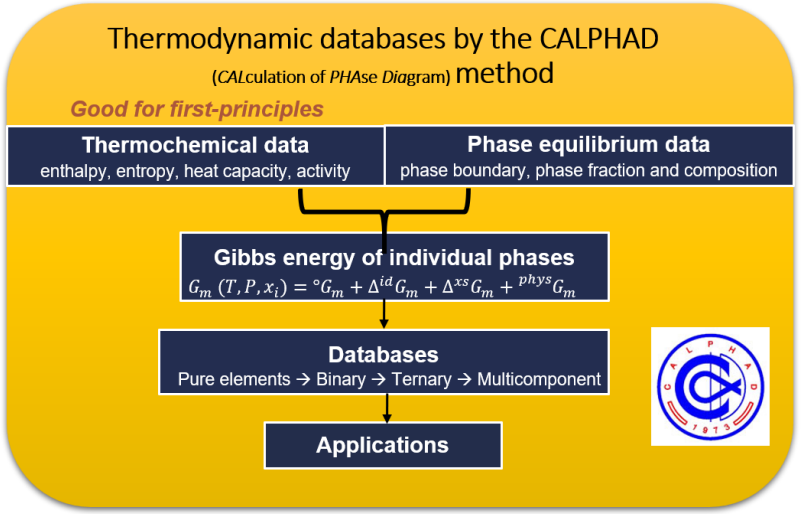

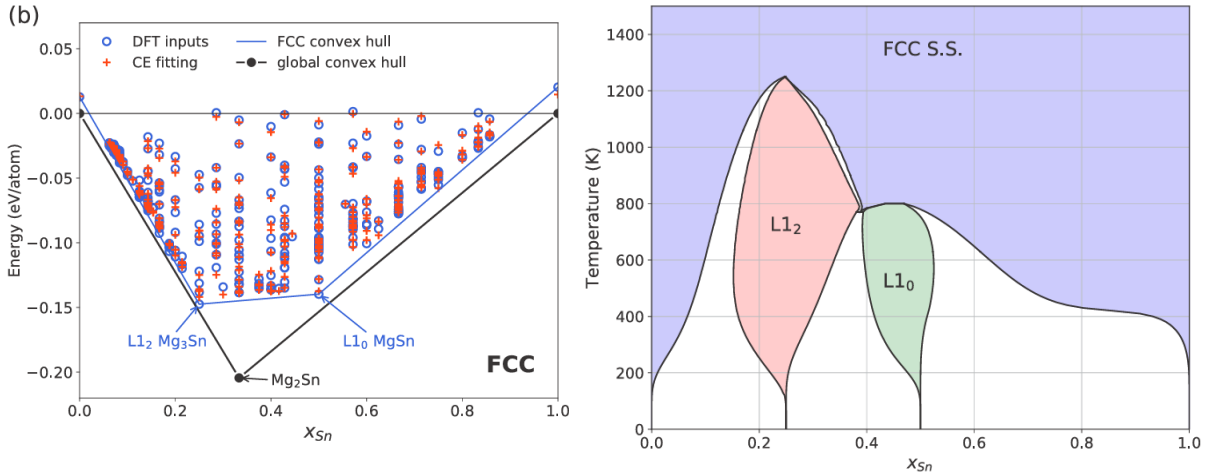

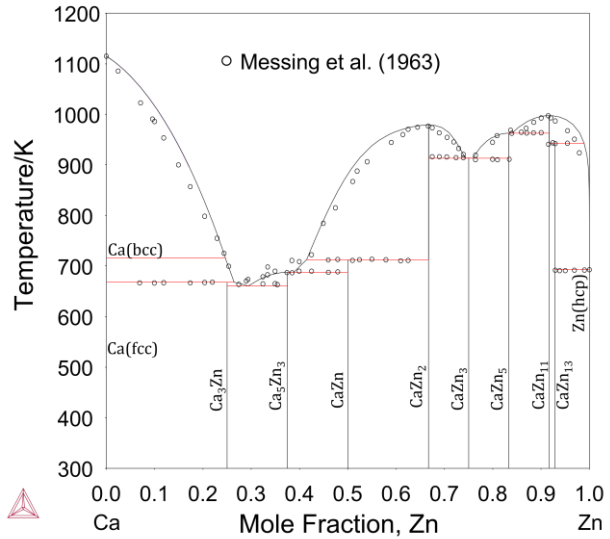

Wang, K., Cheng, D., Fu, C. L., & Zhou, B. C. (2020). First-principles investigation of the phase stability and early stages of precipitation in Mg-Sn alloys. *Physical Review Materials*, *4*(1), 013606.

Strategy: More Physics + Data-based, Better Alignment!

Physical Phenomenon in Solid Solution: Chemical Short-Range Order(SRO) but is overlooked in current CALPHAD

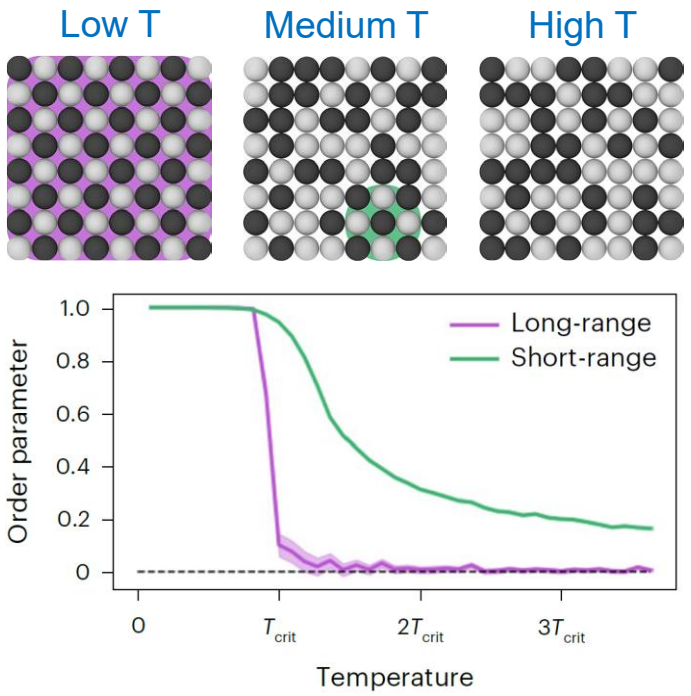

Warren-Cowley SRO parameter: $\alpha_{ij}^{m} = 1 - \frac{p_{ij}^{m}}{c_i c_j}$

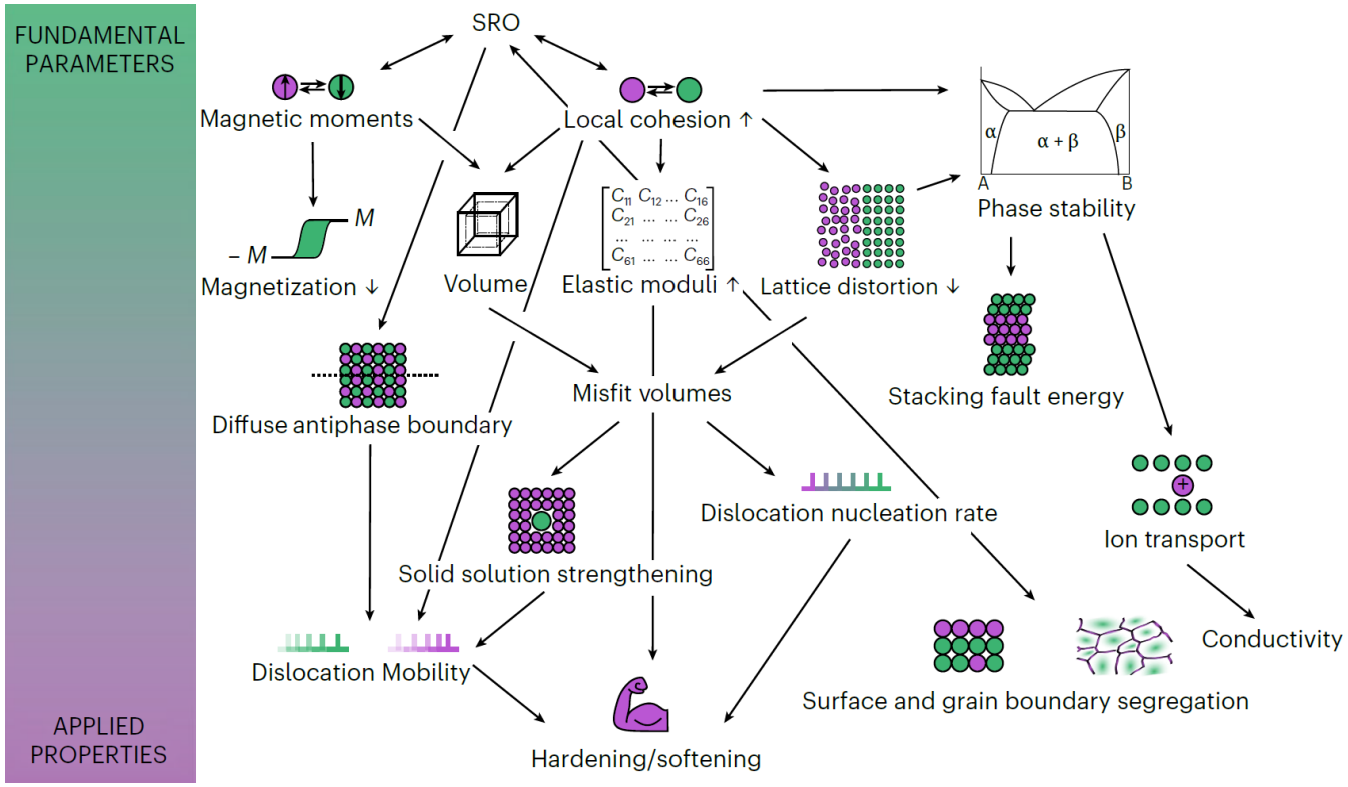

How to introduce chemical short-range order?

Randomly mix the different Cluster(with SRO) but not the atom!

Clarification: Cluster Variation Method (CVM) in a nutshell (1951)

CVM is a systematic recursive correction algorithm to calculate the configurational entropy of a lattice:

$$S_{CVM} = -k_B \sum_{\alpha}^{\alpha_M} a_\alpha \sum_{\sigma(\alpha)} \rho_\alpha \ln \rho_\alpha$$

$$= 2S_4 - 6S_2 + 5S_1$$

$$= -k_B \left(2 \sum_{ijkl}^{16} \rho_{ijkl} \ln \rho_{ijkl} - 6 \sum_{ij}^{4} \rho_{ij} \ln \rho_{ij} + 5 \sum_{i}^{2} x_i \ln x_i \right)$$

Tetrahedron | Pair | Point

Superposition relation: $\sum_j \sum_k \sum_l \rho_{ijkl} = \sum_j \rho_{ij} = x_i$

Kikuchi-Barker coefficients a_α depends on the geometry of the lattice.

- **Basis cluster**: Tetrahedron 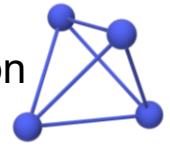 ρ_{ijkl}
- Subclusters:
  - Pair:  ρ_{ij}
  - Point:  x_i

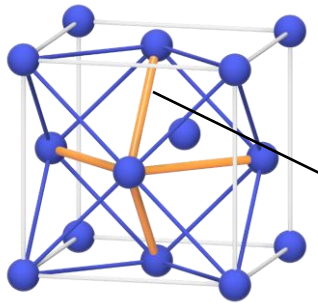

Overlapping pairs

CVM vs. Cluster Expansion

S_{CVM} can also be expanded in terms of correlation function ξ.

Ryoichi Kikuchi

CVM

- A direct approximation of free energy using interrelated **cluster probability ρ** within a basis cluster
- Natural iteration method to minimize the CVM free energy with constraints

Didier de Fontaine

Juan Sanchez

Cluster Expansion

- Expands a lattice model scalar property using multisite **correlation functions ξ** as the orthonormal basis function
- Coupled with Monte Carlo to calculate phase diagrams

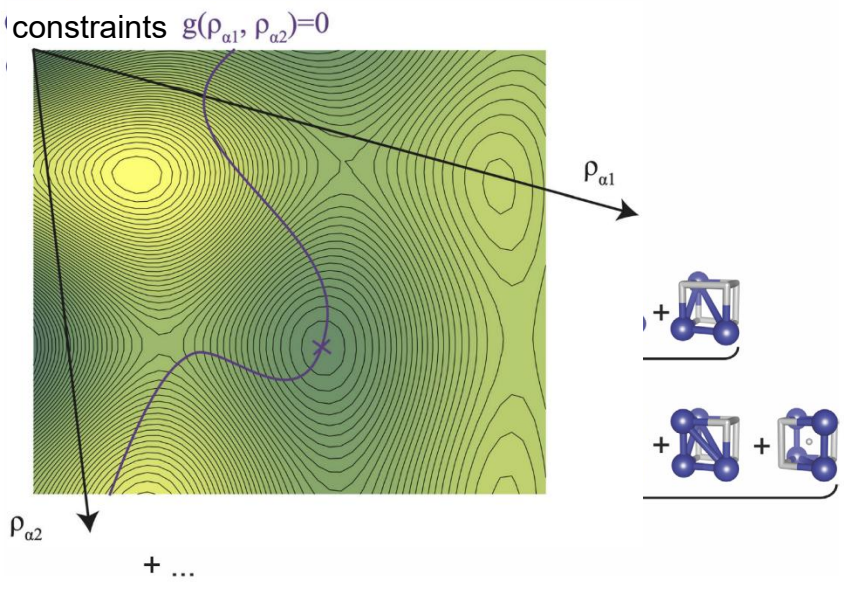

The ener … be
linearly e

E …

= …

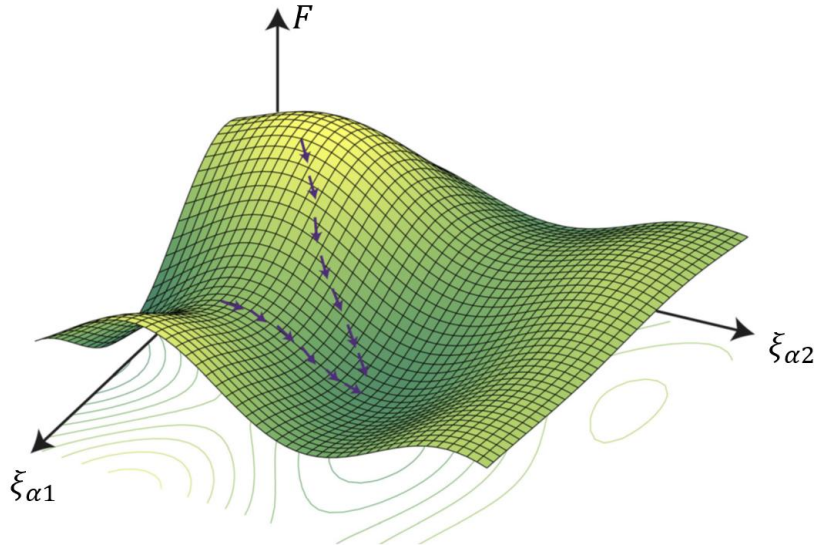

- J_α: Effe…
- $\xi_\alpha(\vec{\sigma})$ = … tion, the averag… each site i in the cluster, represents the average of atomic occupancy

Sanchez et al., Physica A 128, 334 (1984), Chang et al., J. Phys.: Condens. Matter 31 (2019) 325901
Kadkhodaei and Muñoz. *JOM* 73.11 (2021) 3326

Some historical connections

- R. Kikuchi -----friend-----Didier de Fontaine
- Didier de Fontaine's advisor is John Hilliard, the Hilliard in "Cahn-Hilliard equation".
- Didier de Fontaine is the advisor of:
  - Juan Sanchez(UTAustin), Chris Wolverton(co-advised, NWU), Mark Asta(UCB), G. Ceder(MIT→UCB), Dane Morgan(co-advised, UW Madison), …
    - G. Ceder is the advisor of
      - Axel van de Walle(Brown), Anton Van Der Ven(UCSB), Stefano Curtarolo(Duke), Tim Mueller(JHU), Shyue Ping Ong(UCSD), …

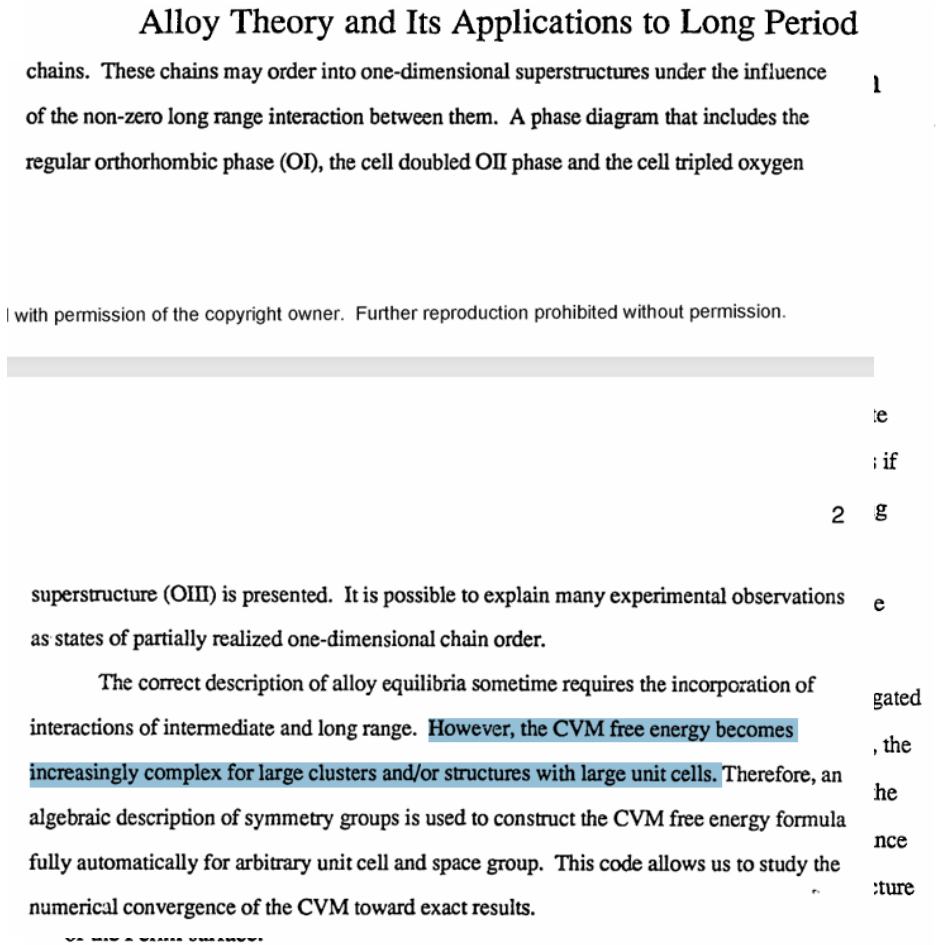

Alloy Theory and Its Applications to Long Period

chains. These chains may order into one-dimensional superstructures under the influence of the non-zero long range interaction between them. A phase diagram that includes the regular orthorhombic phase (OI), the cell doubled OII phase and the cell tripled oxygen

with permission of the copyright owner. Further reproduction prohibited without permission.

2

superstructure (OIII) is presented. It is possible to explain many experimental observations as states of partially realized one-dimensional chain order.

The correct description of alloy equilibria sometime requires the incorporation of interactions of intermediate and long range. However, the CVM free energy becomes increasingly complex for large clusters and/or structures with large unit cells. Therefore, an algebraic description of symmetry groups is used to construct the CVM free energy formula fully automatically for arbitrary unit cell and space group. This code allows us to study the numerical convergence of the CVM toward exact results.

Number of variables during minimization is n^S ...

CVM is a systematic recursive correction algorithm to calculate the configurational entropy of a lattice:

$$S_{CVM} = -k_B \sum_{\alpha}^{\alpha_M} a_\alpha \sum_{\sigma(\alpha)} \rho_\alpha \ln \rho_\alpha$$

$$= 2S_4 - 6S_2 + 5S_1$$

$$= -k_B \left(2 \sum_{ijkl}^{16} \rho_{ijkl} \ln \rho_{ijkl} - 6 \sum_{ij}^{4} \rho_{ij} \ln \rho_{ij} + 5 \sum_{i}^{2} x_i \ln x_i \right)$$

Tetrahedron | Pair | Point

Superposition relation: $\sum_j \sum_k \sum_l \rho_{ijkl} = \sum_j \rho_{ij} = x_i$

Kikuchi-Barker coefficients a_α depends on the geometry of the lattice.

- **Basis cluster**: Tetrahedron 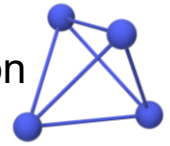 ρ_{ijkl}
- Subclusters:
  - Pair:  ρ_{ij}
  - Point:  x_i

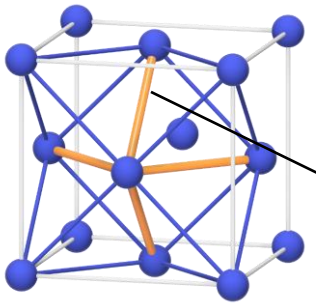

Overlapping pairs

Fowler-Yang-Li(FYL)-transform:

$$n^S \rightarrow n \times S$$

for *number of minimizing variables.*

5 component tetrahedron approximation:

$$625 \rightarrow 20$$

$$Disorder \rightarrow 4$$

History of FYL-transform

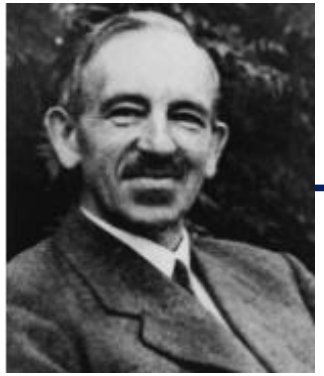

Ralph Fowler

PhD Advisor

Jwu-Shi Wang

Master Advisor

Chen-Ning Yang

Master thesis of Yang

THE JOURNAL OF CHEMICAL PHYSICS VOLUME 13, NUMBER 2 FEBRUARY, 1945

A Generalization of the Quasi-Chemical Method in the Statistical Theory of Superlattices

C. N. YANG*
National Tsing Hua University, Kunming, China
(Received November 17, 1944)

Yin-Yuan Li

Two most important students of Fowler in physics is Dirac and Mott.

Main idea of FYL-transform

$$\rho_{ijkl} = \frac{1}{z} e^{\frac{\mu_{ijkl} - \epsilon_{ijkl}}{k_B T}}$$

FYL transform is analogous to the mass action in gaseous chemical equilibria:

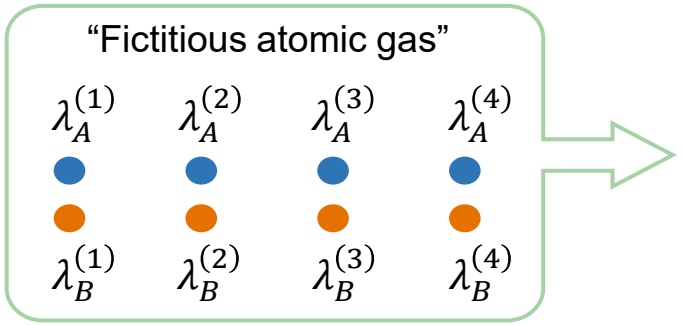

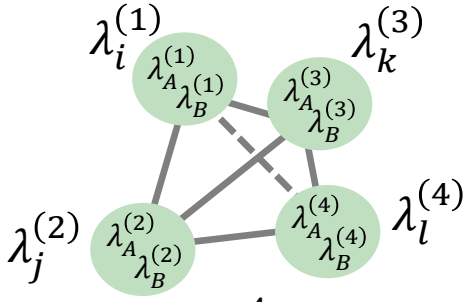

$$\mu_\alpha(\rho_{ijkl}) = \sum_{s=1}^{4} \sum_{n=A,B} \mu_n^{(s)}$$

Number of variables: n^s → $n \times s$

- **Yang's generalized quasi-chemical method (Cluster Site Approximation)**:

  Two key approximations (ansatzes) to enable analytical calculation of thermodynamics:

  1. **FYL transform** to simplify the minimization of free energy
  2. **Non-interference assumption** to simplify the treatment of atomic correlation

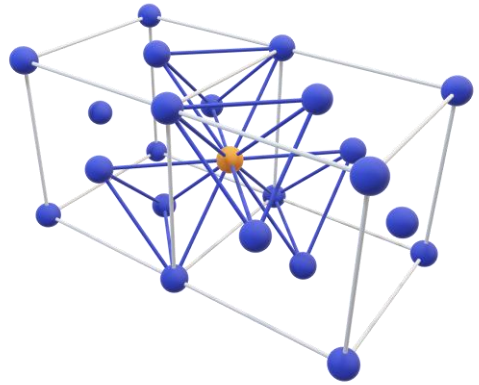

- **Our contribution: combine FYL transform with Kikuchi's CVM**

  Generalized quasi-chemical method = FYL transform + non-interference assumption — Clusters/pairs are independent

  ↓

  FYL-CVM = FYL transform + CVM recursive relation — Clusters are interrelated

FCC binary prototype phase diagrams for FYL-CVM

Nearest-neighbor bond energy: **J**

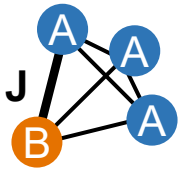

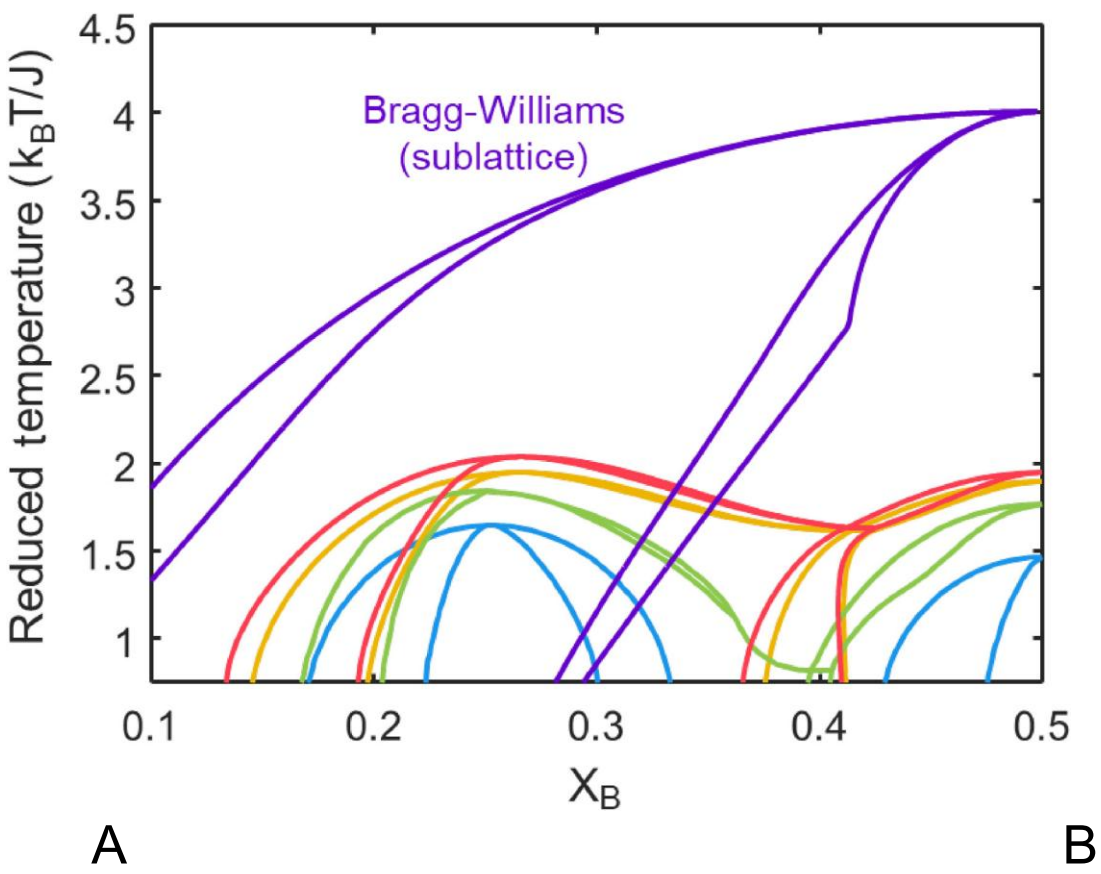

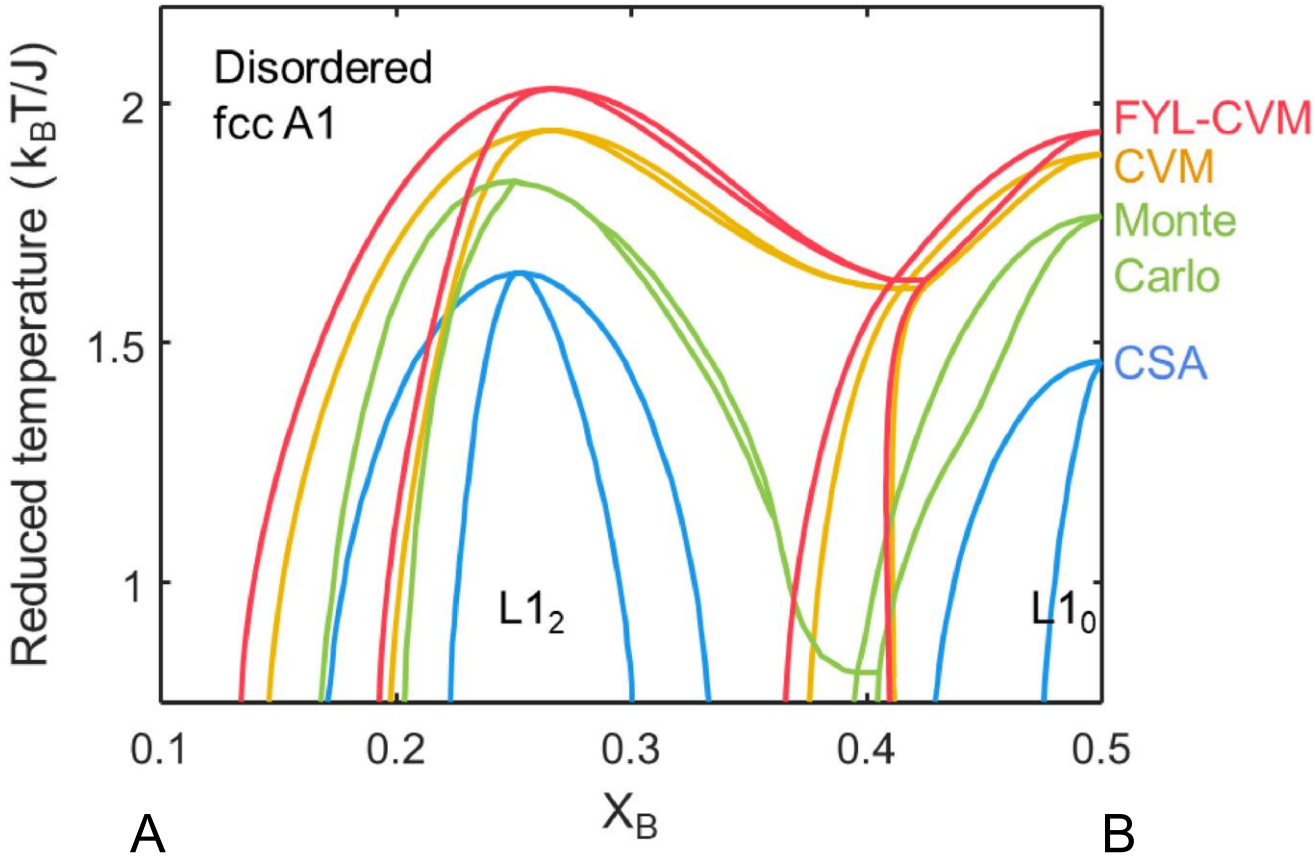

Cu-Au phase diagram

$$G_{mix} = G_{conf}$$

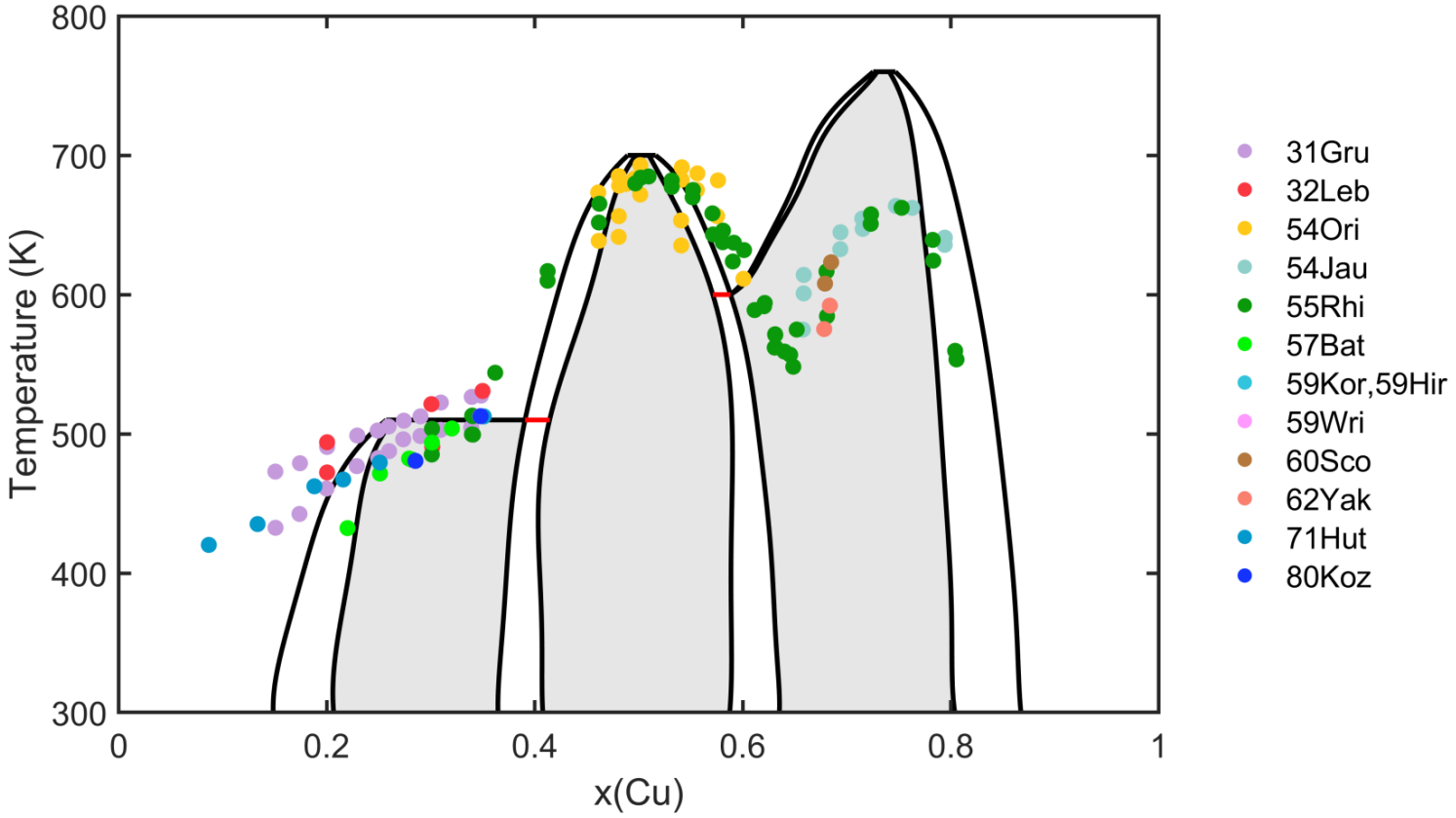

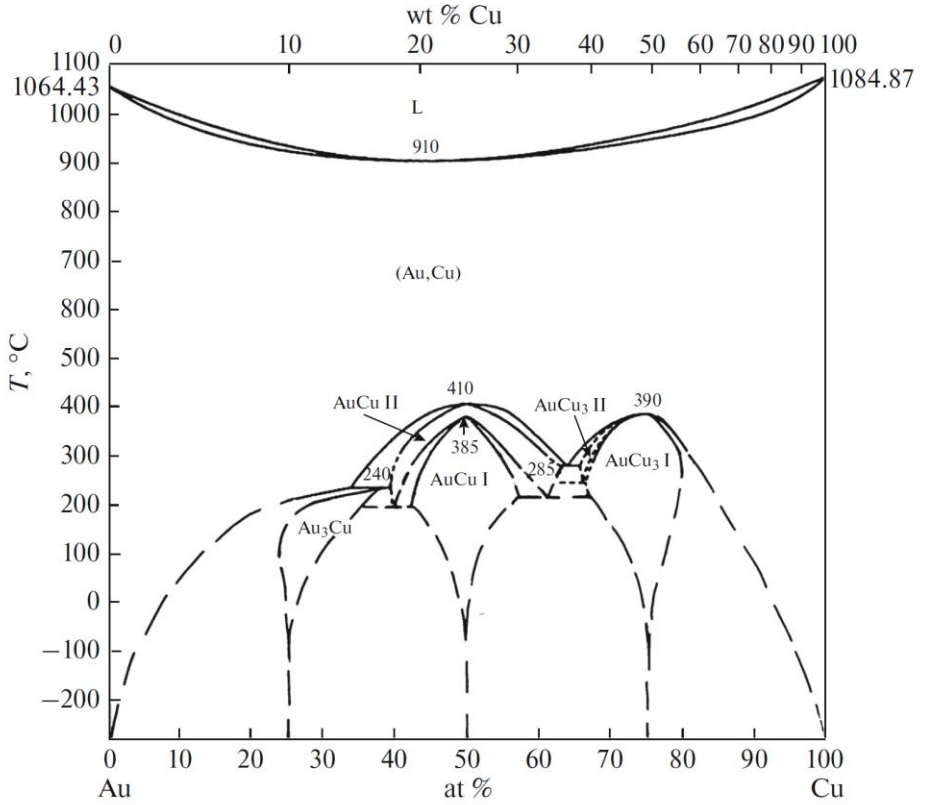

Fedorov, P. P. & S. N. Volkov. "Au−Cu phase diagram." *Russ. J. Inorg. Chem.* 61 (2016) 772

Okamoto, H., Chakrabarti, D. J., Laughlin, D. E., & Massalski, T. B. "The Au−Cu (gold-copper) system." *J. Phase Equil.* 8 (1987) 454

Adding More Physics:

$$G_{tot} = G_{conf} + G_{vib} + G_{elastic} + G_{ele} + \cdots$$

Observation of Vibrational Contributions: two main effects to be considered

$$G_{mix} = G_{confi} + G_{non-config} = G_{config} + \boldsymbol{G_{vib}} + G_{elastic} + G_{ele}$$


Gerbrand Ceder


Axel van de Walle

The "Bond Proportion" Mechanism

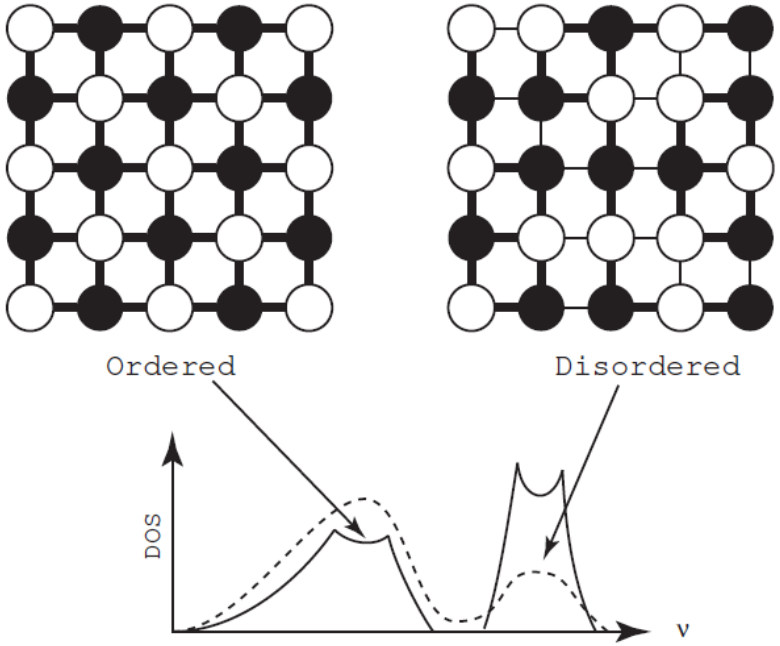

Size mismatch effect

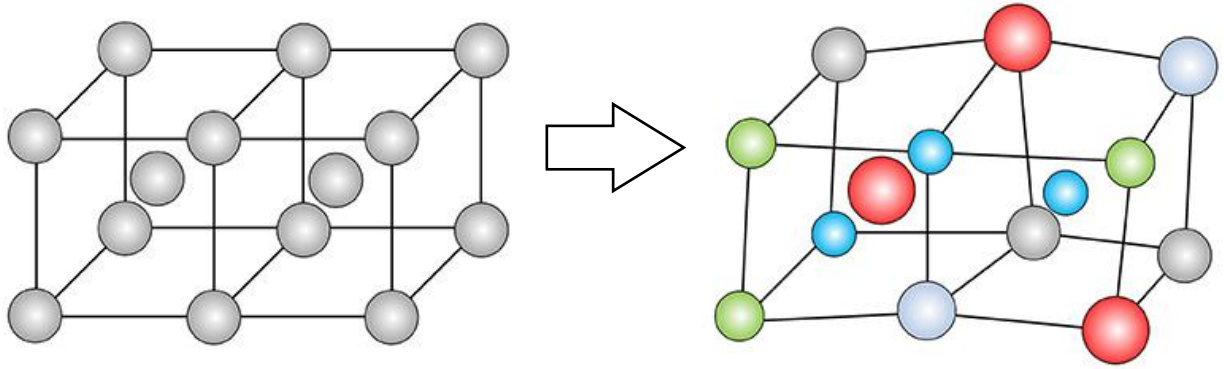

Strategy for Elastic Contributions: Separate it

$$G_{mix} = G_{config} + G_{non-config} = G_{config} + G_{vib} + \boldsymbol{G_{elastic}} + G_{ele}$$


Alex Zunger

- ε-G approach based on Zunger's work (1988)

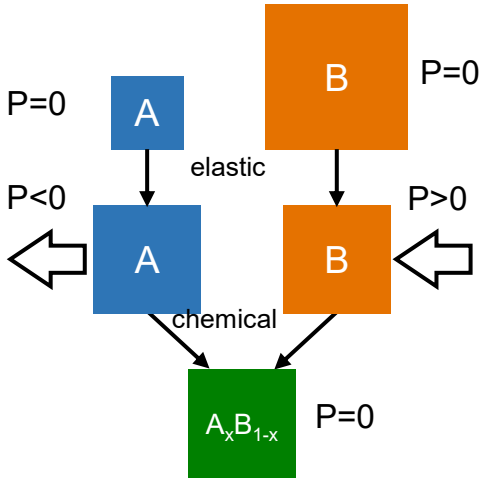

Molar volume changes on alloying

$$G = N \sum_{ij, i \neq j} \Omega_{ij} x_i x_j$$

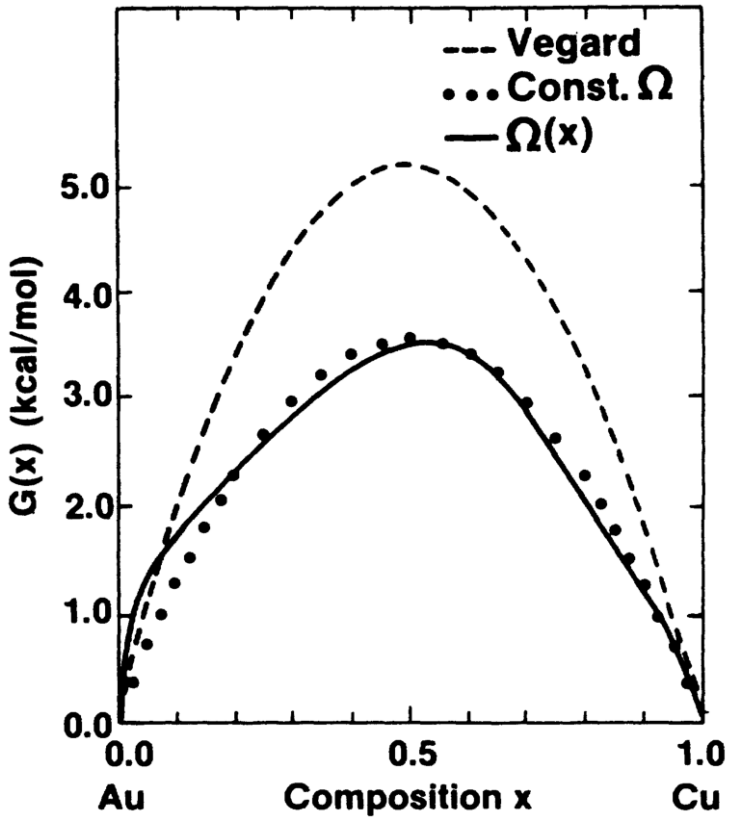

$$G_{mix} = G_{conf}$$

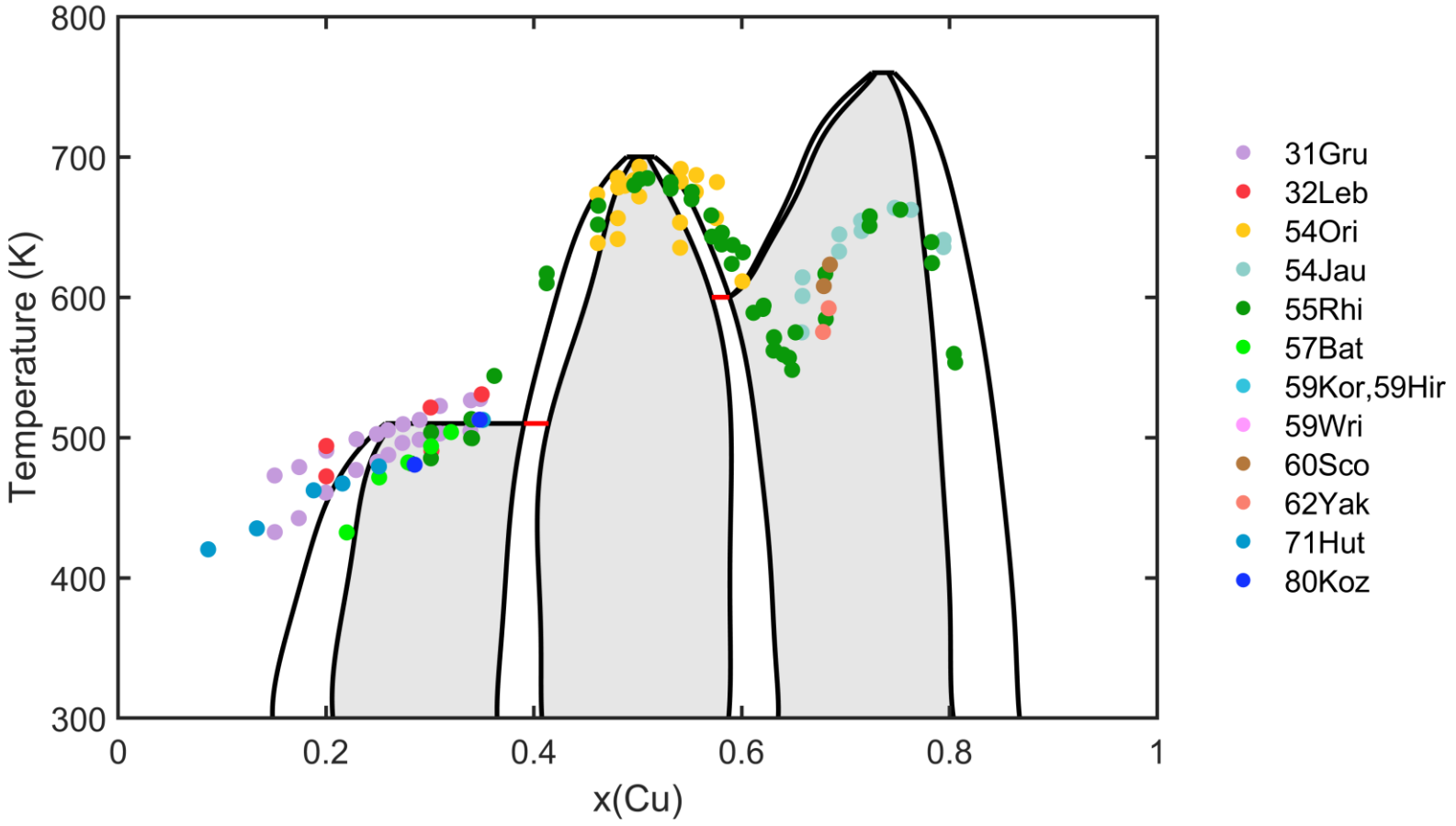
800
700
600
500
400
300
Temperature (K)
0
0.2
0.4
0.6
0.8
1
x(Cu)
31Gru
32Leb
54Ori
54Jau
55Rhi
57Bat
59Kor,59Hir
59Wri
60Sco
62Yak
71Hut
80Koz

$$G_{mix} = G_{conf} + G_{elastic}$$

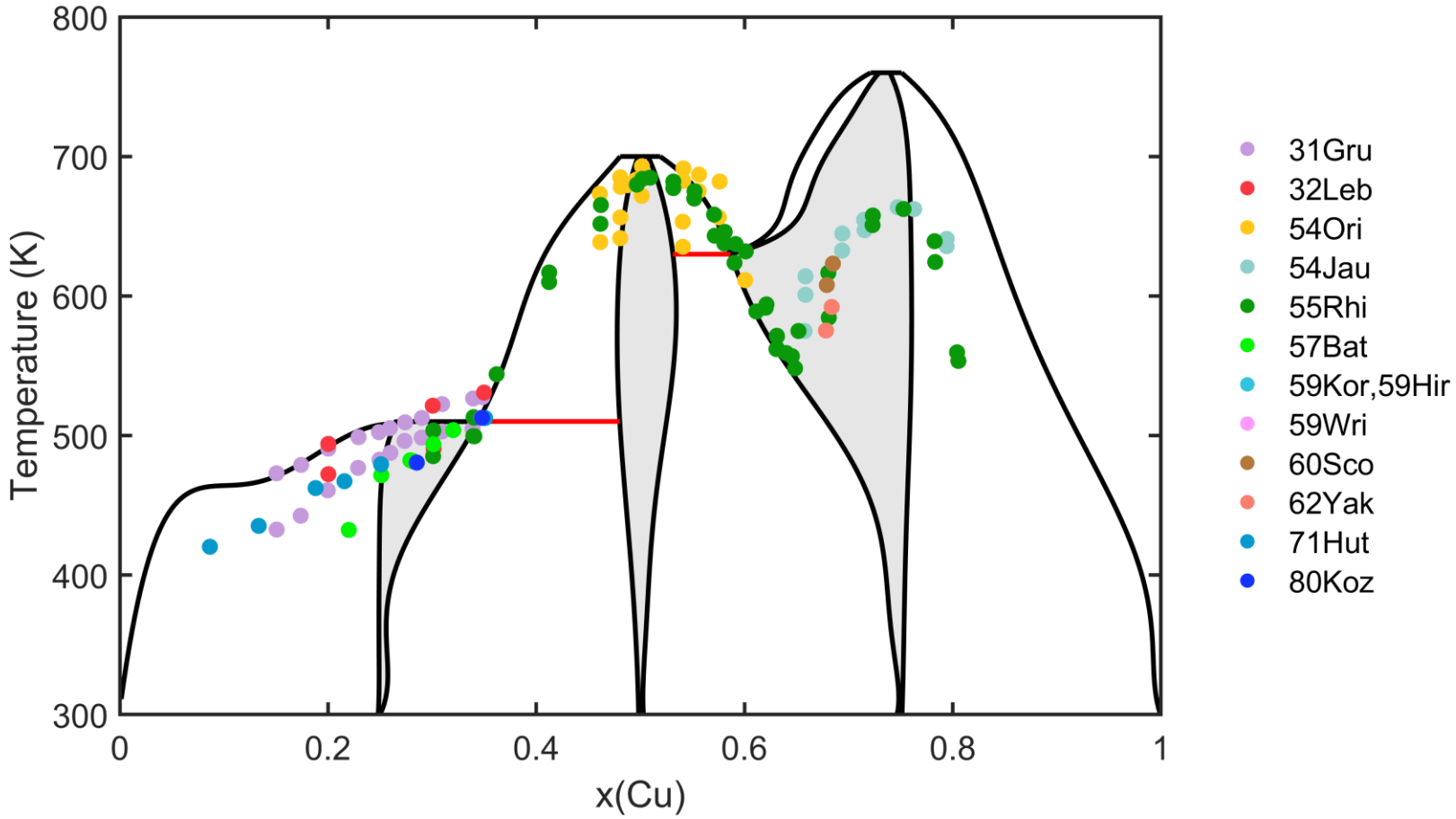

$$G_{mix} = G_{conf} + G_{elastic} + G_{vib}$$

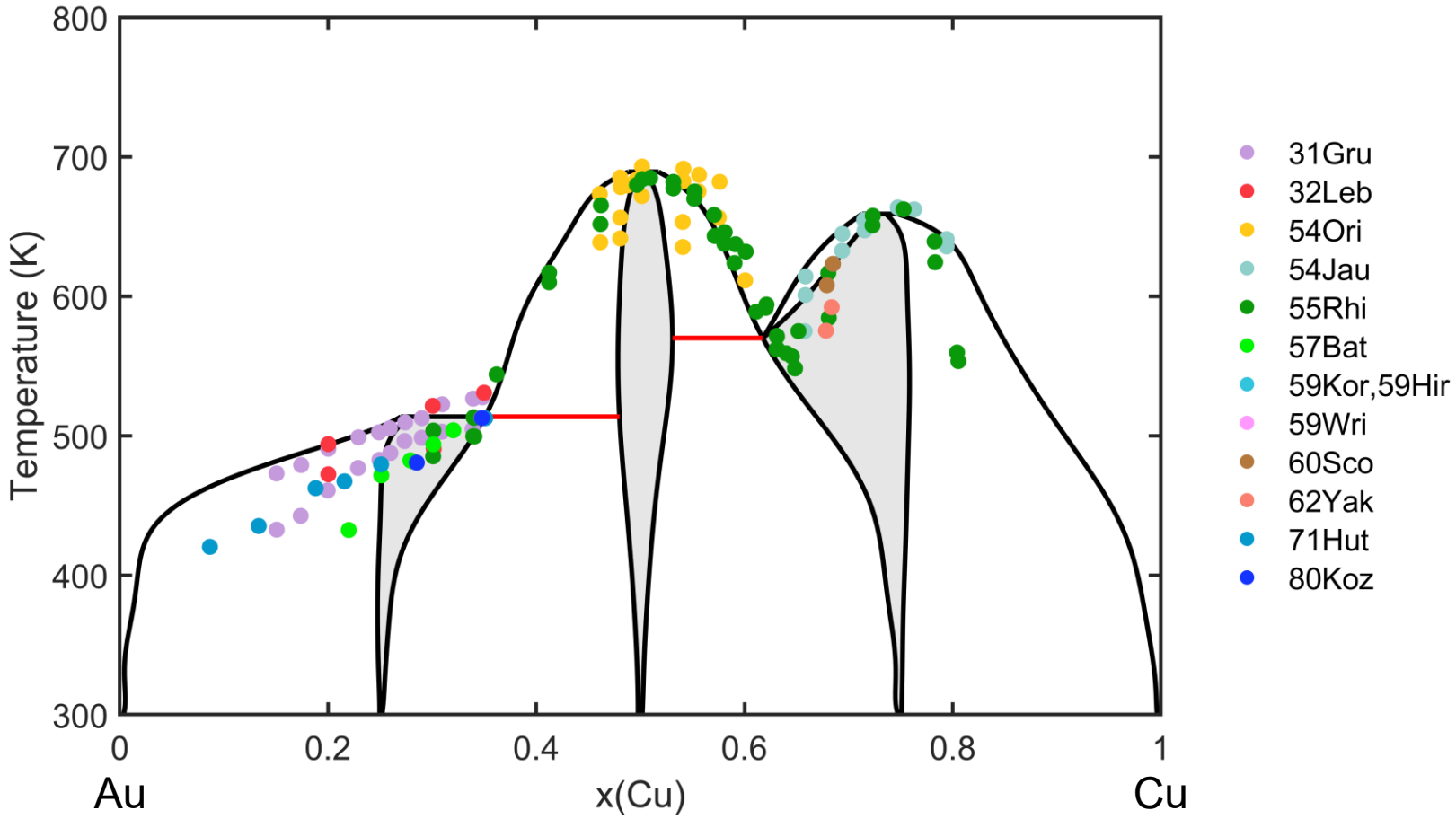

$$G_{mix} = G_{conf} + G_{elastic} + G_{vib} + G_{elec}$$

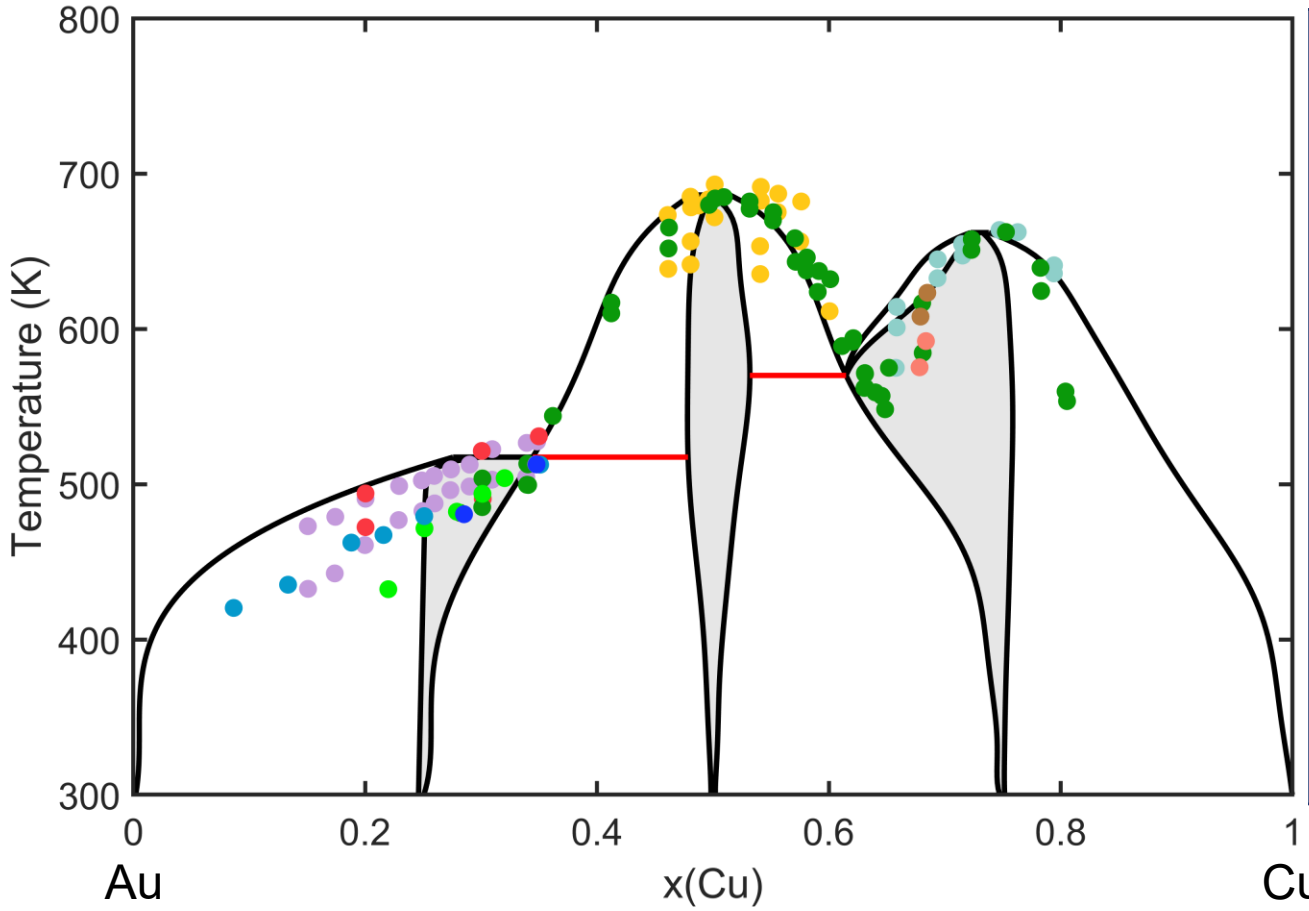

	# of fitting parameters	Source of fitting data
Chemical cluster energy	0	DFT formation energies
Elastic	1 Ω=56.1kJ/mol	Exp.
Vibrational	3 r=1.06 $p_{lc}(Cu_3Au)$=1.05 $p_{lc}(CuAu_3)$=0.98	Exp.
Electronic	0	DFT EDOS
CVM-CALPHAD	**4**	**DFT+Exp.**
Bragg-Williams CALPHAD	**10**	**Exp.**

Sundman, Bo, et al. *CALPHAD* 22.3 (1998) 335

Warren-Cowley SRO parameter α_{CuAu} in Cu-Au

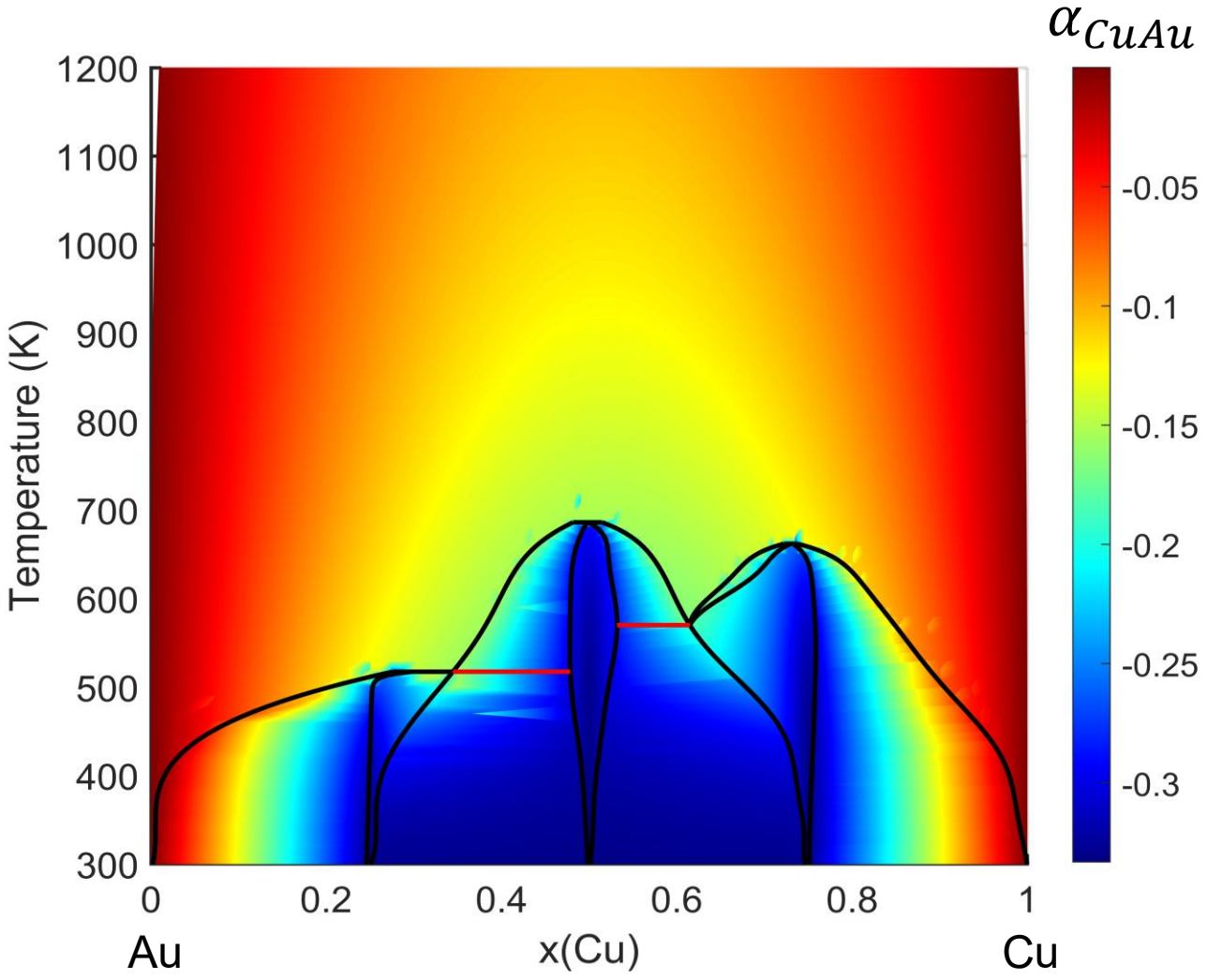

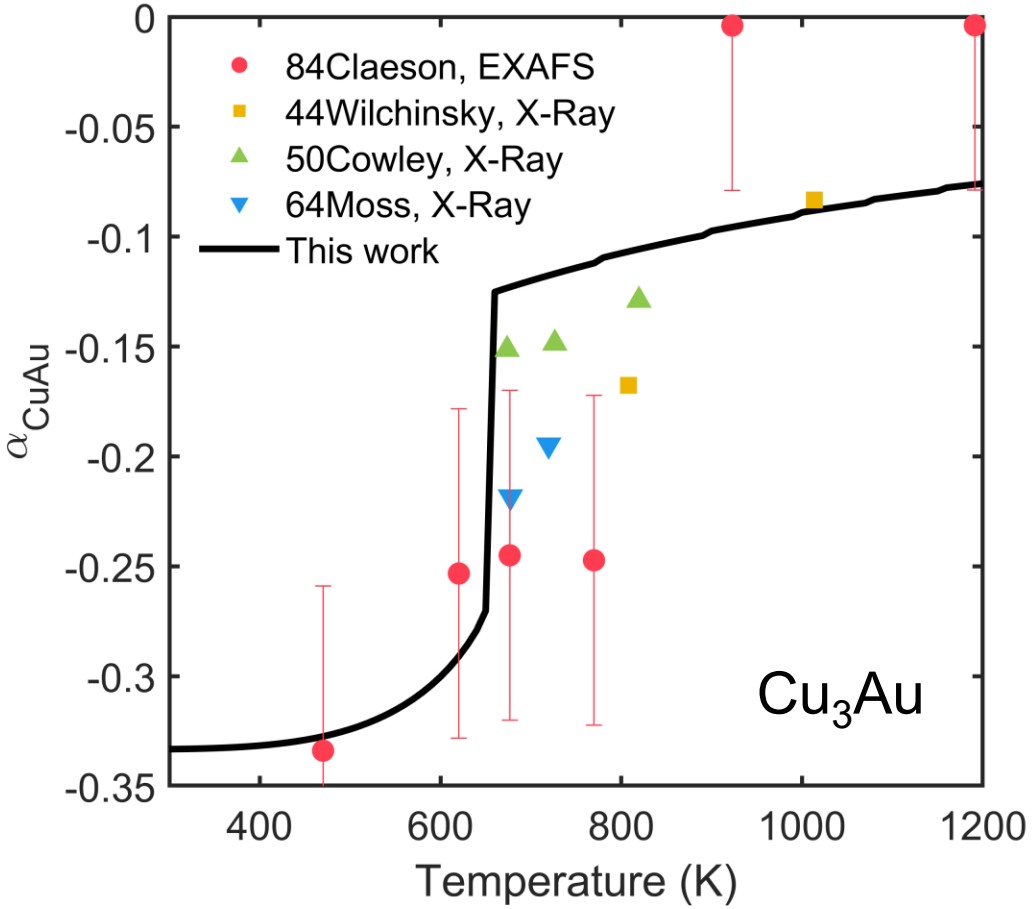

Warren-Cowley SRO parameters in Cu-Au-Ag at T=800K

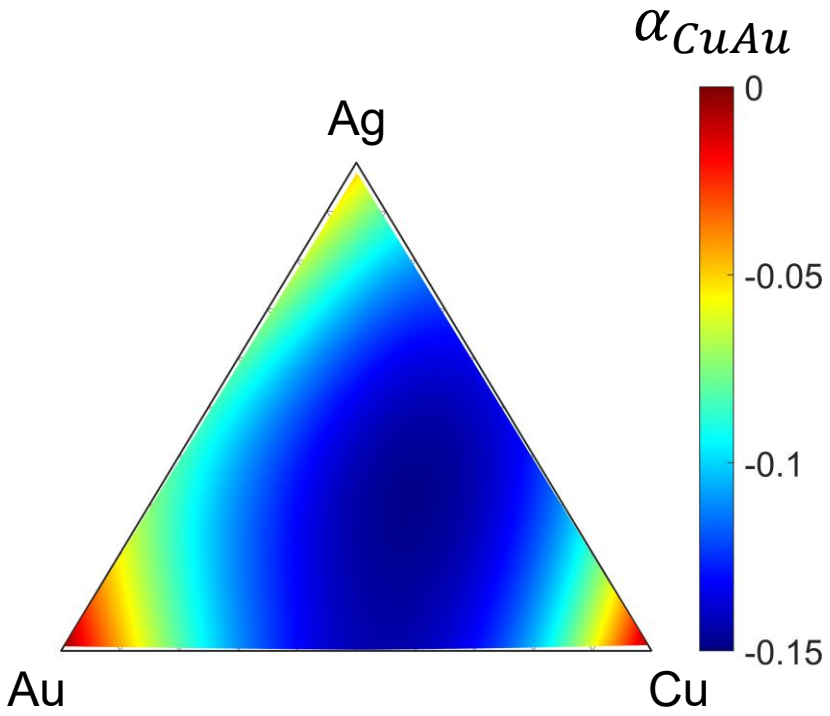

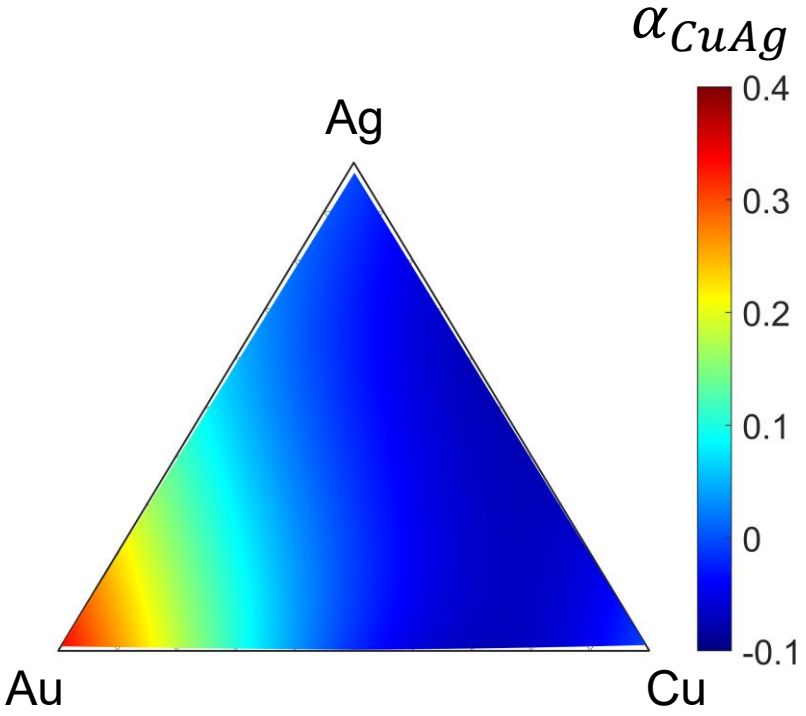

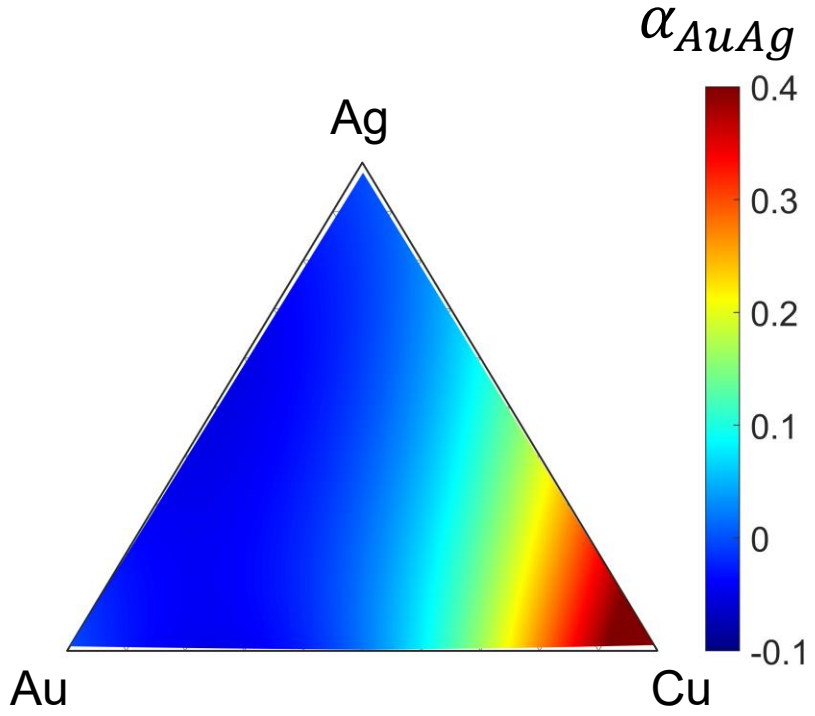

Take-Home Message

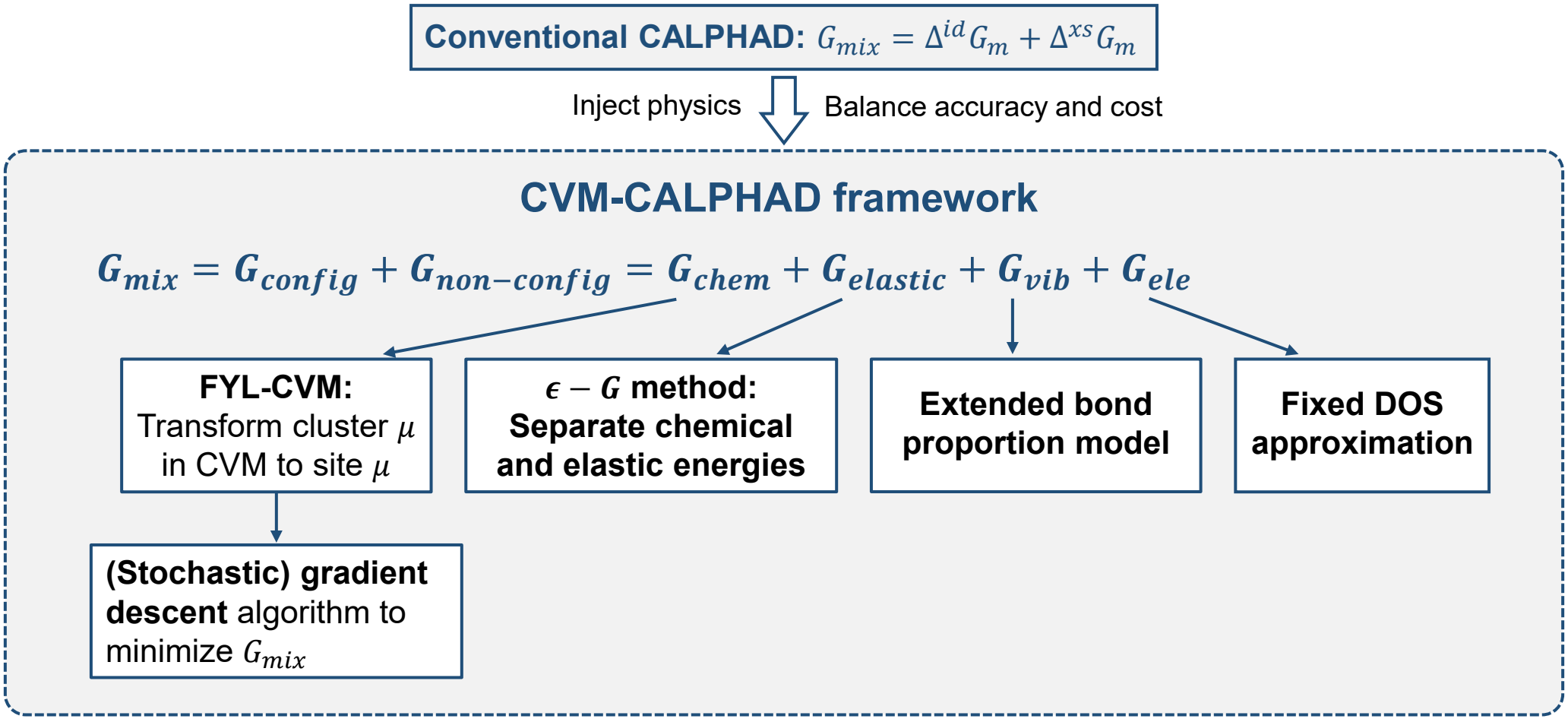

Push to kinetics with the duality consideration

- CALPHAD4Phase Field: $\mu_i^{t+1} = \mu_i^t - \alpha \frac{\partial \Omega}{\partial \mu_i^t}$ $\partial_t \mu = -\alpha' \nabla_\mu \Omega$ Cahn-Hilliard/time-dependent G-L

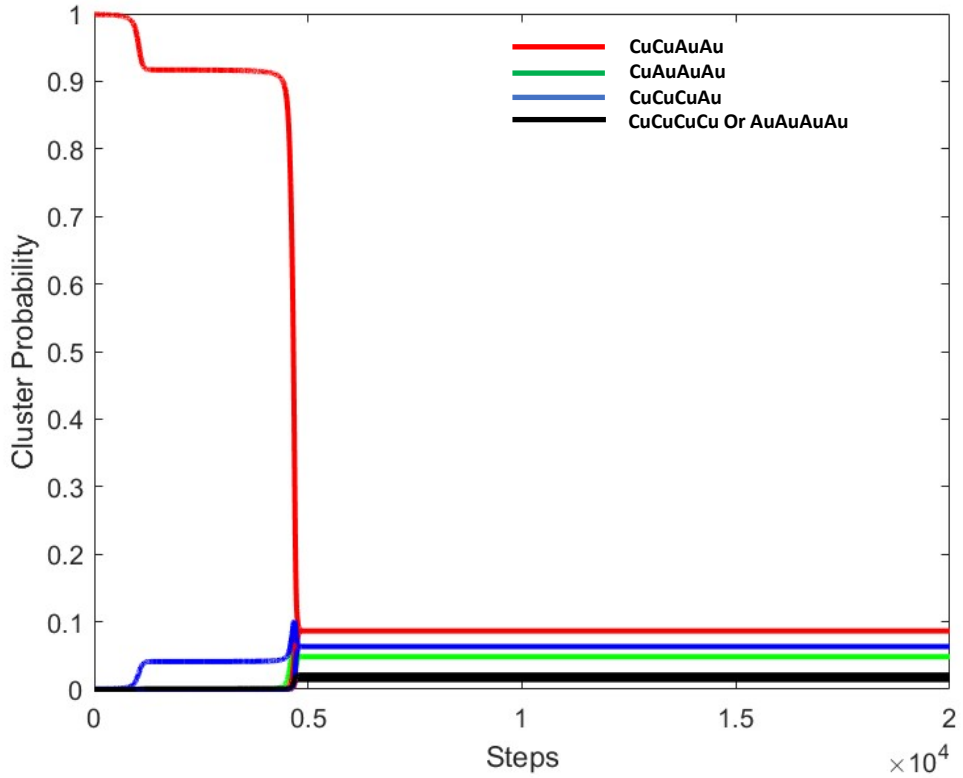

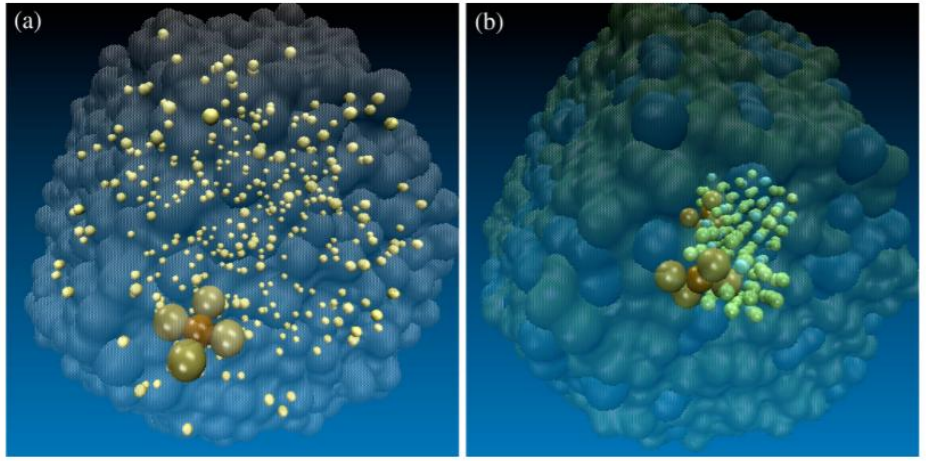

FIG. 4. $L1_2$ ordered clusters of Cu_3Au in the supercooled liquid (a) and in a configuration containing a critical nucleus (b). For clarity, only the central Cu atom (ochre) and the four closest Au (tan) are shown as large spheres and liquidlike atoms are translucent. In (a), atoms in icosahedra are shown as small yellow spheres. In (b), atoms from the critical nucleus are shown as small blue spheres (Au) and small green spheres (Cu).

Liquid	→	$L1_2$precursor	→	Solid solution
(structural disorder)		(structural order)		(structural order)
(chemical disorder)		(chemical order)		(chemical disorder)

Outline:

- High entropy alloy, combinatorial disorder
- Cluster based thermodynamics modeling

- Measuring in-plane thermal transport with wrinkle
- Modified conduction equation

- electron-phonon coupling within localized state, interplay between disorder and the electron-phonon interaction
- Anomalous Neutron Nuclear-Magnetic Interference Spectroscopy

Energy challenge in computing system and thermal management

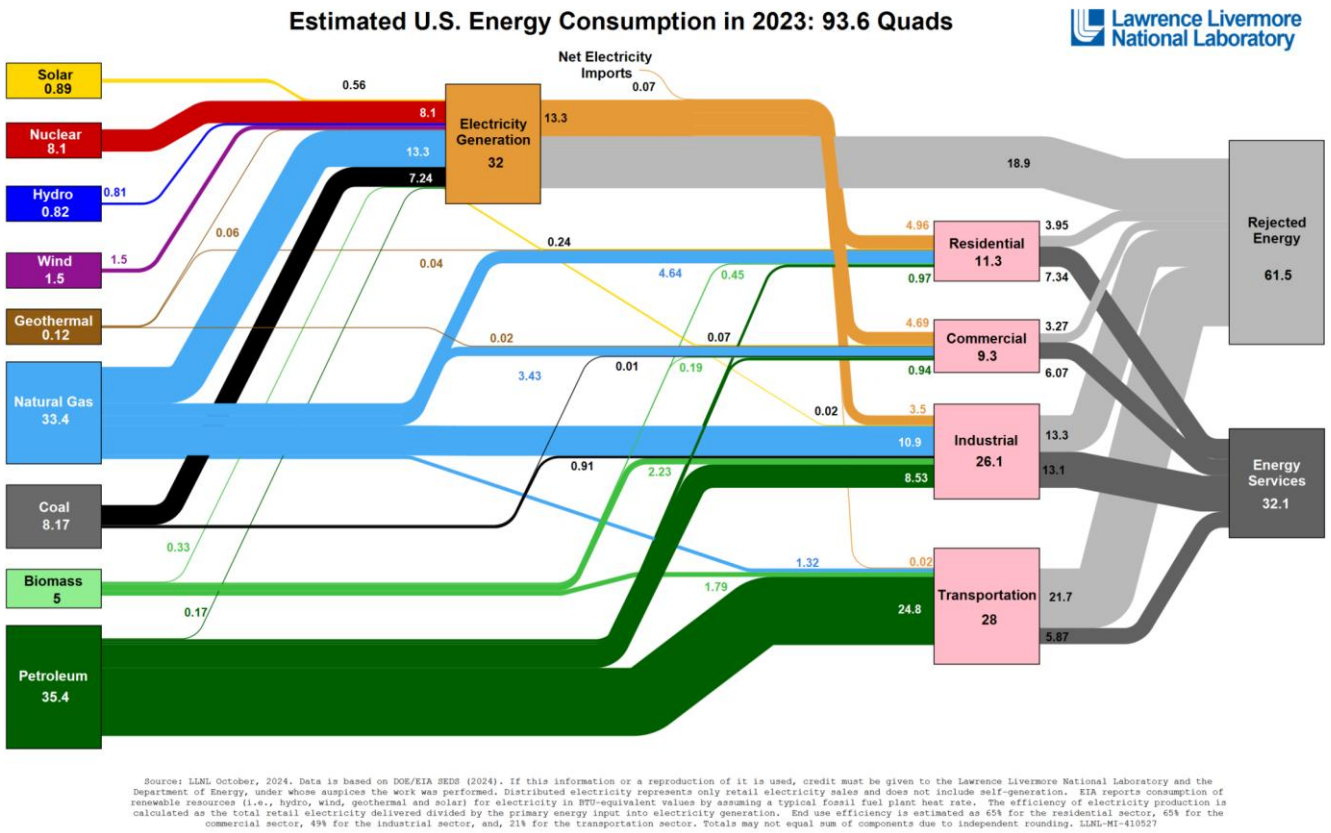

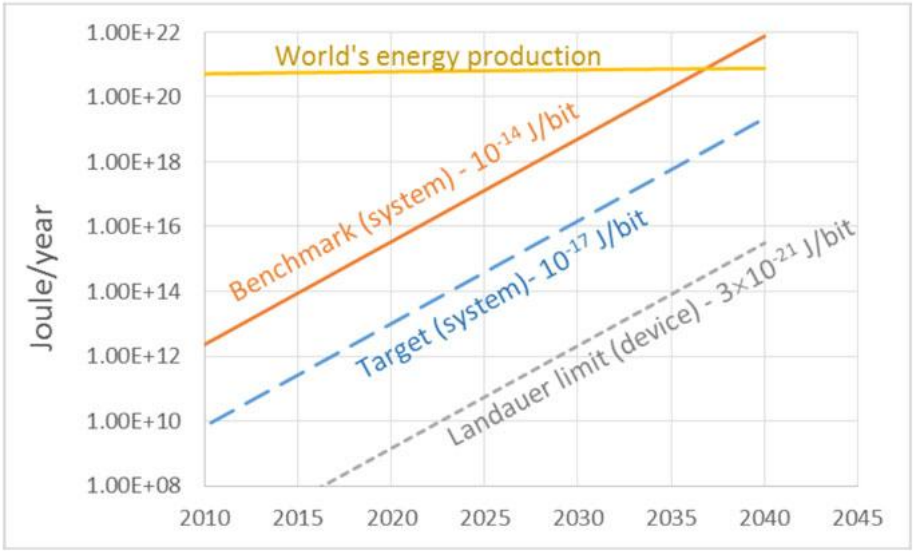

Fig. A8. Total energy of computing.

(SIA Report 2015)

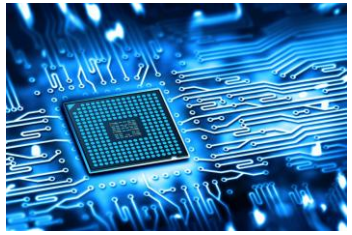

Energy transport within multilayered semiconductor device

- **Heterogeneity** and **multilayered** structure in the device level for functionality and the protection(dielectric, thermal dissipation, strain, degradation…).

- **Thermal management** is even more important for semiconductor device for **its performance and sustainability**.

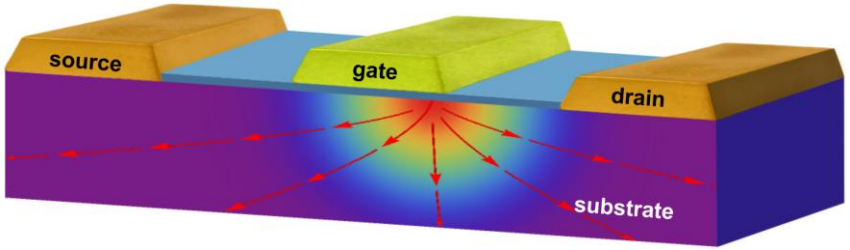

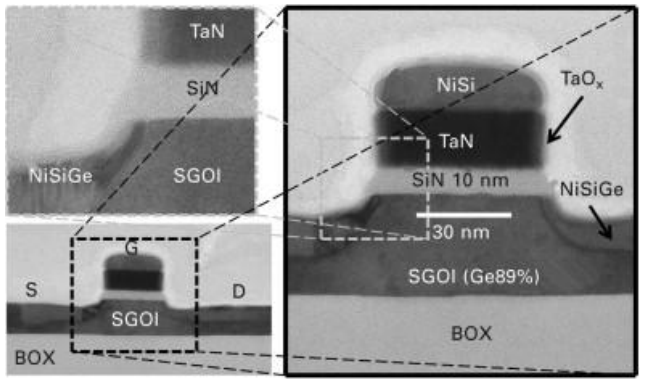

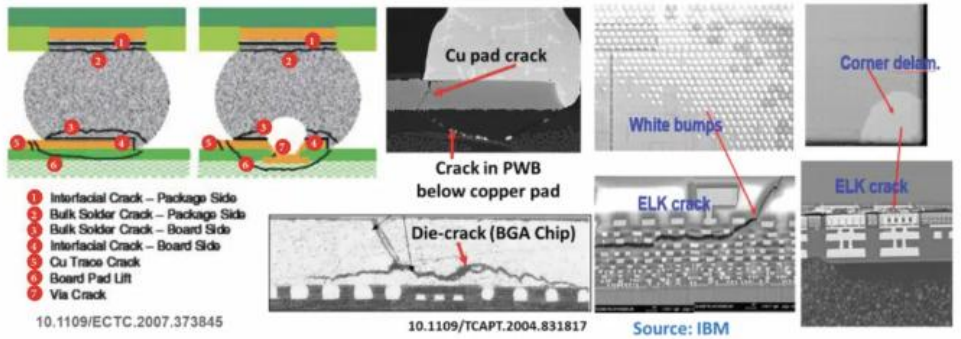

Thermal management of gallium nitride

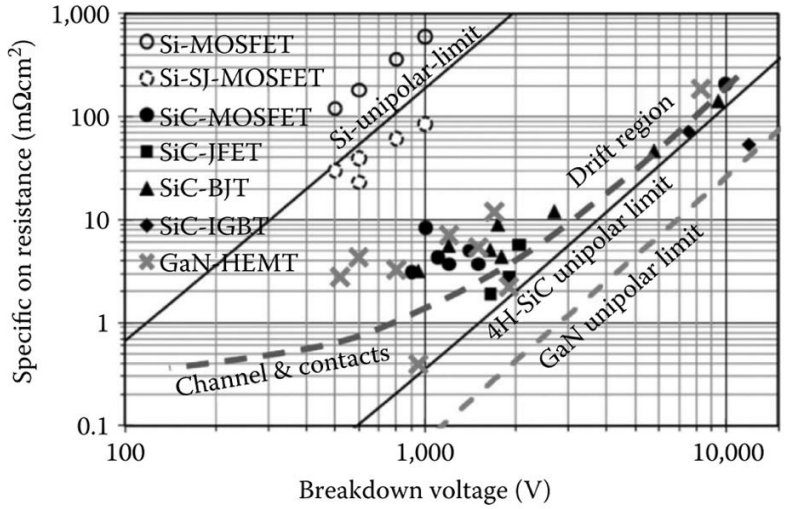

Medjdoub, F. Gallium Nitride (GaN) - Physics, Devices, and Technology (2017)

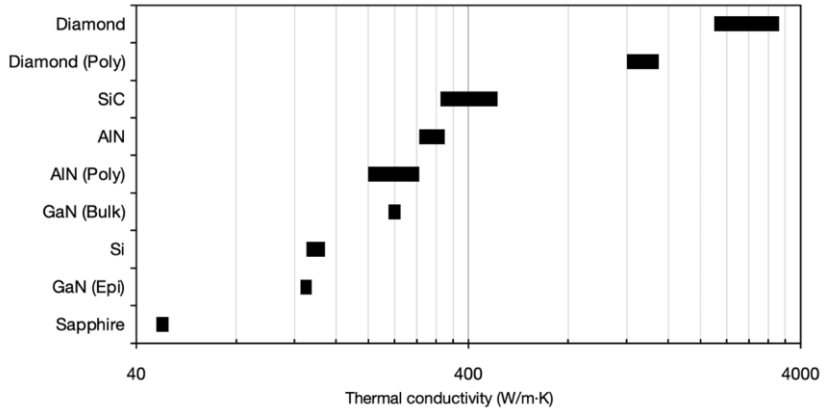

Qiao, K. Gallium Nitride Remote Epitaxy (2022)

Time-domain thermoreflectance

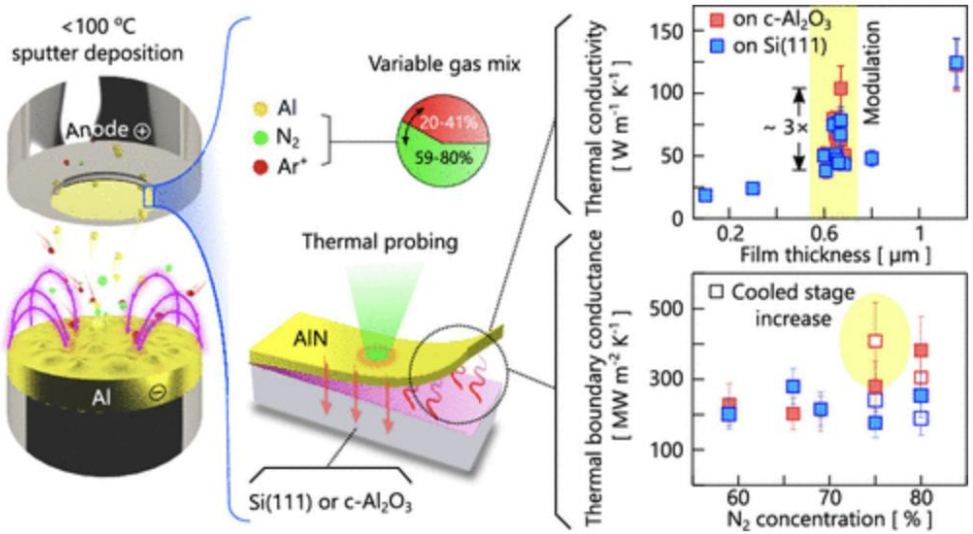

ACS Nano 17, 21240–21250 (2023)

Pump-probe X-ray diffraction experimental setup: spatial resolved for in-plane measurement?

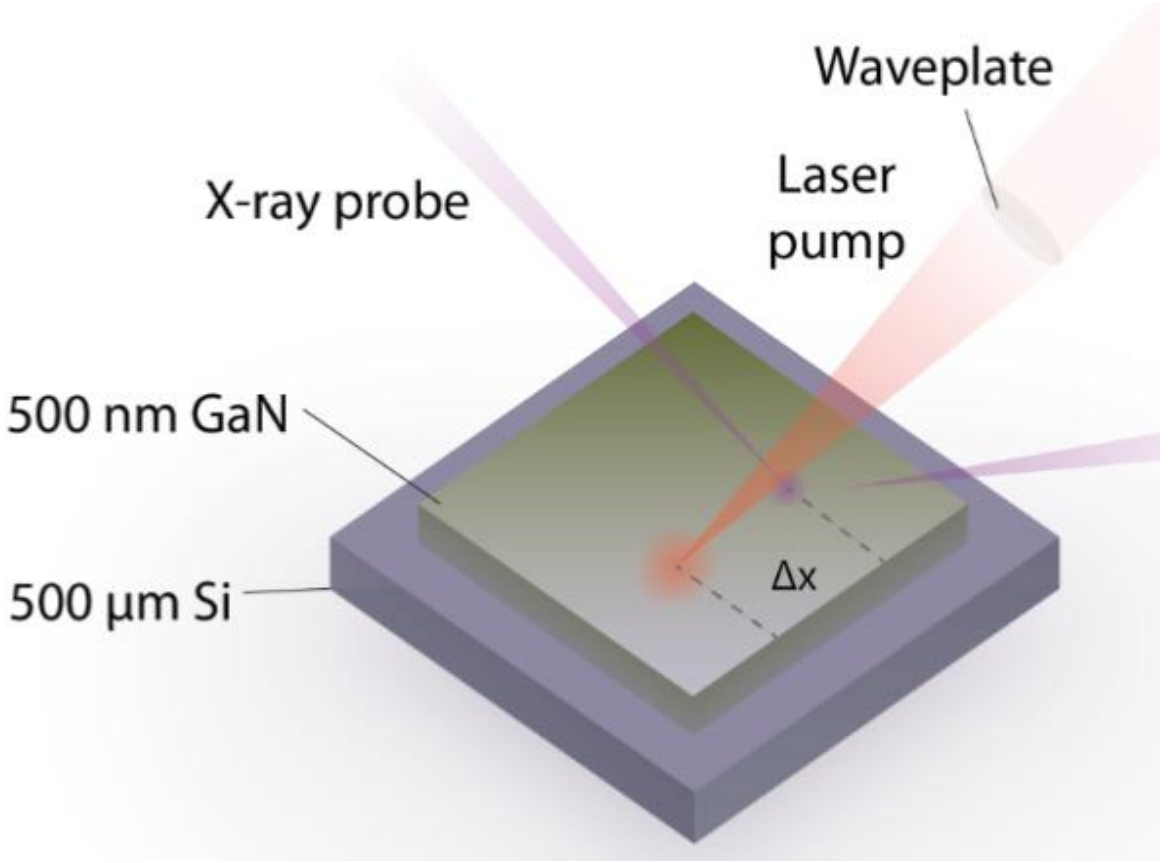

Measurement of (002) Bragg peak 2θ variation

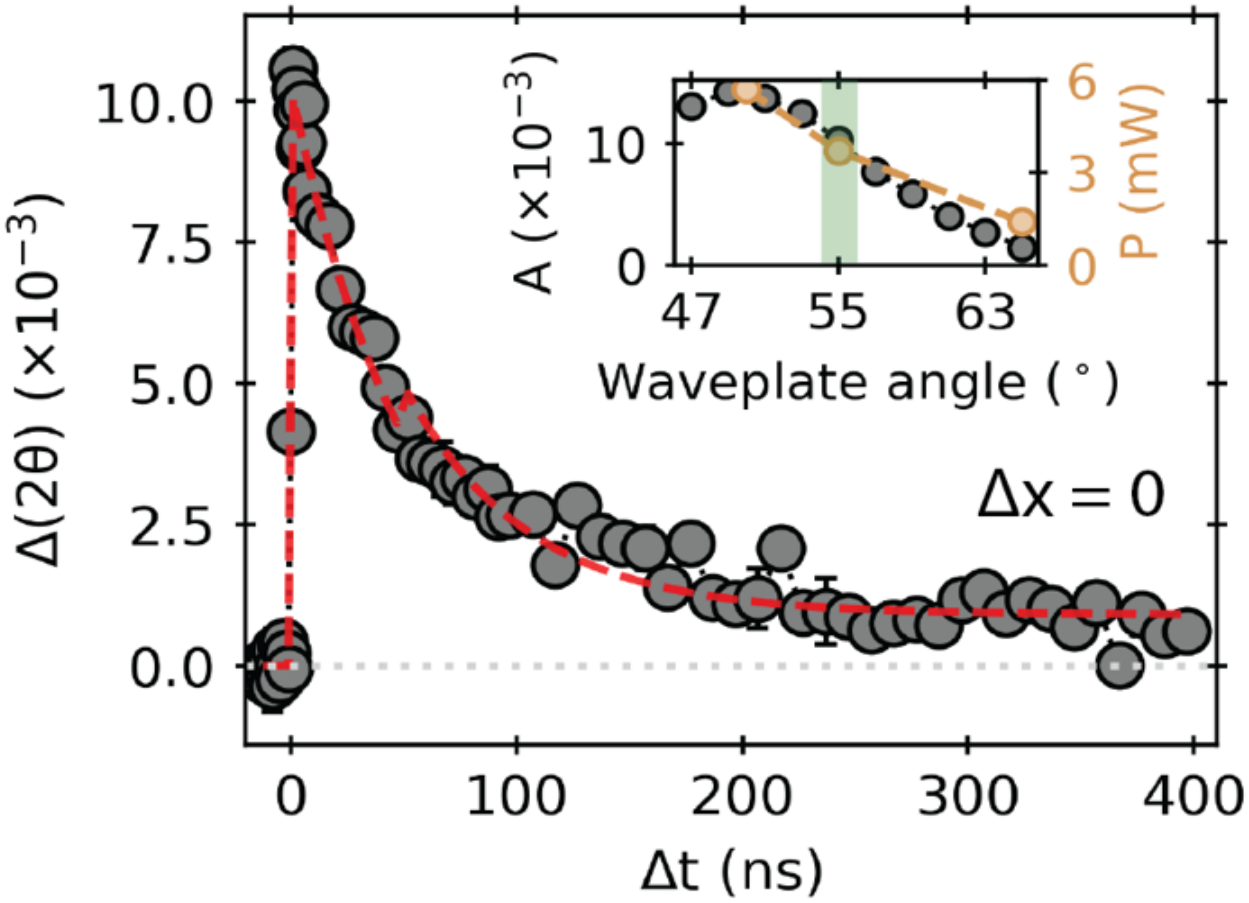

With spatial resolution of the relaxation
Several measurements → sections of process

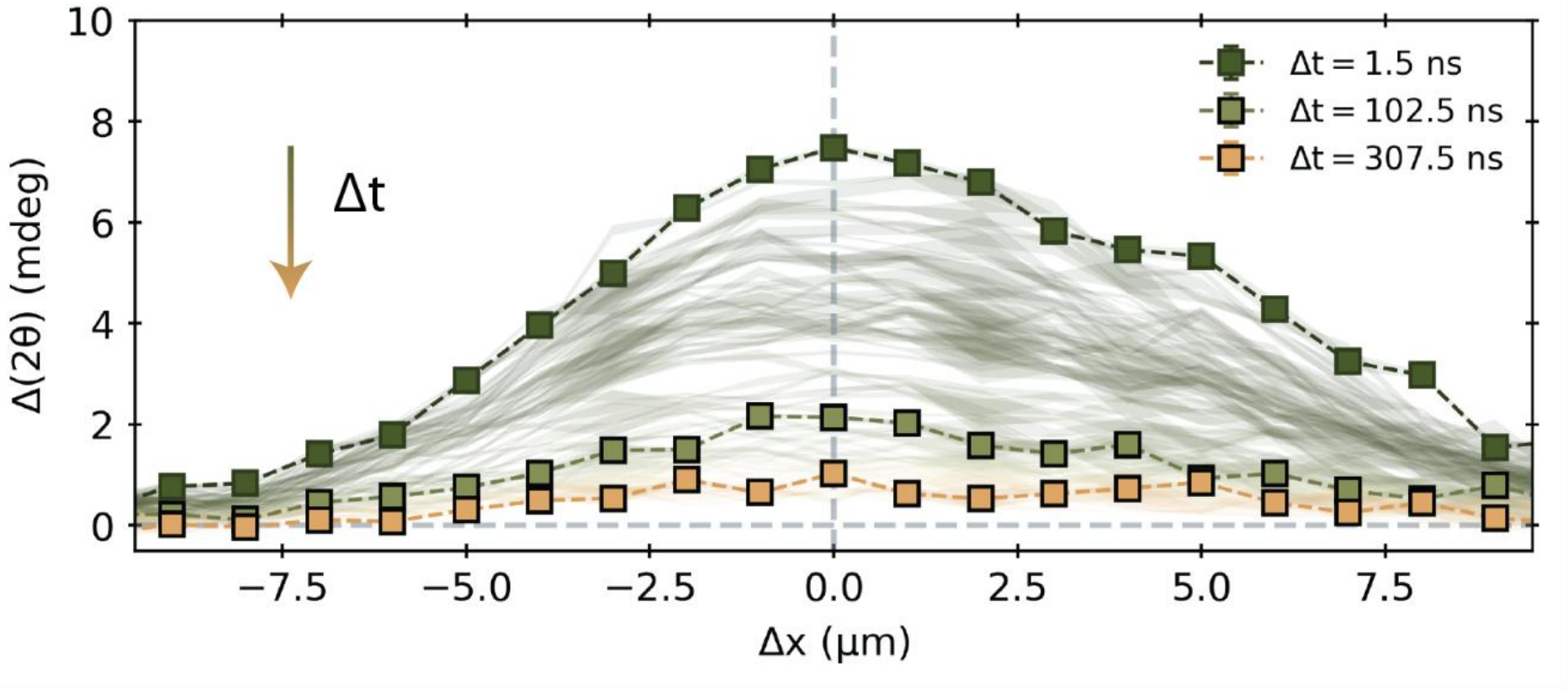

With wrinkle, unsymmetric signal

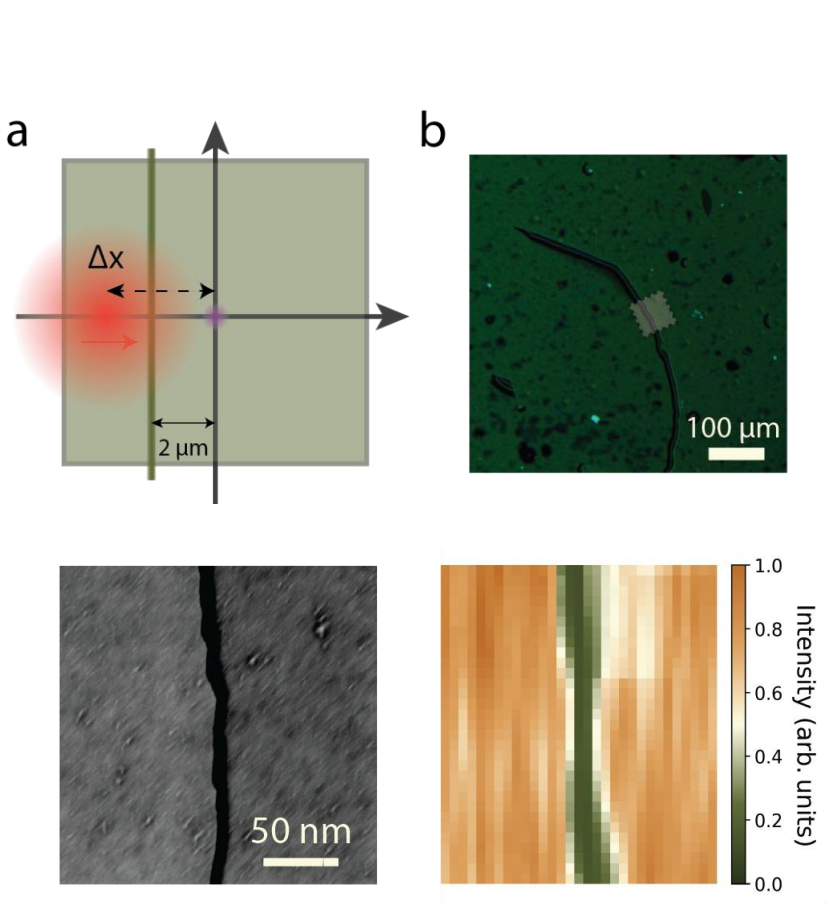

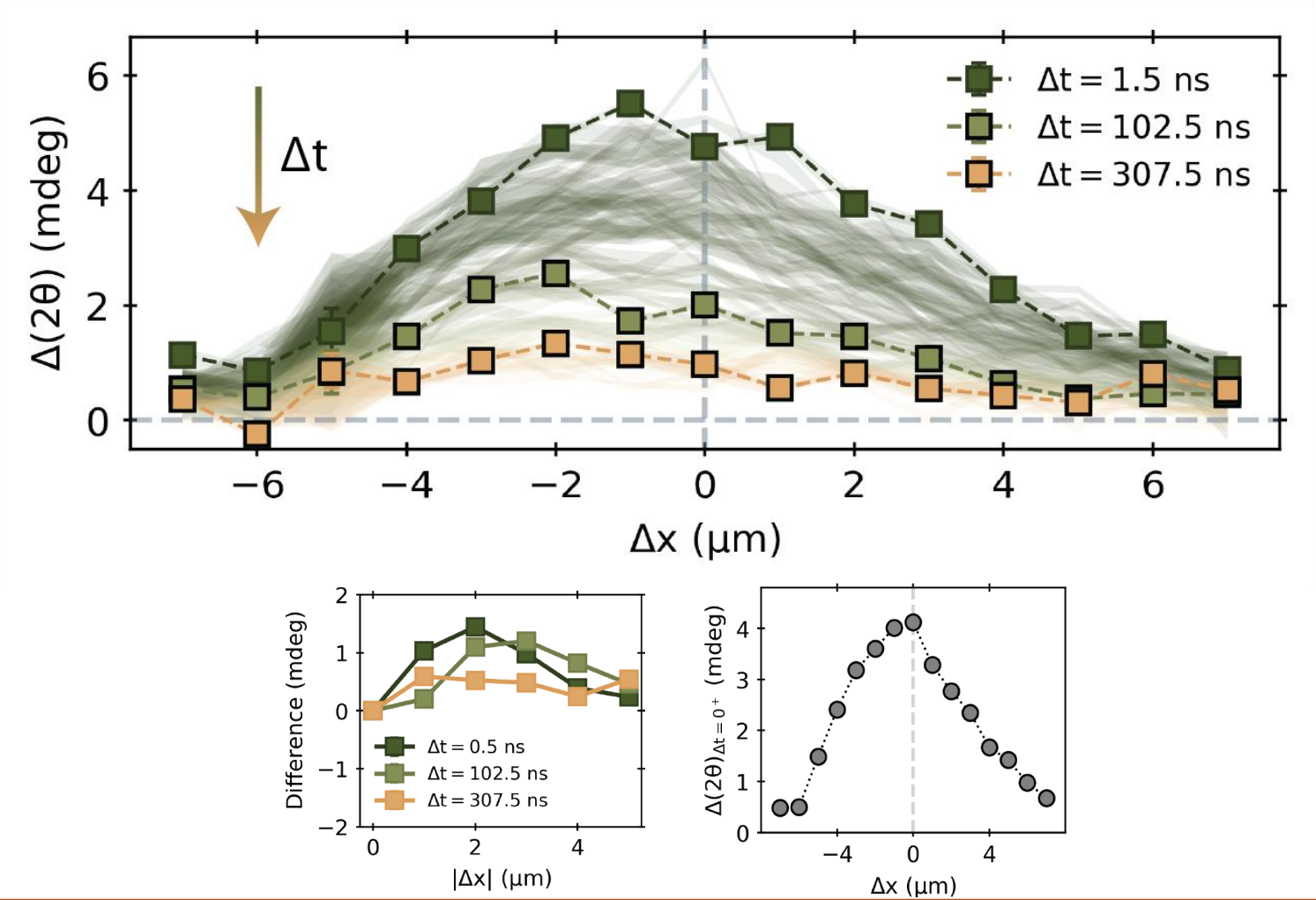

How to extract the information? How to simulate the process?

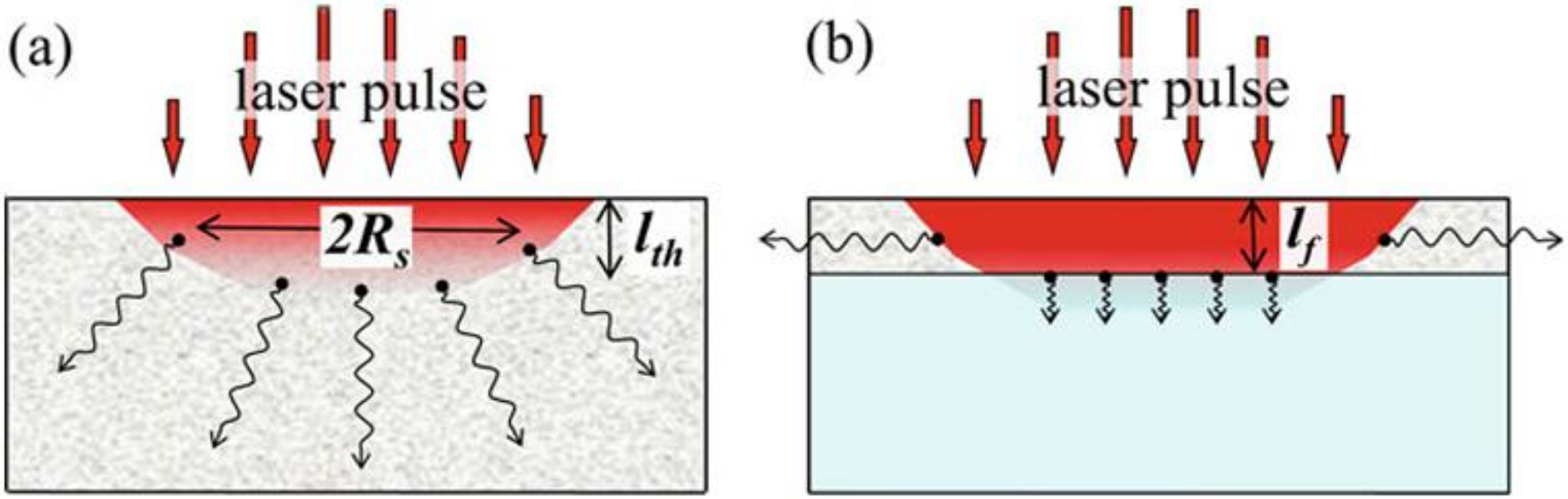

Fig. 6 Schematic representation of the laser energy deposition and redistribution in a strongly absorbing bulk target (**a**) and a film deposited on a substrate (**b**)

1D to 3D to have the in-plane resolution

Shugaev, Maxim V., et al. "Laser-induced thermal processes: heat transfer, generation of stresses, melting and solidification, vaporization, and phase explosion." *Handbook of Laser Micro-and Nano-Engineering*. Cham: Springer International Publishing, 2021. 83-163.

Adding Thermal Boundary Conductance (TBC) into the diffusion mechanism:

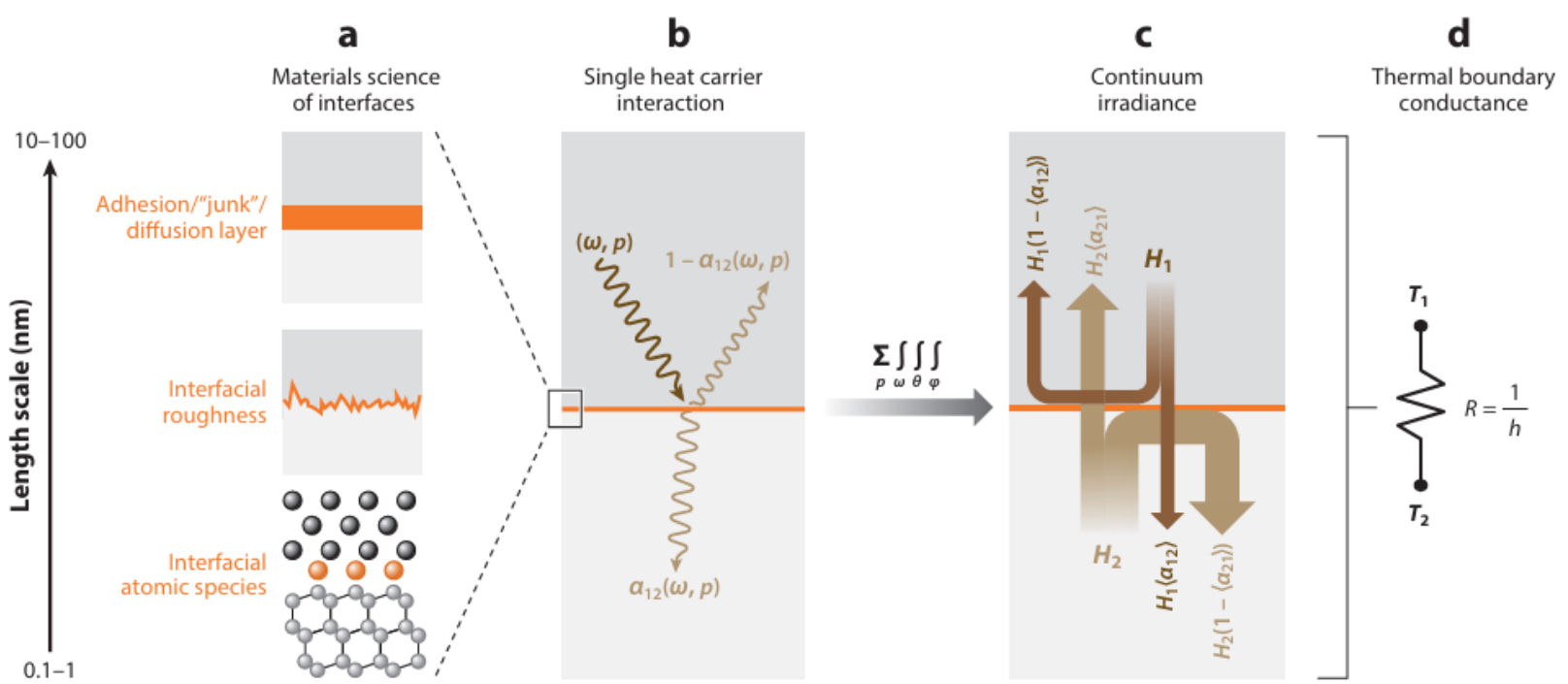

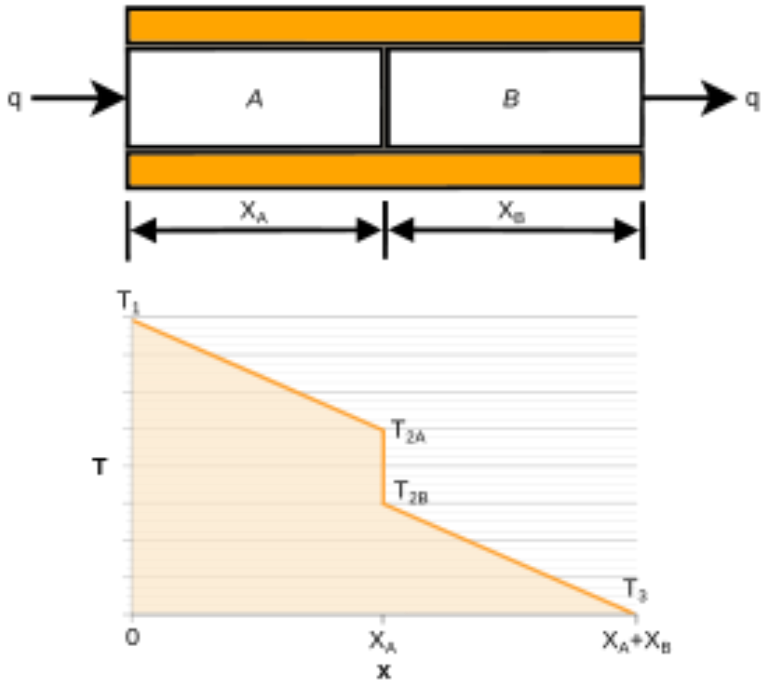

Variable Neumann boundary condition

$$q_2 = G_{12}(T_2 - T_1)$$
$$q_1 = G_{12}(T_1 - T_2)$$

$$q = -k\frac{\partial T}{\partial \mathbf{n}}$$

$$c\rho\frac{\partial T_i}{\partial t} = \nabla \cdot (k_i \nabla T_i), T_i \in \Omega_i$$
$$-k_i\frac{\partial T_i}{\partial \mathbf{n_i}} = \sum_j G_{ij}(T_i - T_j), T_i, T_j \in \partial_i\Omega, T_j \in \partial_j\Omega$$

$$\Omega = \sum_i \Omega_i$$
$$\partial\Omega = \cap_{ij}\partial_{ij}\Omega$$

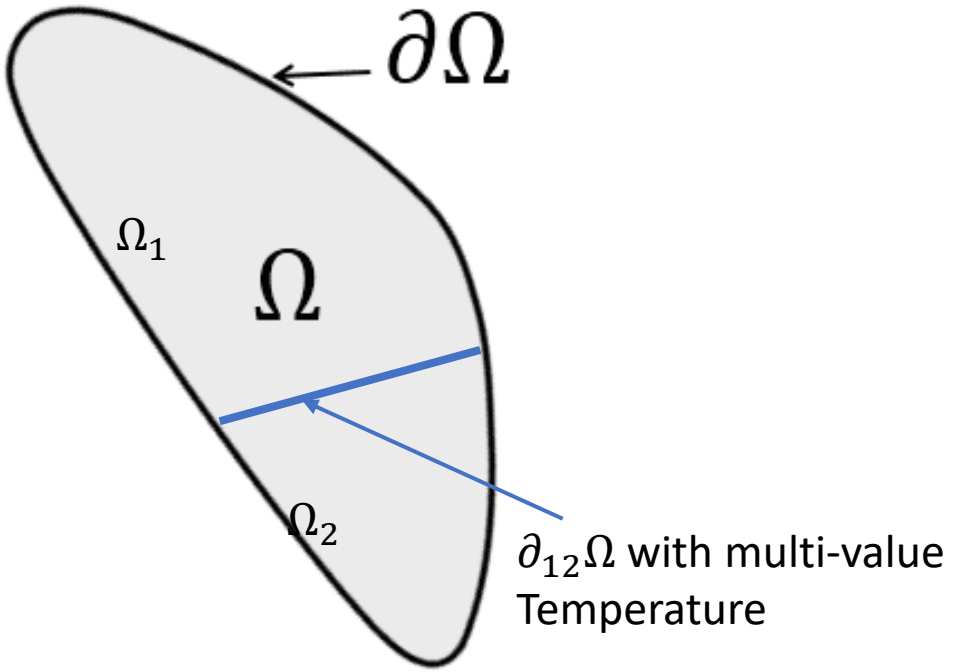

Partial Different Equations-driven inverse problem Solver (Optimization)

$$c\rho\frac{\partial T_i}{\partial t} = \nabla\cdot(k_i\nabla T_i), T_i \in \Omega_i$$

$$-k_i\frac{\partial T_i}{\partial \mathbf{n_i}} = \sum_j G_{ij}(T_i - T_j), T_i, T_j \in \partial_i\Omega, T_j \in \partial_j\Omega$$

$$\Omega = \sum_i \Omega_i$$

$$\partial\Omega = \cap_{ij}\partial_{ij}\Omega$$

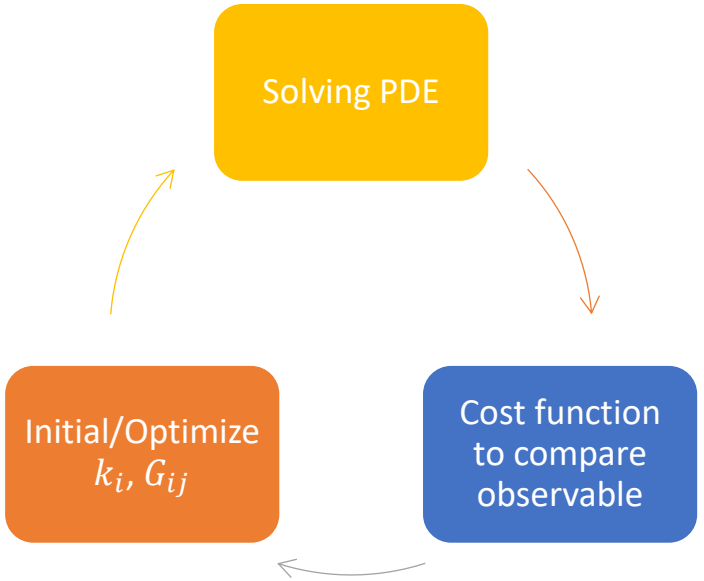

T_{exp}, $L = |T_{exp} - T_{sim}|$ + first derivative deviation +…

The General Computational Framework (for multi-layer, defected)

PDE Simulation Part

Foundation Module: *Profile Class*: the temperature field/conductivity with spatial resolution

Selective Transport Solver: Boundary condition solver, different transport mechanism(diffusion, …)

Main Process: Optimizer

Loss Function Construction

Optimizer: quasi-Newton methods, evolutional global optimization algorithm, AutoDiff-opt…

Assistant Pre/Post Process

Local Temperature Construction and Initial Profile Construction:
Based on experimental data

Temperature Profile Plotting:
Position and time resolved Profile to compare with EXP

Fix cross-plane transport to get in-plane information (with FDTR)

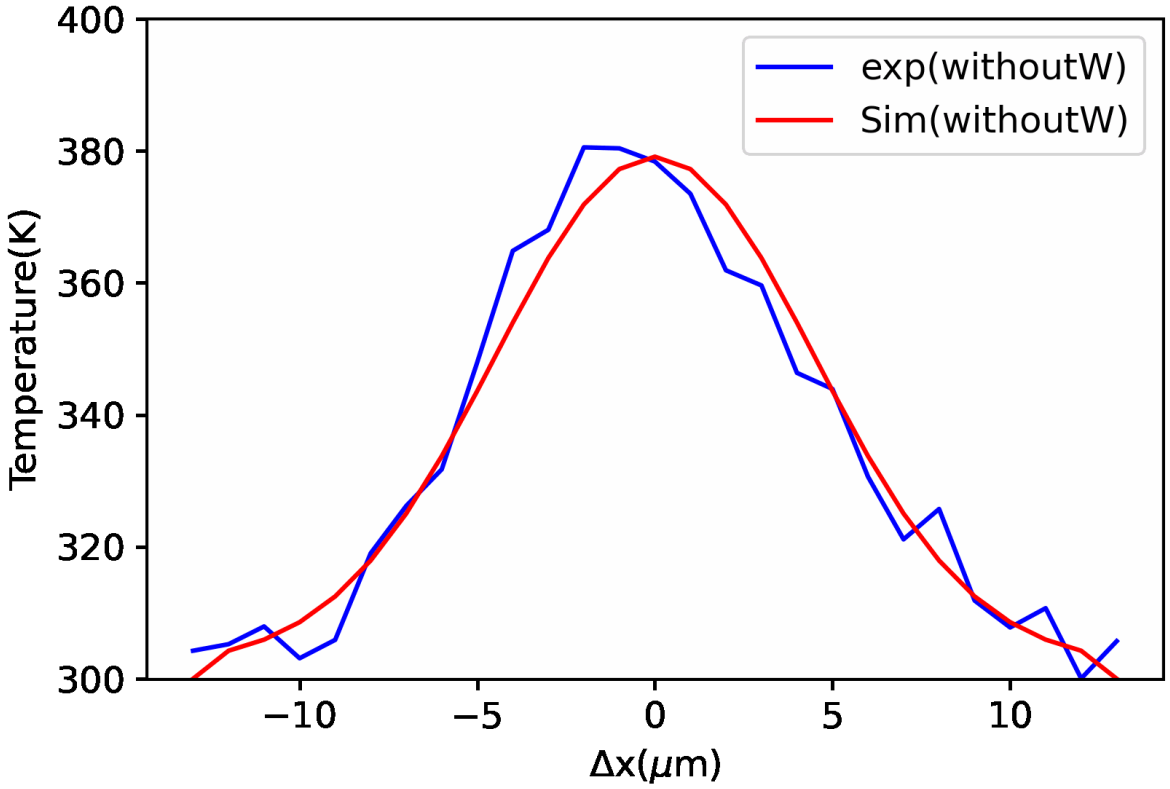

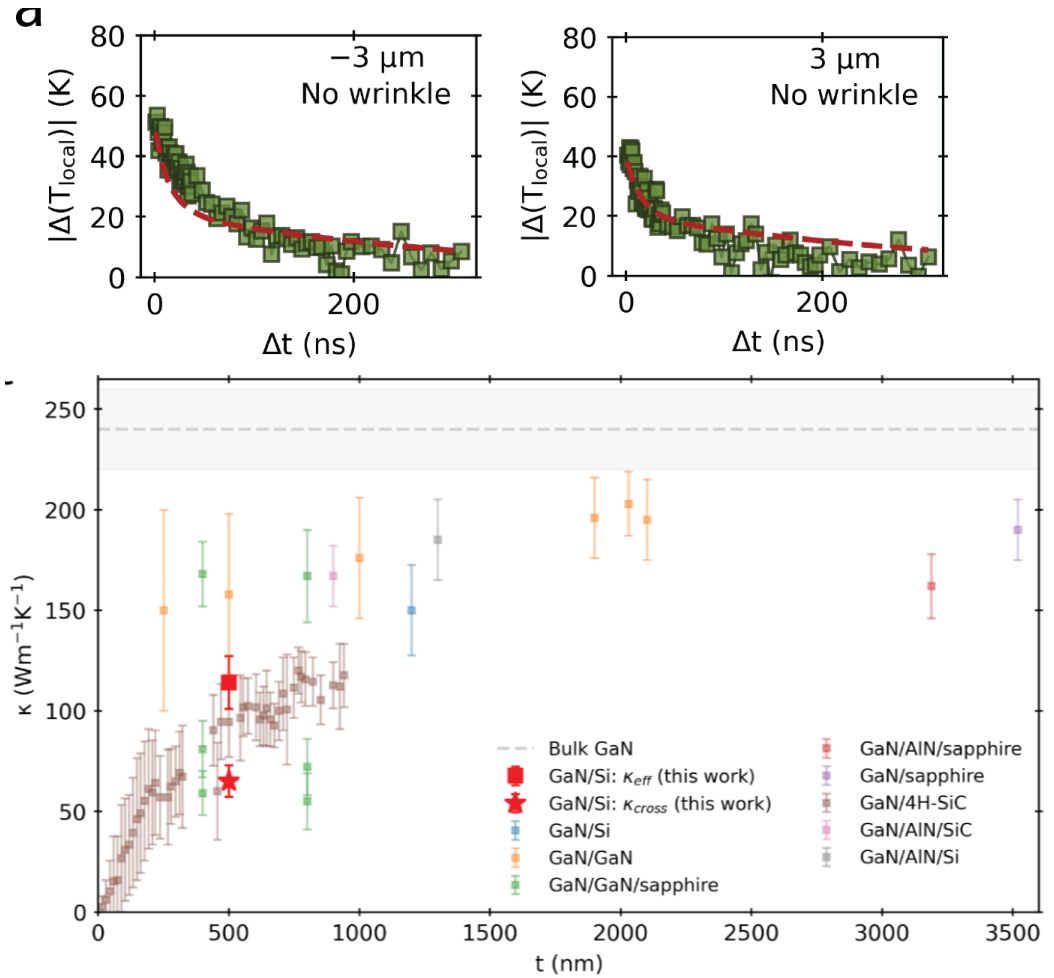

$\kappa = 106.22\mathrm{W/mK}$ While $\kappa_{cross} = 65\mathrm{W/mK}$, $TBC = 2.82 \times 10^{7}\mathrm{W/m^2K}$

Fix cross-plane transport, fit both local κ and TBC to track wrinkle's effect

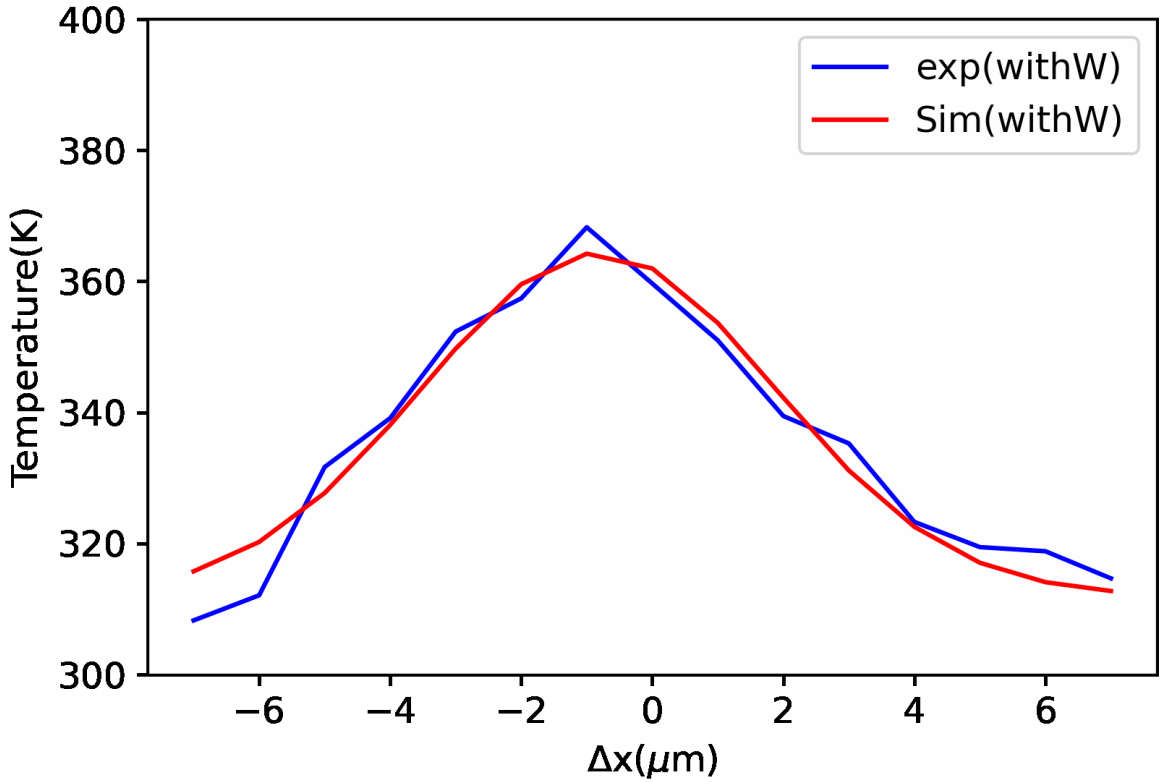

$\kappa = 106.22\text{W/mK}$ While $\kappa_{cross} = 65\ \text{W/mK}$,
$TBC = 2.15 \times 10^7 \text{W/m}^2\text{K}$ $\kappa_w = 21.5\text{W/mK}$

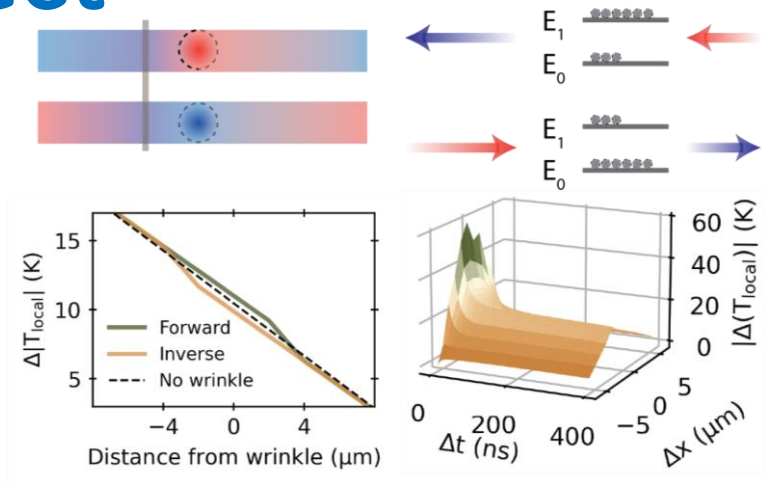

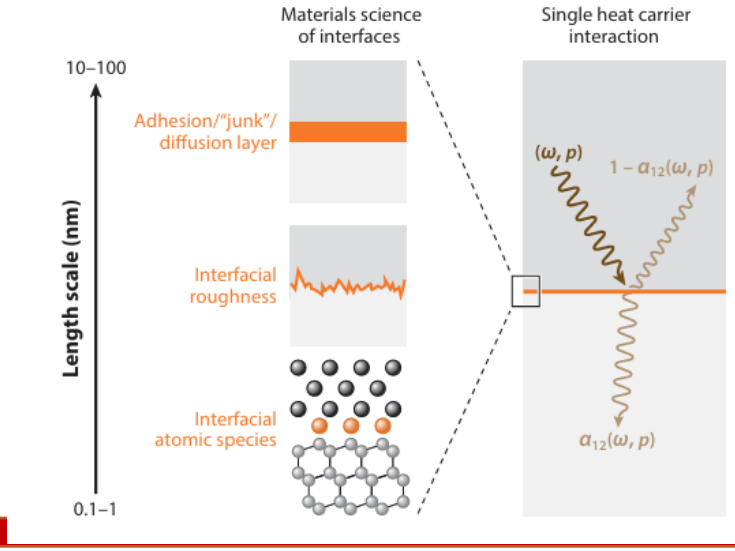

Take-home Message

- Time-resolved X-ray diffraction(TR-XRD) is employed to measure the in-plane thermal conductivity.
- Wrinkle-induced thermal transport is explored with TR-XRD.
- A general comprehensive numerical framework is constructed to resolve the experimental data and for future similar study.

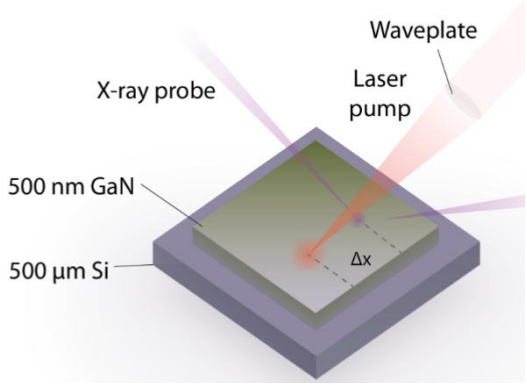

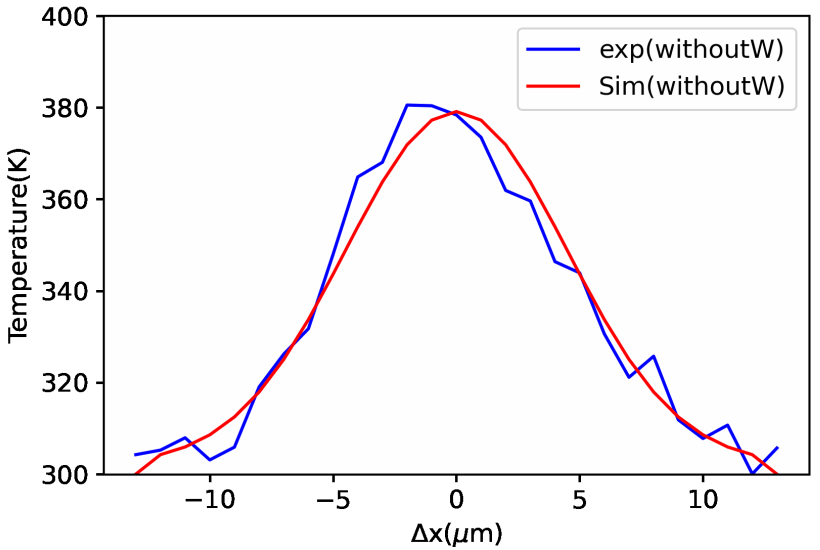

Multi-modality time-resolved measurement and Data-driven inverse problem

- One measurement only give you one perspective, not enough for complex materials behavior.
- while we can manage huge amount of data now, as in the wave of data science.

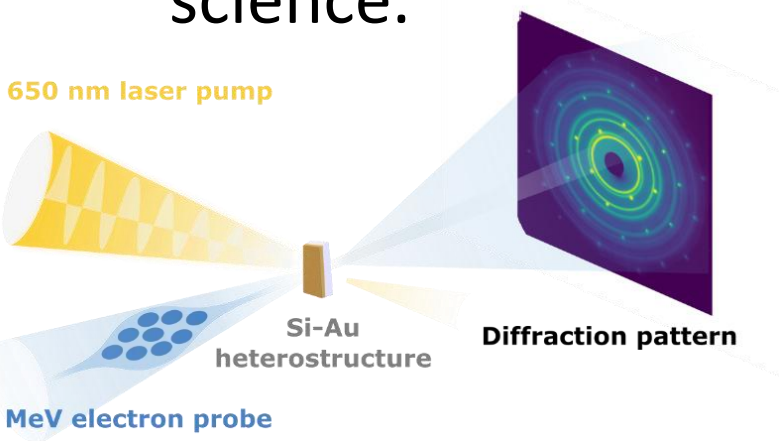

Ultrafast electron scattering

Chen, Zhantao, et al. "Panoramic mapping of phonon transport from ultrafast electron diffraction and scientific machine learning." *Advanced Materials* 35.2 (2023): 2206997.

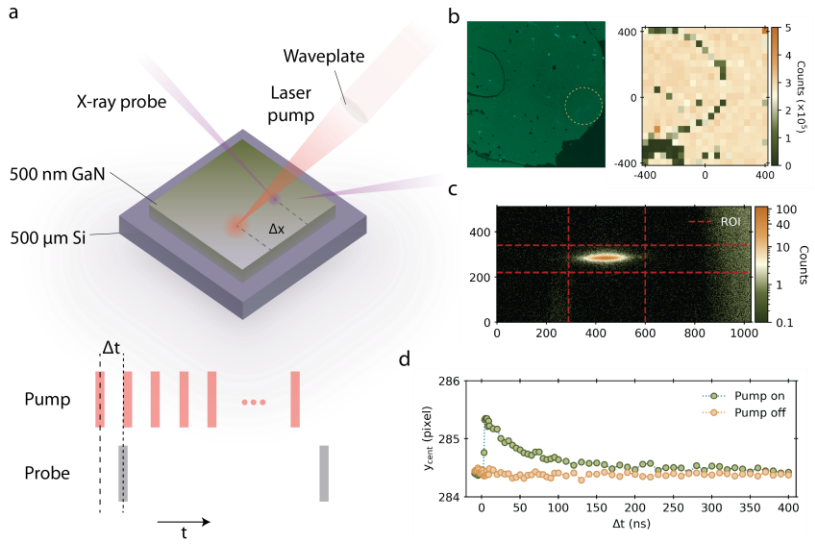

Time-resolved X-ray scattering

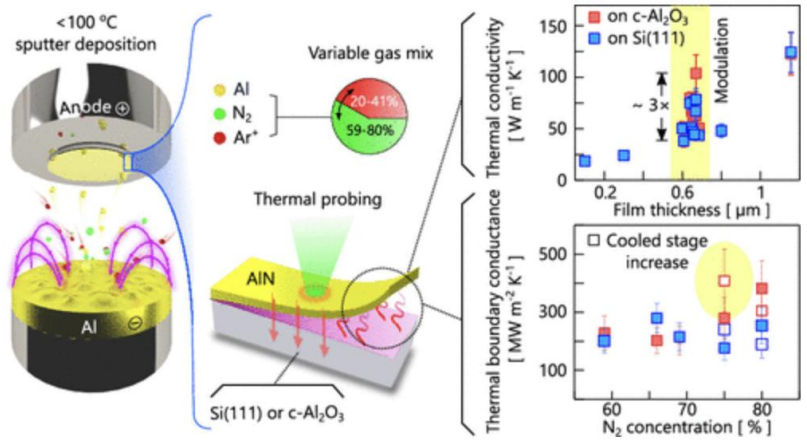

Time-domain thermoreflectance

Outline:

- High entropy alloy, combinatorial disorder
- Cluster based thermodynamics modeling

- Measuring in-plane thermal transport with wrinkle
- Modified diffusion equation

- electron-phonon coupling within doped materials, interplay between disorder and the electron-phonon interaction
- Anomalous Neutron Nuclear-Magnetic Interference Spectroscopy

Electron-Phonon coupling: fundamental interactions of quasiparticles in solids

$$H = H_{\mathrm{el}} + V_{\mathrm{el-el}} + H_{\mathrm{ph}} + H_{\mathrm{el-ph}}.$$

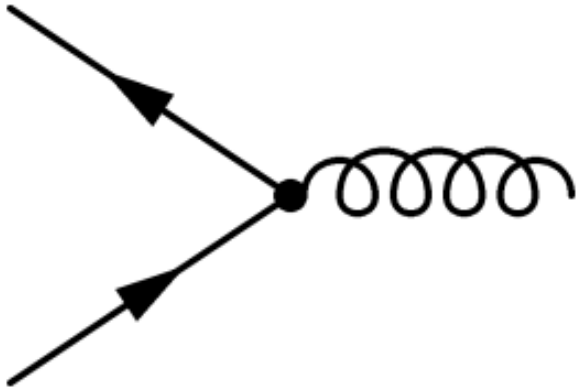

Electron-Phonon coupling: fundamental interactions of quasiparticles in solids

$$H = H_{\mathrm{el}} + V_{\mathrm{el-el}} + H_{\mathrm{ph}} + H_{\mathrm{el-ph}}$$

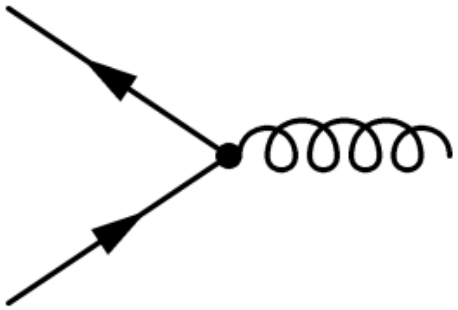

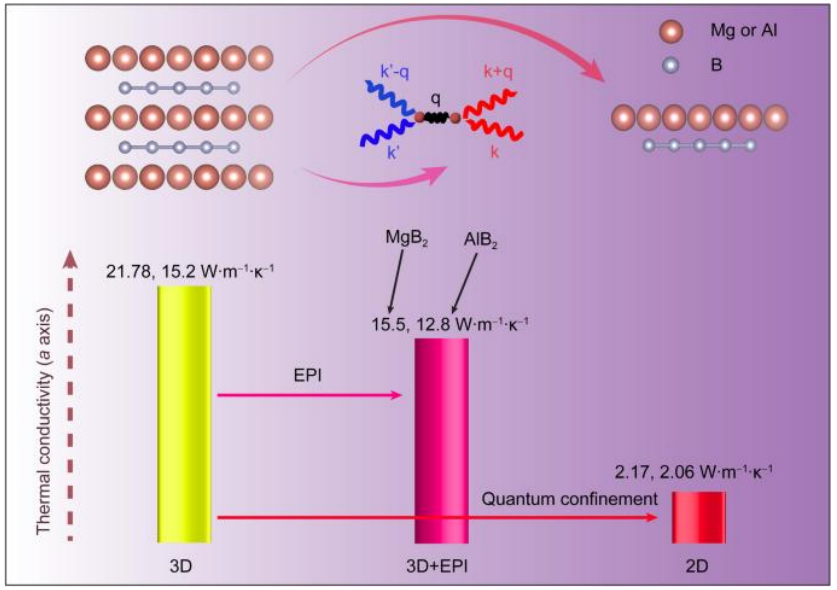

Liu, Sen, et al. "Phonon thermal transport properties of XB2 (X= Mg and Al) compounds: considering quantum confinement and electron–phonon interaction." *Rare Metals* 42.9 (2023): 3064-3074.

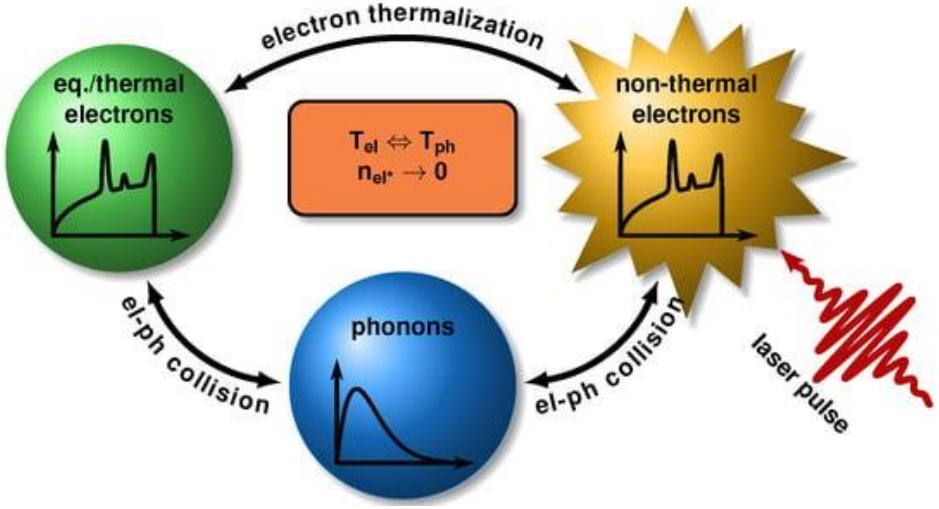

Uehlein, Markus, Sebastian T. Weber, and Baerbel Rethfeld. "Influence of Electronic Non-Equilibrium on Energy Distribution and Dissipation in Aluminum Studied with an Extended Two-Temperature Model." *Nanomaterials* 12.10 (2022): 1655.

Strong electron-phonon coupling and phonon-induced superconductivity in tetragonal C_3N_4 with hole doping

Alexander N. Rudenko,[1,*] Danis I. Badrtdinov,[1] Igor A. Abrikosov,[2] and Mikhail I. Katsnelson[1]
[1]*Radboud University, Institute for Molecules and Materials, Heijendaalseweg 135, 6525AJ Nijmegen, The Netherlands*
[2]*Department of Physics, Chemistry, and Biology (IFM), Linköping University, SE-581 83 Linköping, Sweden*

Interface-enhanced electron-phonon coupling and high-temperature superconductivity in potassium-coated ultrathin FeSe films on $SrTiO_3$

Chenjia Tang,[1] Chong Liu,[1] Guanyu Zhou,[1] Fangsen Li,[1] Hao Ding,[1] Zhi Li,[1] Ding Zhang,[1] Zheng Li,[1] Canli Song,[1,2] Shuaihua Ji,[1,2] Ke He,[1,2] Lili Wang,[1,2,*] Xucun Ma,[1,2] and Qi-Kun Xue[1,2,†]
[1]*State Key Laboratory of Low-Dimensional Quantum Physics, Department of Physics, Tsinghua University, Beijing 100084, People's Republic of China*
[2]*Collaborative Innovation Center of Quantum Matter, Beijing 100084, People's Republic of China*

Ubiquitous strong electron–phonon coupling at the interface of FeSe/$SrTiO_3$

Chaofan Zhang, Zhongkai Liu, Zhuoyu Chen, Yanwu Xie, Ruihua He, Shujie Tang, Junfeng He, Wei Li, Tao Jia, Slavko N. Rebec, Eric Yue Ma, Hao Yan, Makoto Hashimoto, Donghui Lu, Sung-Kwan Mo, Yasuyuki Hikita, Robert G. Moore, Harold Y. Hwang, Dunghai Lee & Zhixun Shen

Nature Communications **8**, Article number: 14468 (2017) | Cite this article

6549 Accesses | **49** Citations | **1** Altmetric | Metrics

How to measure electron-phonon interaction?

The way to measure electron-phonon interaction

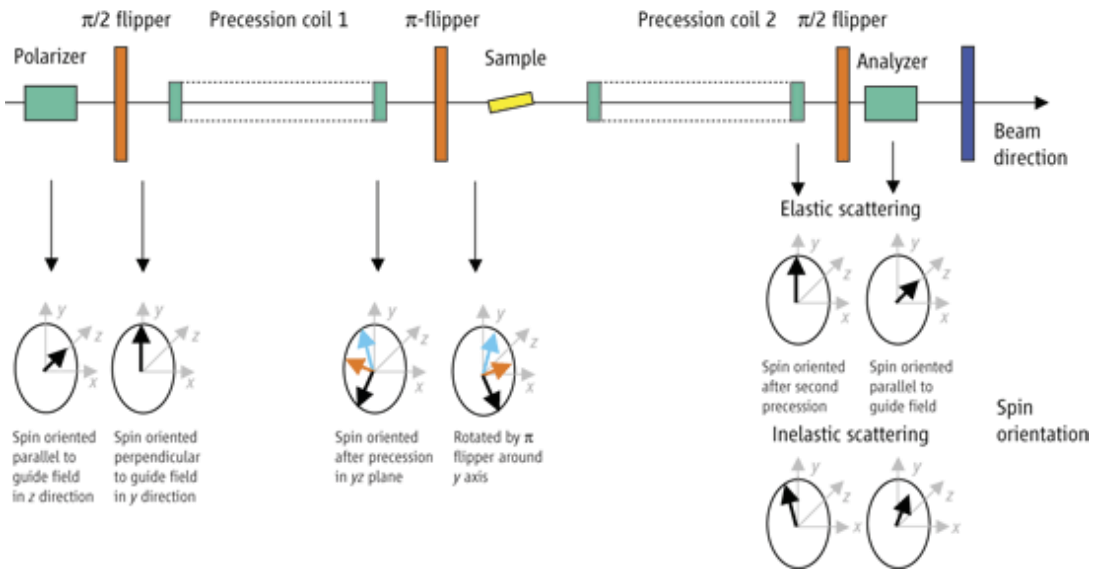

inelastic spin-echo spectroscopy(phonon linewidth)
Difficult to set up; quadratic

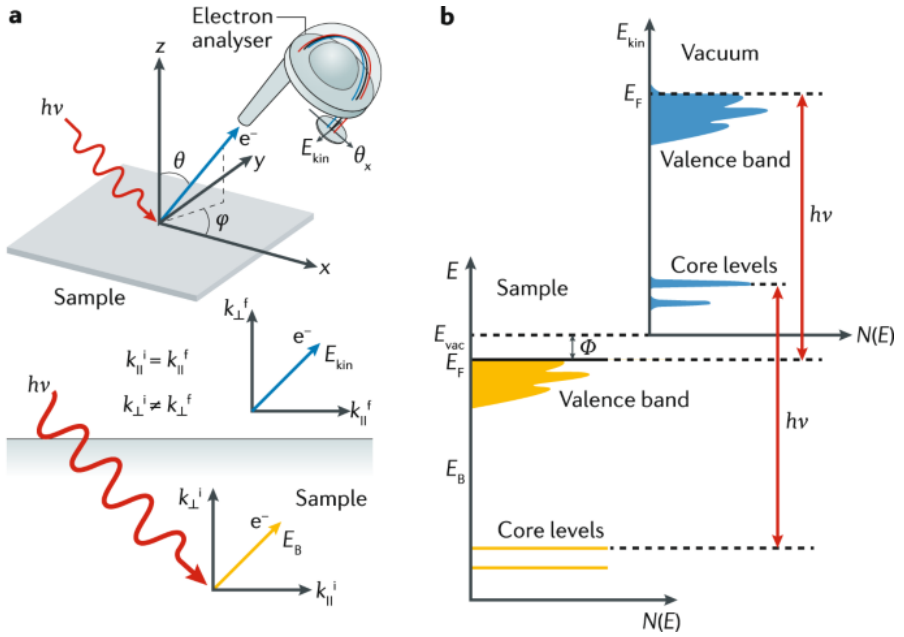

Angle-resolved photoemission spectroscopy(electron wavevector resolved)

Any other method?

- Could be linear dependence?

- Could be phonon wavevector resolved?

Neutron Scattering: Probe Phonon structure and Magnetic structure

- Nuclear Scattering

$$H_{I,\mathrm{nuc}} = \frac{g}{L^3} \sum_{\mathbf{kq}} \Psi^{+}_{N\mathbf{k}+\mathbf{q}} \Psi_{N\mathbf{k}} \rho(\mathbf{q})$$

$$\chi^{R}_{\rho\rho}(\mathbf{q}, t_1 - t_2) = -i\theta(t_1 - t_2)\langle[\rho(\mathbf{q}, t_1), \rho(-\mathbf{q}, t_2)]\rangle_E$$

- Magnetic Scattering

$$H_I = -\frac{2\pi\hbar^2\gamma r_e}{m_N L^3} \sum_{\mathbf{qk}} \Psi^{+}_{N\mathbf{k}+\mathbf{q}} \sigma_N \Psi_{N\mathbf{k}} \cdot \mathbf{M}_{\perp}(\mathbf{q})$$

$$S^{j}_{MM\perp}(\mathbf{q}, E) = \int_{-\infty}^{\infty} \left\langle M^{j}_{\perp}(\mathbf{q}, t)\, M^{j}_{\perp}(-\mathbf{q}, 0) \right\rangle e^{iEt/\hbar} dt$$

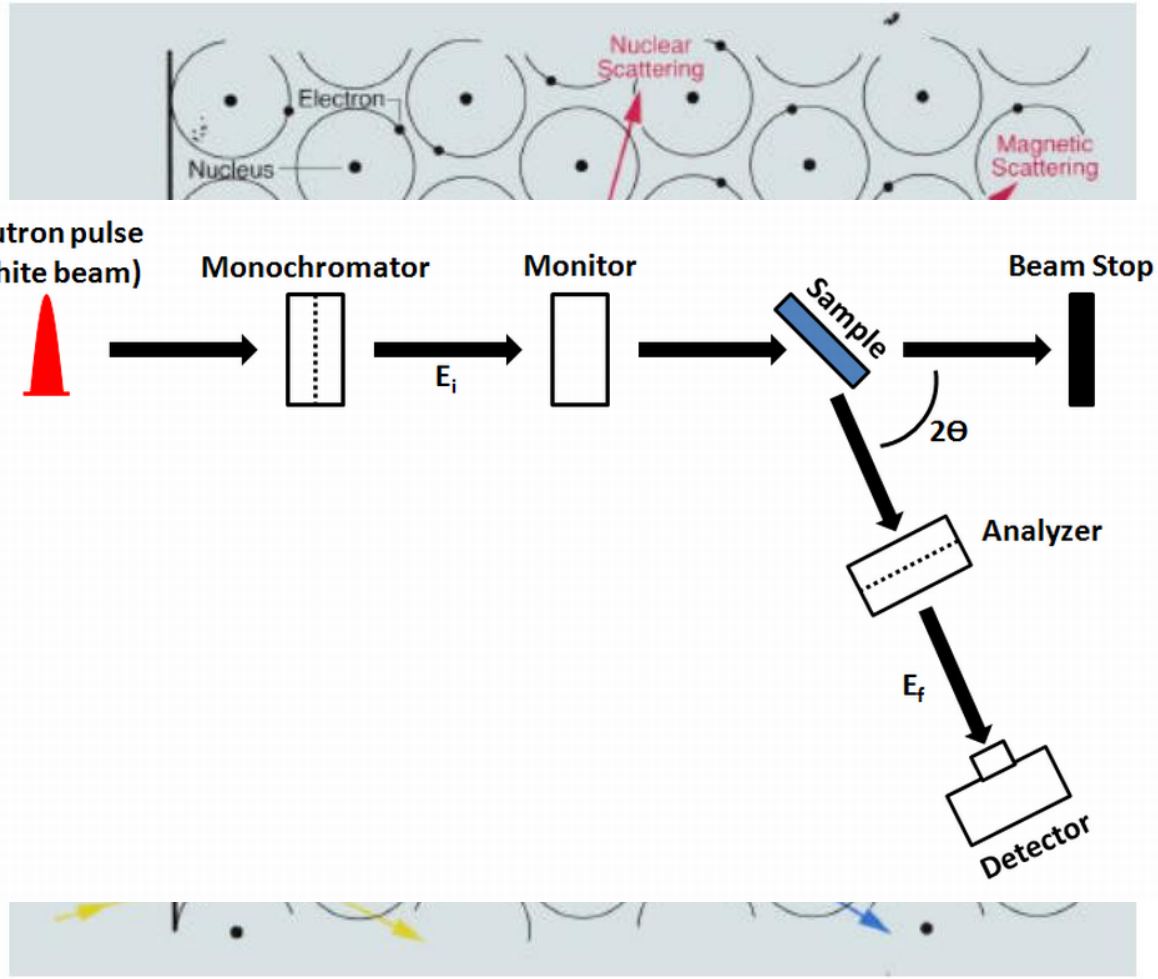

Construction of many-body theory of the neutron scattering

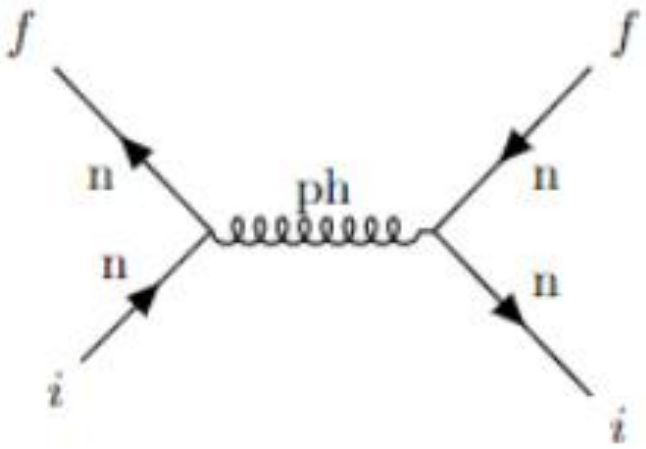

(a) Nuclear-Nuclear scattering

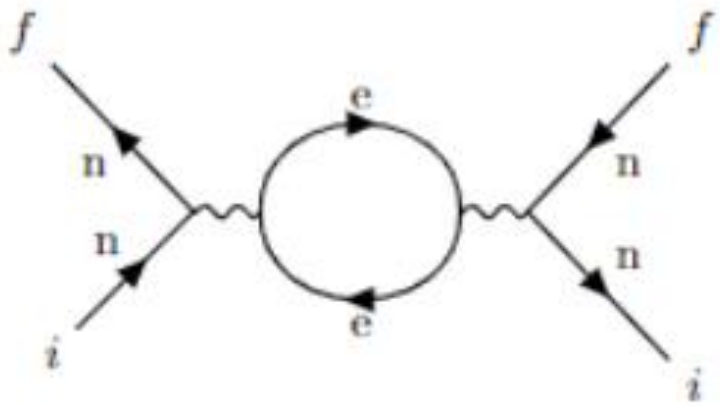

(b) Magnetic-Magnetic scattering

$$H_{I,\mathrm{nuc}} = \frac{g}{L^3}\sum_{\mathbf{kq}} \Psi^{+}_{N\mathbf{k}+\mathbf{q}} \Psi_{N\mathbf{k}} \rho_{\mathbf{q}}$$

$$H_{I,\mathrm{mag}} = -\frac{g\gamma r_e}{L^3}\sum_{\mathbf{qk}} \Psi^{+}_{N\mathbf{k}+\mathbf{q}} \boldsymbol{\sigma}_N \Psi_{N\mathbf{k}} \cdot \mathbf{M}_{\perp\mathbf{q}}$$

Write them together, when they coexist…interference term emerged from the Quadratic Form

When both neutron nuclear interaction $H_{I,\text{nuc}}$ and neutron magnetic interaction $H_{I,\text{mag}}$ co-exist, the total neutron-matter interaction Hamiltonian can be written as

$$S_{\text{tot}}(\mathbf{q},E) = S_{\rho\rho}(\mathbf{q},E) + (\gamma r_e)^2 S_{MM}(\mathbf{q},E) - 2\gamma r_e S_{\text{ano}}(\mathbf{q},E)$$

$$= \underbrace{\begin{pmatrix} S_{\rho\rho,\uparrow\uparrow}(\mathbf{q},E) & 0 \\ 0 & S_{\rho\rho,\downarrow\downarrow}(\mathbf{q},E) \end{pmatrix}}_{\text{nuclear scattering}} + \underbrace{(\gamma r_e)^2 \begin{pmatrix} S_{M^zM^z}(\boldsymbol{q},E) & S_{M^-M^+}(\boldsymbol{q},E) \\ S_{M^+M^-}(\boldsymbol{q},E) & S_{M^zM^z}(\boldsymbol{q},E) \end{pmatrix}}_{\text{magnetic scattering}}$$

$$\underbrace{- 2\gamma r_e \begin{pmatrix} S^z_{\rho M\uparrow}(\mathbf{q},E) & 0 \\ 0 & -S^z_{\rho M\downarrow}(\mathbf{q},E) \end{pmatrix}}_{\text{anomalous scattering}}$$

$$S_{\rho\rho}(\mathbf{q},E)=\begin{pmatrix} S_{\rho\rho,\uparrow\uparrow}(\mathbf{q},E) & 0 \\ 0 & S_{\rho\rho,\downarrow\downarrow}(\mathbf{q},E)\end{pmatrix}$$

$$S_{\rho\rho,\uparrow\uparrow}(\mathbf{q},E)=\int_{-\infty}^{+\infty}\langle\rho_{\mathbf{q}\uparrow}(t)\rho_{-\mathbf{q}\uparrow}(0)\rangle_H\, e^{iEt/h}dt$$

$\boldsymbol{\rho^2}$

$$S_{MM}(\mathbf{q},E)=\begin{pmatrix} S_{M^zM^z}(\boldsymbol{q},E) & S_{M^-M^+}(\boldsymbol{q},E) \\ S_{M^+M^-}(\boldsymbol{q},E) & S_{M^zM^z}(\boldsymbol{q},E)\end{pmatrix}$$

$$S_{M^jM^l}(\mathbf{q},E)=\int_{-\infty}^{\infty}\left\langle M^j_{\mathbf{q}\perp}(t)M^l_{-\mathbf{q}\perp}(0)\right\rangle_H e^{iEt/h}dt$$

$$M^{\pm}=M^x\mp iM^y$$

$$(j,l=+,-,z)$$

$\boldsymbol{M^2}$

$\boldsymbol{(\rho+M)^2}$

$$S_{\text{ano}}\,(\mathbf{q},E)=\begin{pmatrix} S^z_{\rho M\uparrow}(\mathbf{q},E) & 0 \\ 0 & -S^z_{\rho M\downarrow}(\mathbf{q},E)\end{pmatrix}$$

$$S^z_{\rho M\uparrow/\downarrow}(\mathbf{q},E)=\int_{-\infty}^{+\infty}\langle\rho_{\mathbf{q}\uparrow/\downarrow}(t)M^z_{-\mathbf{q}\perp}(0)\rangle_H\, e^{iEt/h}dt$$

$\boldsymbol{\rho M}$

a) We will need polarized neutrons.

b) For spin-non-flip anomalous scattering, it will only detect the **q**-projected magnetization *parallel to* the neutron spin direction (*z* direction, $\mathbf{m}^z_{\perp}(\mathbf{q})$).

$$S_{\text{ano}}(\mathbf{q}, E) = \begin{pmatrix} S^z_{\rho M\uparrow}(\mathbf{q}, E) & 0 \\ 0 & -S^z_{\rho M\downarrow}(\mathbf{q}, E) \end{pmatrix}$$

$$S^z_{\rho M\uparrow/\downarrow}(\mathbf{q}, E) = \int_{-\infty}^{+\infty} \left\langle \rho_{\mathbf{q}\uparrow/\downarrow}(t) M^z_{-\mathbf{q}\perp}(0) \right\rangle_H e^{iEt/h} dt$$

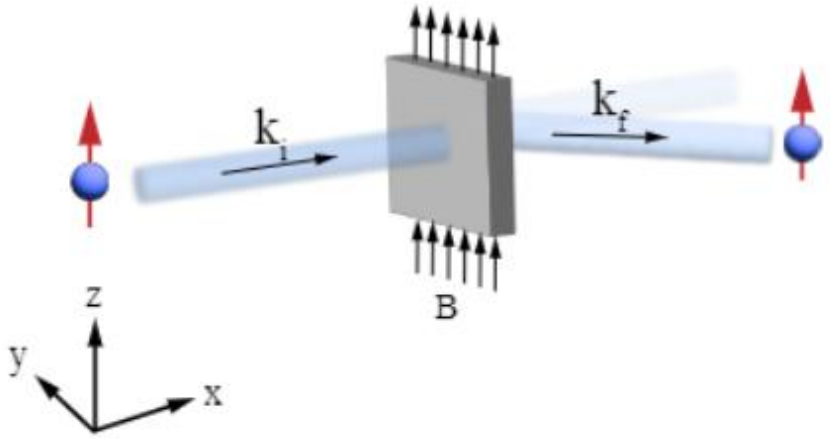

a) We will need polarized neutrons.

b) For spin-non-flip anomalous scattering, it will only detect the **q**-projected magnetization *parallel to* the neutron spin direction (*z* direction, $\mathbf{m}^z_\perp(\mathbf{q})$).

interference term exists somewhere before…

9. Nuclear – magnetic interference in elastic scattering

We discuss here some of the results from magnetic studies using the interference of nuclear and magnetic scattering (see also Section 10). Since the magnetic scattering amplitude is proportional to the neutron spin, the cross section of polarized neutrons has an interference contribution, which can lead to a scattering-induced polarization and its rotation.

Maleev, Sergei V. "Polarized neutron scattering in magnets." *Physics-Uspekhi* 45.6 (2002): 569.

Nuclear–magnetic interference

Finally, let us mention the possibility that magnetic and nuclear scattering occurs in the same Bragg reflection. Examples of this are $\mathbf{q} = 0$ magnetic structures, and structures with $\mathbf{q} \neq 0$ in which magnetic order is coupled to a structural distortion with the same $\mathbf{q}$. In such cases, nuclear–magnetic interference can occur, and SNP can determine the relationship between the amplitudes and phases of the magnetic and nuclear scattering. If a model for the nuclear structure factors is available then it is possible to determine the size of the ordered moments by SNP, without the need for additional intensity measurements.

Boothroyd, Andrew T. *Principles of neutron scattering from condensed matter*. Oxford University Press, 2020.

$$P_f\sigma_{\text{total}} = \boldsymbol{P}_i(N^*N - \boldsymbol{M}_\perp^* \cdot \boldsymbol{M}_\perp) + (\boldsymbol{P}_i \cdot \boldsymbol{M}_\perp)\boldsymbol{M}_\perp^* + (\boldsymbol{P}_i \cdot \boldsymbol{M}_\perp^*)\boldsymbol{M}_\perp + \mathrm{i}\boldsymbol{P}_i \times (N\boldsymbol{M}_\perp^* - N^*\boldsymbol{M}_\perp) + (N\boldsymbol{M}_\perp^* + N^*\boldsymbol{M}_\perp) - \mathrm{i}(\boldsymbol{M}_\perp^* \times \boldsymbol{M}_\perp) \quad , \tag{3b}$$

$$\boldsymbol{M}_\perp = (\boldsymbol{Q} \times \boldsymbol{M} \times \boldsymbol{Q})/|Q|^2 \quad . \tag{3c}$$

化。(3)式定义了所有与极化中子散射相关的信息，并将散射分为了四大类：核散射 N^*N 、非手性磁散射 $\boldsymbol{M}_\perp^* \cdot \boldsymbol{M}_\perp$ 、核磁相干散射 $N\boldsymbol{M}_\perp^* + N^*\boldsymbol{M}_\perp$ ，以及手性磁散射 $\boldsymbol{M}_\perp^* \times \boldsymbol{M}_\perp$ 。在这一理论基础上，极化中子实验得以依据所探测样品的特性选择适合的极化中子实验方法，并对实验结果进行有效的分析。

tion analysis)。完全极化分析可以作为一种极化调控手段安装在单晶衍射谱仪[25]上或三轴散射谱仪[11]上，测量核磁相干散射及手性磁性散射信号。这其中，核磁相干散射揭示了磁性系统中电子轨道、电荷扰动和晶格扭曲效应的相互竞争，因此在研究量子材料这一热门学科时具有决定性的作

Xin, T. O. N. G. "Polarized neutron techniques." *Physics* 49.11 (2020): 765-773.

Mathematical observation: the electron-phonon coupling emerged from the interference term

$$\chi^{j}_{\rho M}(\mathbf{q},\tau_1-\tau_2)\approx \mathrm{T}_\tau\int_0^\beta d\tau\sum_{l=1}^{N} b_l e^{-i\mathbf{q}\cdot\mathbf{R}_l^0}\left\langle \hat{H}_{\text{e-ph}}(\tau)(-i)\mathbf{q}\cdot\hat{\mathbf{u}}_l(\tau_1)\hat{M}^{j}_{-\mathbf{q}\perp}(\tau_2)\right\rangle_{H_0}$$

$$=\frac{N^{1/2}}{V}\int_0^\beta d\tau\sum_{l=1}^{N} b_l e^{-i\mathbf{q}\cdot\mathbf{R}_l^0}\mathrm{T}_\tau\left\langle \begin{array}{l}\sum\limits_{\mathbf{k}'\mathbf{q}'\sigma} g_{\mathbf{q}'}c^{+}_{\mathbf{k}'+\mathbf{q}'\sigma}(\tau)c_{\mathbf{k}'\sigma}(\tau)\left(a_{\mathbf{q}'}(\tau)+a^{+}_{-\mathbf{q}'}(\tau)\right)\\ \times\sum\limits_{\mathbf{q}''}\sqrt{\dfrac{\hbar}{2MN\omega_{\mathbf{q}''}}}\left(a_{\mathbf{q}''}(\tau_1)+a^{+}_{-\mathbf{q}''}(\tau_1)\right)e^{i\mathbf{q}''\cdot\mathbf{R}_l^0}\left(-i\mathbf{q}\cdot\varepsilon_{\mathbf{q}''}\right)\\ \times\sum\limits_{\mathbf{k}''\sigma'\sigma''} c^{+}_{\mathbf{k}''\sigma'}(\tau_2)\mathbf{m}^{j}_{\perp\sigma'\sigma''}(-\mathbf{q})c_{\mathbf{k}''-\mathbf{q}\sigma''}(\tau_2)\end{array}\right\rangle_{H_0}$$

$$=\frac{1}{V}\int_0^\beta d\tau\sum_{l=1}^{N} b_l \sum_{\substack{\mathbf{k}'\mathbf{q}'\sigma\\ \mathbf{q}''\mathbf{k}''\sigma'\sigma''}} g_{\mathbf{q}'}\sqrt{\frac{\hbar}{2M\omega_{\mathbf{q}''}}}e^{-i\mathbf{q}\cdot\mathbf{R}_l^0}e^{i\mathbf{q}''\cdot\mathbf{R}_l^0}\left(-i\mathbf{q}\cdot\varepsilon_{\mathbf{q}''}\right)\mathbf{m}^{j}_{\perp\sigma'\sigma''}(-\mathbf{q})$$
$$\times\mathrm{T}_\tau\left\langle c^{+}_{\mathbf{k}'+\mathbf{q}'\sigma}(\tau)c_{\mathbf{k}'\sigma}(\tau)c^{+}_{\mathbf{k}''\sigma'}(\tau_2)c_{\mathbf{k}''-\mathbf{q}\sigma''}(\tau_2)\right\rangle_0\left\langle\left(a_{\mathbf{q}'}(\tau)+a^{+}_{-\mathbf{q}'}(\tau)\right)\left(a_{\mathbf{q}''}(\tau_1)+a^{+}_{-\mathbf{q}''}(\tau_1)\right)\right\rangle_0$$

electron spin degrees of freedom

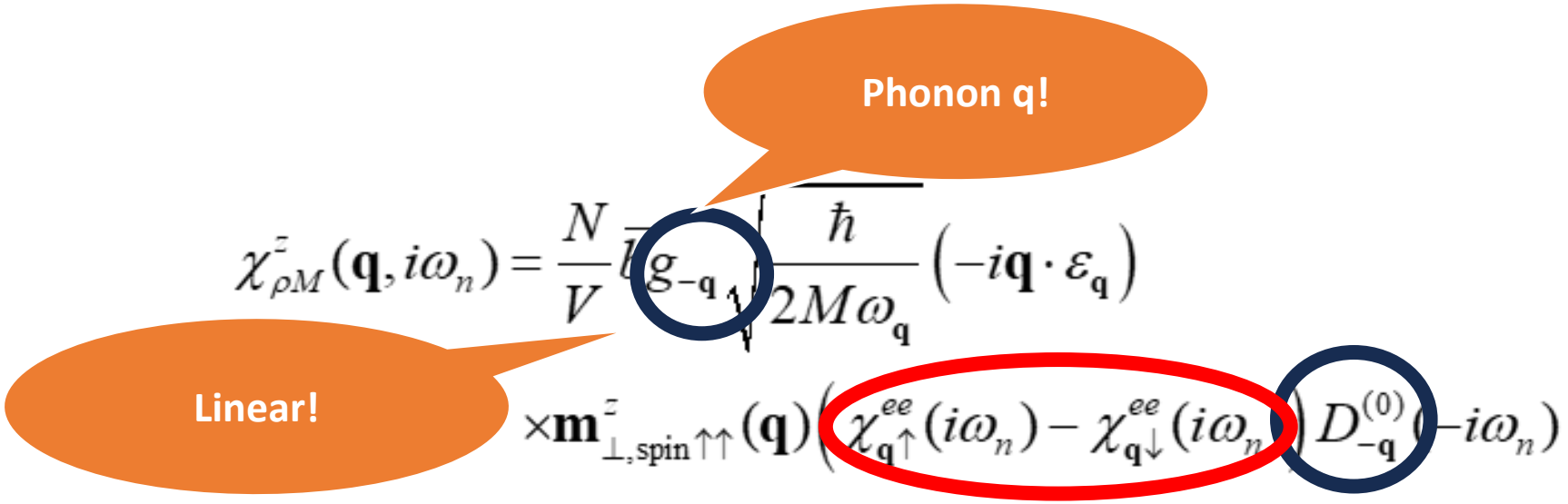

Numerical results

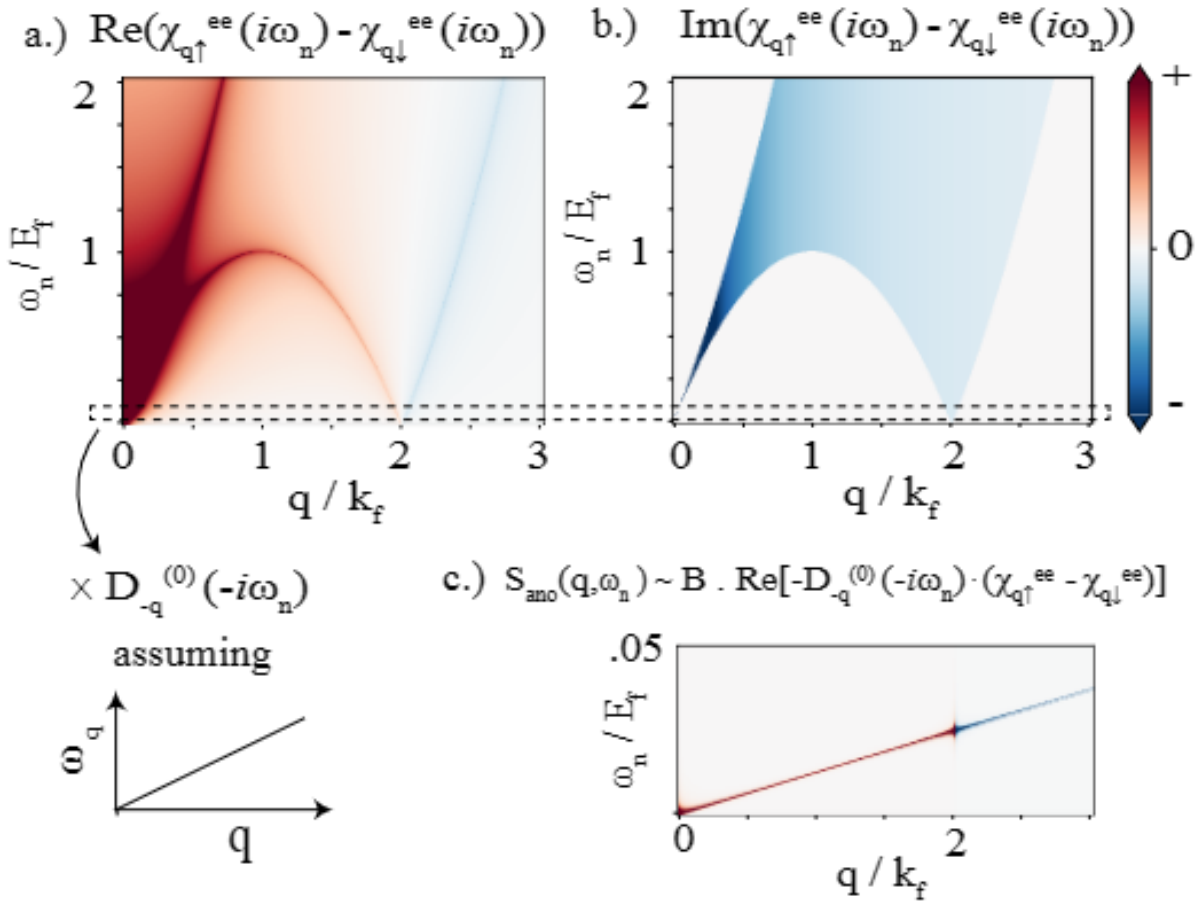

$$\chi^z_{\rho M}(\mathbf{q}, i\omega_n) = N\bar{b} g_{-\mathbf{q}} \sqrt{\frac{\hbar}{2M\omega_{\mathbf{q}}}} (-i\mathbf{q}\cdot\varepsilon_{\mathbf{q}}) D^{(0)}_{-\mathbf{q}}(-i\omega_n) \times \frac{m_e^2}{q\pi^2\hbar^4} \ln\left|\frac{q+2k_F}{q-2k_F}\right| \mu_B B_z$$

If we consider the Thomas-Fermi dielectric function, to estimate signal strength estimation

$$\frac{I_{ANUBIS}}{I_{phonon}} = \frac{2\gamma r_e S^j_{\rho M}}{S_{\rho\rho}}$$

$$\left(\frac{1}{\varepsilon_{\uparrow}(\mathbf{q}, i\omega_n)} - \frac{1}{\varepsilon_{\downarrow}(\mathbf{q}, i\omega_n)} \right) = \frac{4\pi a_0 q^2 k_F \mu_B B_z}{\left(\pi a_0 q^2 + 4k_F\right)^2 \varepsilon_F}$$

Materials	Parameters	Signal strength
Cu(fcc)	$Z = 29$, $\varepsilon_F = 7eV$, $\bar{b} \approx 7.718fm$	2.585×10^{-4}
Ag(fcc)	$Z = 47$, $\varepsilon_F = 5.49eV$, $\bar{b} \approx 5.922fm$	7.405×10^{-4}
Au(bcc)	$Z = 79$, $\varepsilon_F = 5.53eV$, $\bar{b} \approx 7.63fm$	9.574×10^{-4}
Nb(bcc)	$Z = 41$, $\varepsilon_F = 5.32eV$, $\bar{b} \approx 7.054fm$	5.639×10^{-4}
Mg(hcp)	$Z = 12$, $\varepsilon_F = 7.08eV$, $\bar{b} \approx 5.375fm$	1.514×10^{-4}
Tl(hcp)	$Z = 81$, $\varepsilon_F = 8.15eV$, $\bar{b} \approx 8.776fm$	5.233×10^{-4}
Sn(bct)	$Z = 50$, $\varepsilon_F = 10.2eV$, $\bar{b} \approx 6.225fm$	3.411×10^{-4}
Ga(orthorhombic)	$Z = 31$, $\varepsilon_F = 10.4eV$, $\bar{b} \approx 7.288fm$	1.762×10^{-4}
Sb(rhombohedral)	$Z = 51$, $\varepsilon_F = 10.9eV$, $\bar{b} \approx 5.57fm$	3.567×10^{-4}

TABLE I. The table of order-of-magnitude w.r.t. phonon scattering for several common metal systems.

Initial experimental data, Nb

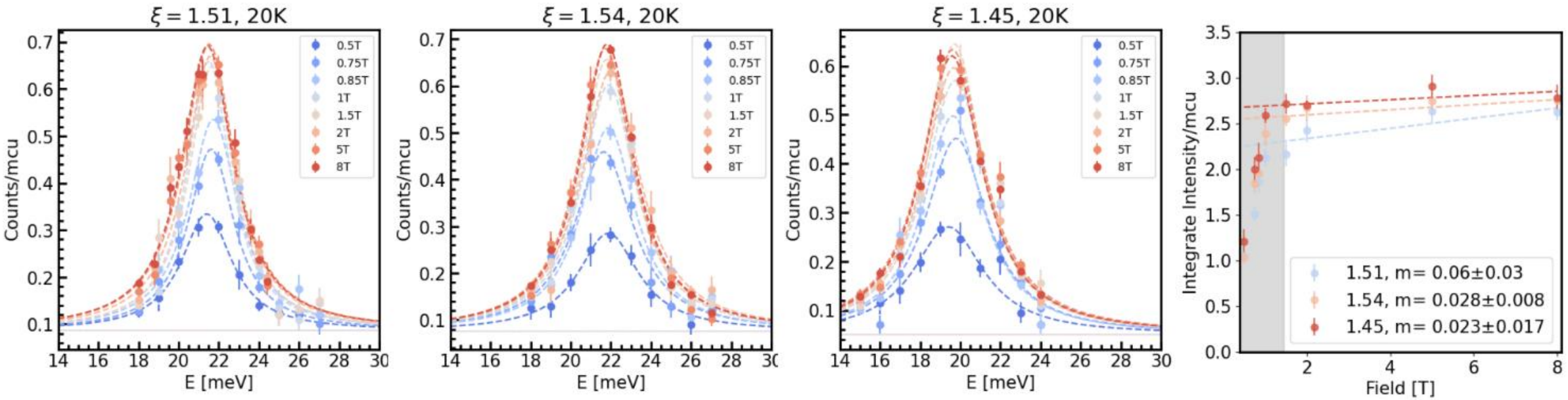

Future Benefits:

- Make electron-phonon coupling accessible through the future neutron facility.
- Combine with the advanced in-situ technique and time-resolved technique.

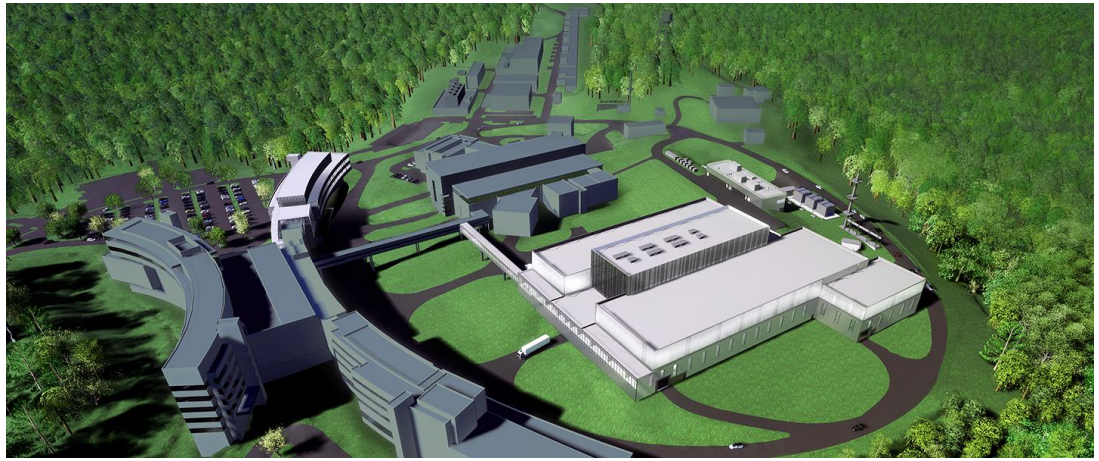

https://neutrons.ornl.gov/sts

Take-home message

- Deeply observe the interference term between neutron nuclear-nuclear scattering and magnetic-magnetic scattering, which is usually ignored.

$$S_{\text{ano}}(\mathbf{q}, E) = \begin{pmatrix} S^z_{\rho M\uparrow}(\mathbf{q}, E) & 0 \\ 0 & -S^z_{\rho M\downarrow}(\mathbf{q}, E) \end{pmatrix}$$

$$S^z_{\rho M\uparrow/\downarrow}(\mathbf{q}, E) = \int_{-\infty}^{+\infty} \left\langle \rho_{\mathbf{q}\uparrow/\downarrow}(t) M^z_{-\mathbf{q}\perp}(0) \right\rangle_H e^{iEt/\hbar} dt$$

- Propose the configuration to measure the electron-phonon coupling through the polarized neutron scattering.

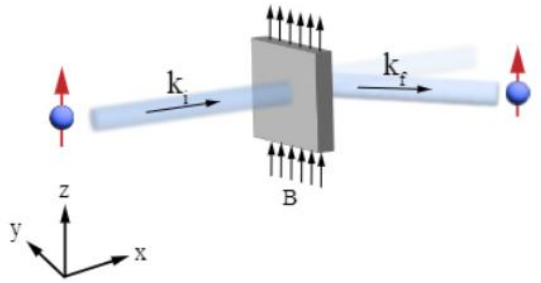

Similar work in filling the gap between experiments and theory

- Thickness-dependent Polaron crossover, Raman spectroscopy

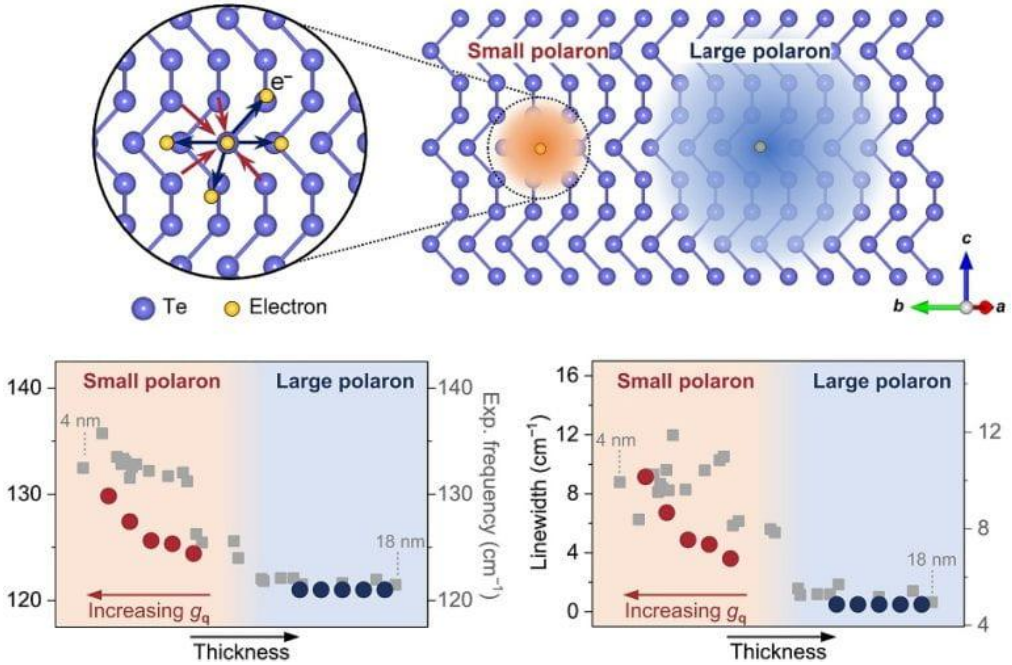

K Zhang†, C Fu†, S Kelly, L Liang, SH Kang, J Jiang, R Zhang, Y Wang, G Wan, P Siriviboon, M Yoon, P Ye, W Wu, M Li*, S Huang*, "Thickness-Dependent Polaron Crossover in Tellurene," Science Advances **11**, eads4763 (2025).

- Embedded Quantum dots, Photoluminescence Spectroscopy

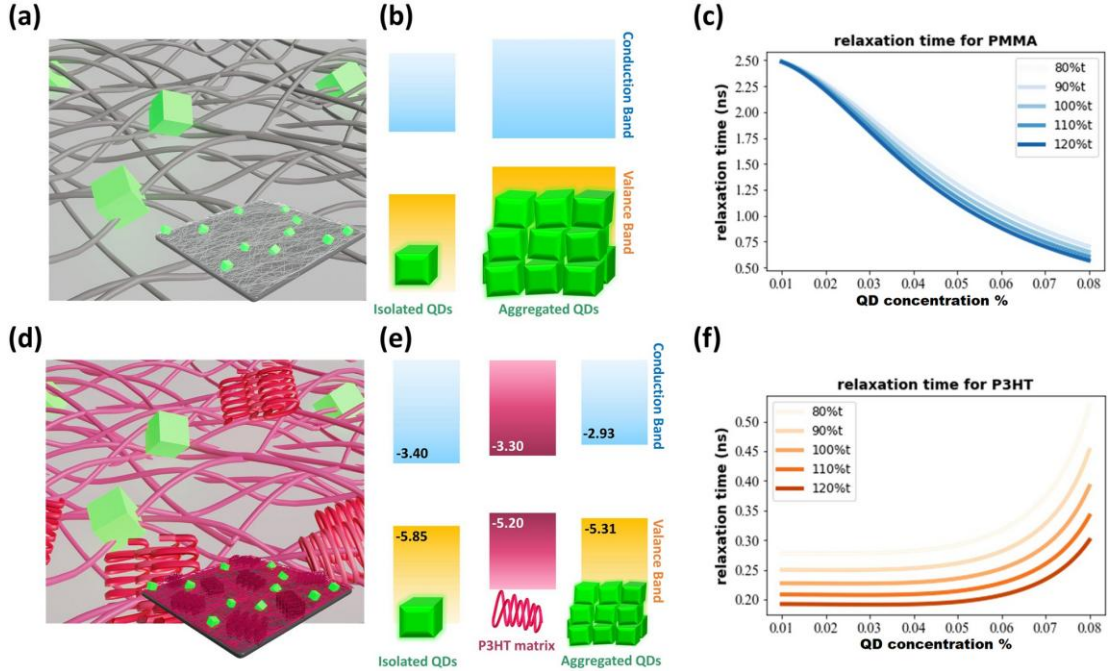

M-C Wu*, K-C Hsiao, C Fu, T-H Lin, Y-H Chang, Y-C Huang, M-P Nieh, W-F Su and M Li*, "Giant, non-perturbative tuning of light-matter interaction of embedded quantum dots in semiconducting matrices," Advanced Composites and Hybrid Materials **8**, 281 (2025).

Similar theoretical characterization design

- Quantum Theory of X-ray Photon Correlation Spectroscopy:

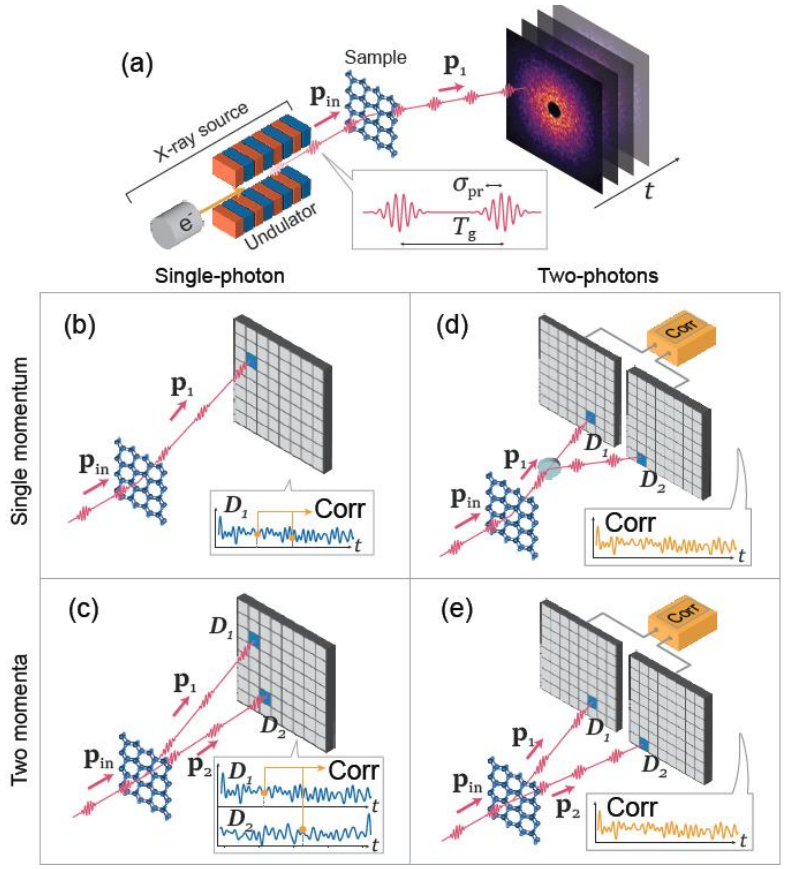

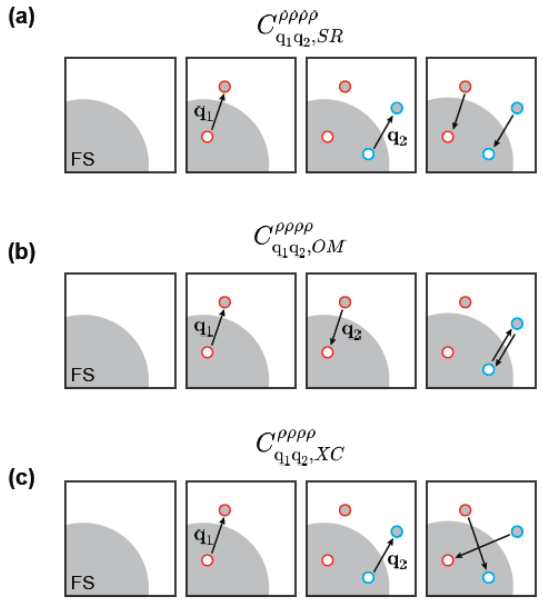

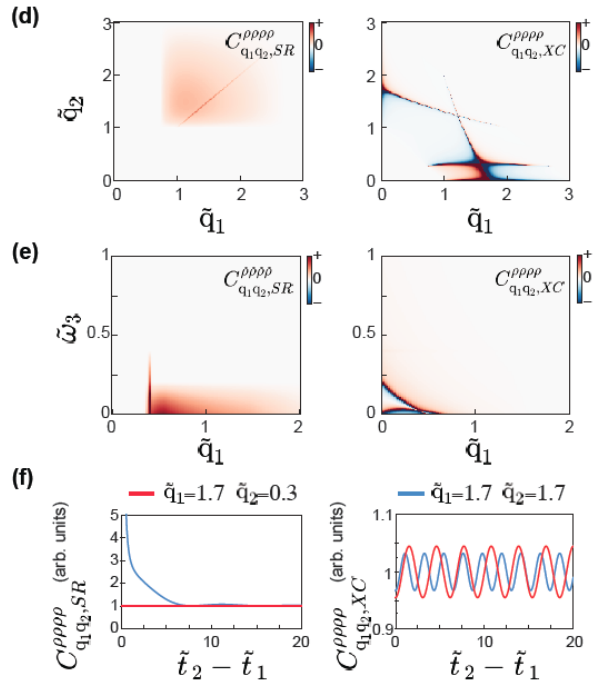

Combined Machine learning into resolving spectroscopy measurements with defects

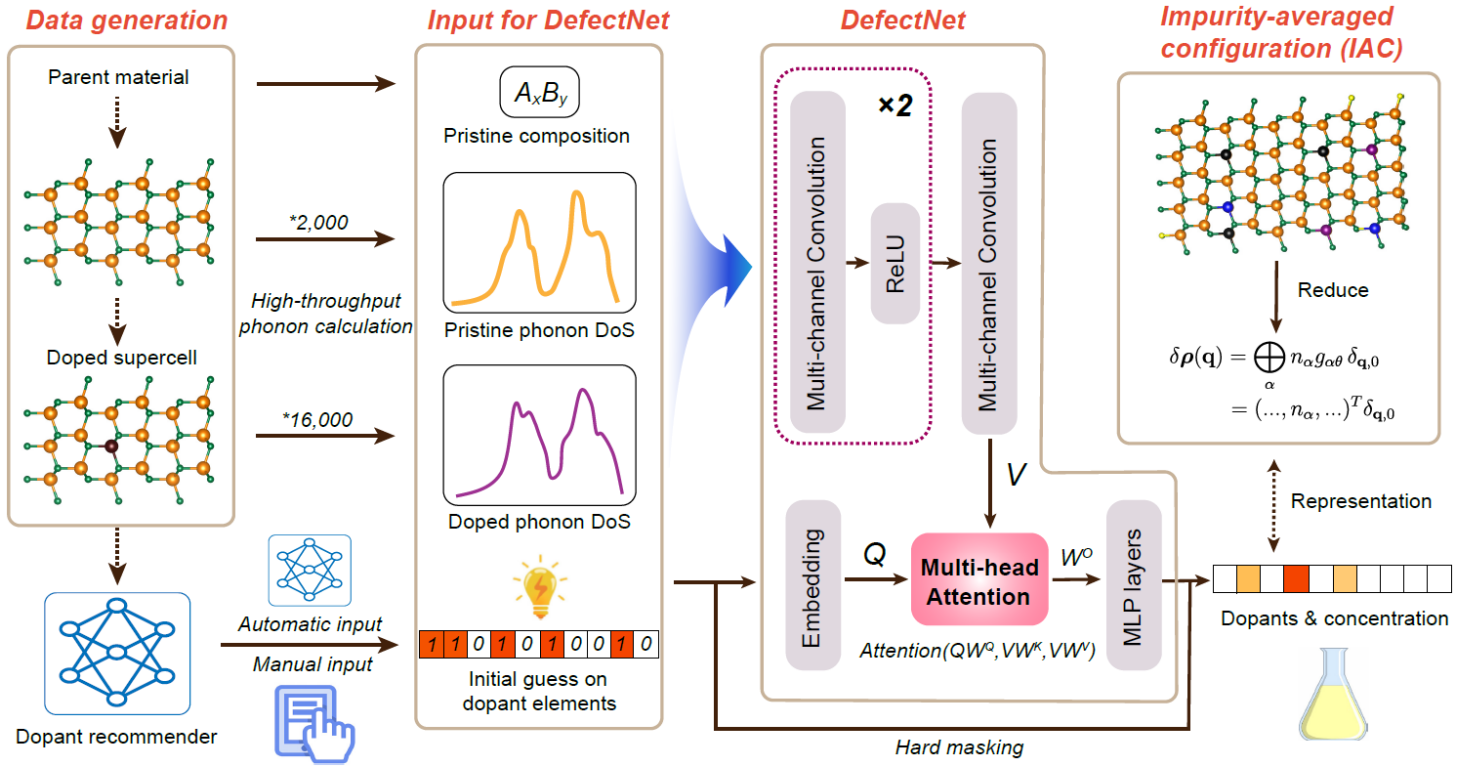

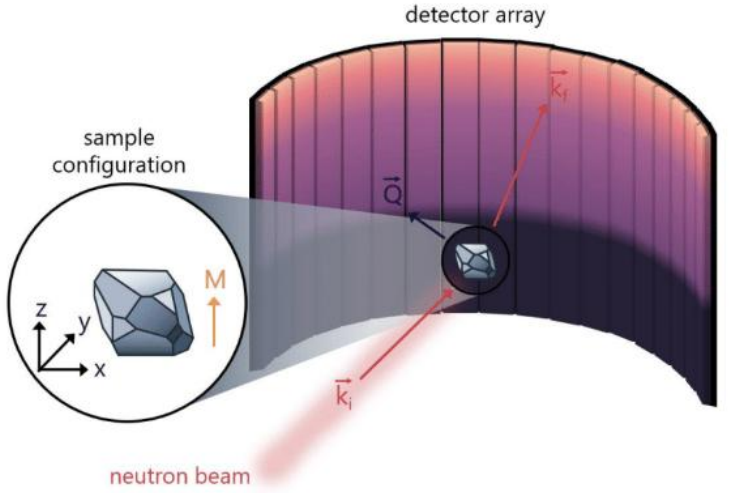

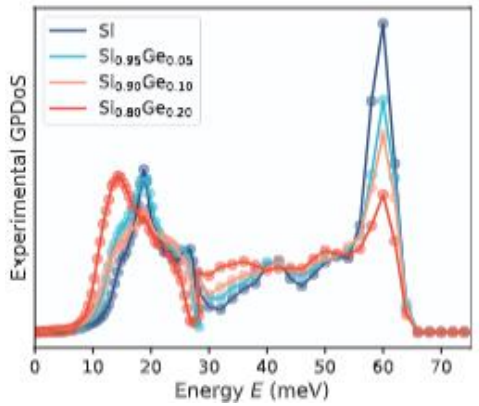

M Cheng*†, C Fu†, B Yu†, E Rha, A Chotrattanapituk, DL Abernathy, YQ Cheng and M Li*, "A Foundation Model for Non-Destructive Defect Identification from Vibrational Spectra," arXiv:2506.00725, submitted.

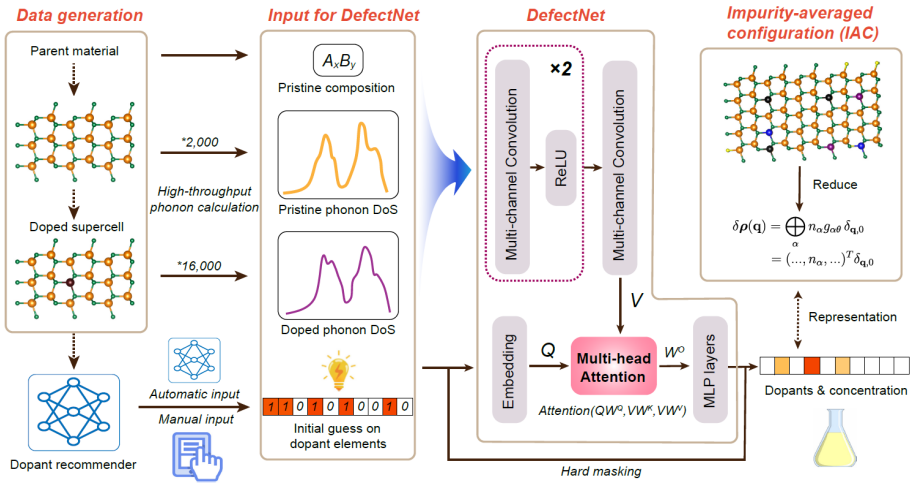

Learning Defect Engineering

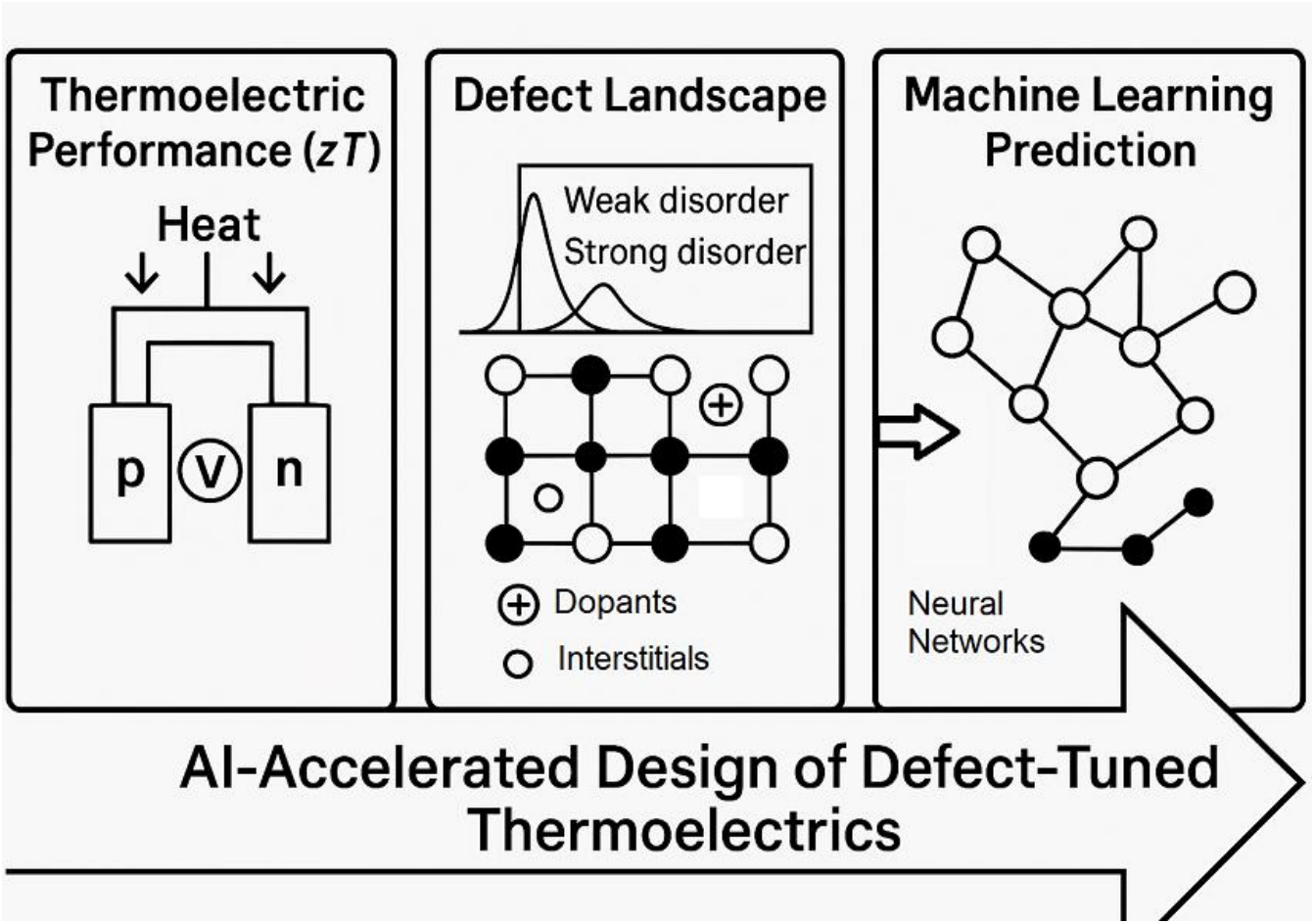

Summary: three-level expansion to characterize delicacy with the “imperfection”

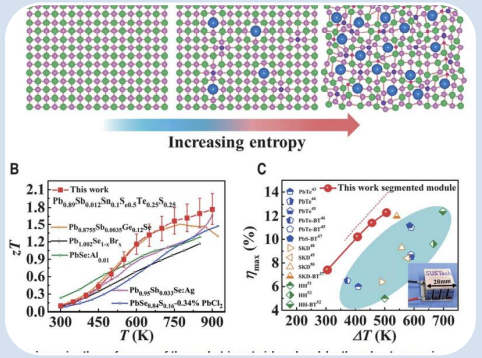

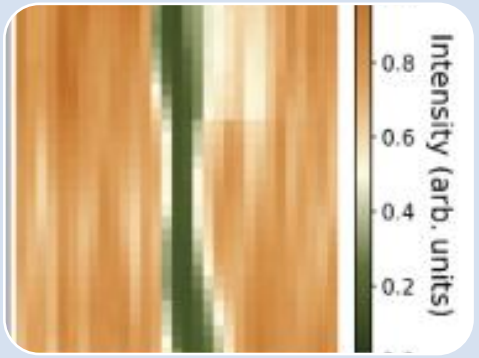

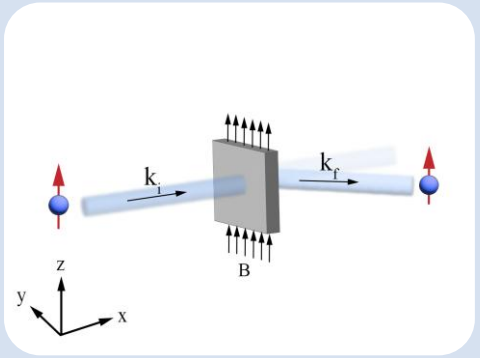

cluster-based model for fitting data in CALPHAD

Configurational disorder

Statistical method with FYL-transform

In-plane thermal conductivity measurement

Wrinkle

Simulate Singularity and TBC in conduction Eq.

Measurement of the electron-phonon coupling

Electron-phonon coupling

Interference term in N-B

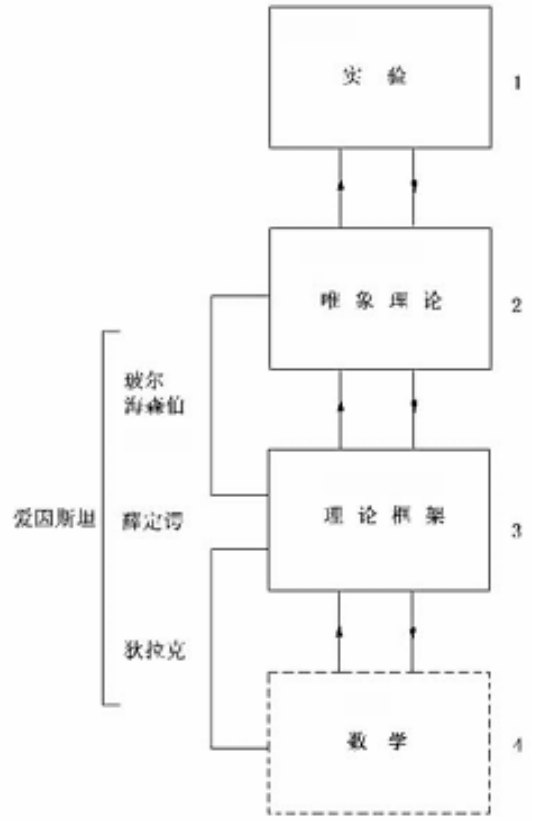

杨振宁. "美与物理学." *物理* 31.04 (2002): 0-0.

One More Thing……

未来? Push to the extreme?

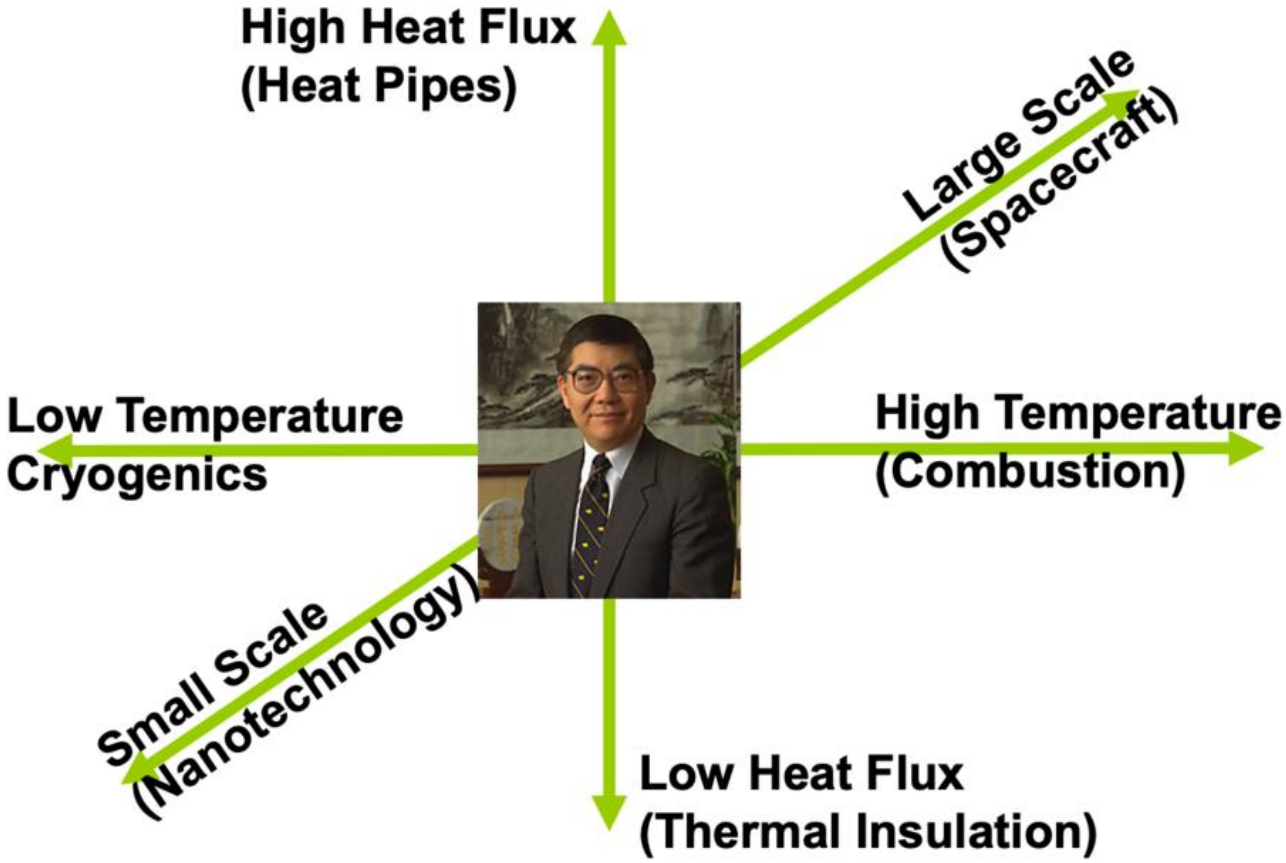

未来? Push to the extreme?

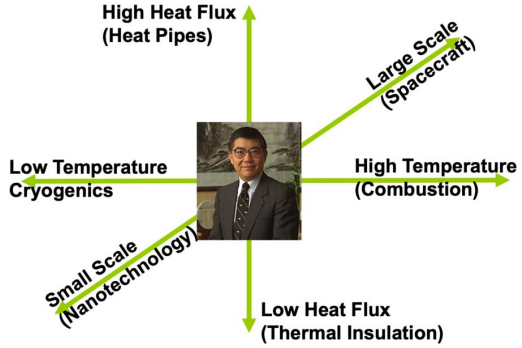

- Push equilibrium thermodynamics to the case with (charge) defects/ionic system
  - nanoscale phase stability or highly defected structure.
  - Interface/grain boundary (phase) stability and the condition.
  - Ionic system's thermodynamics modeling.

- Extend to the long-time scale simulation
  - Any new method can be developed in long-time scale? Rare event? Revive PPM in some way(add spatial information?)?

- Push transport onto real interface
  - Thermal/electrical transport on real interface with various structure.
  - Will interface related energy (stability) play a role?
  - Liquid as thermal interface materials? Is water the best?

- Understand or design new experimental characterization techniques for extreme observation while resolving the data
  - Deeper understanding of electrochemical impedance spectroscopy? Or replace it?
  - Real space characterization (r x k/E) for heterogeneity at large scale such as device level.

未来？越过山丘！

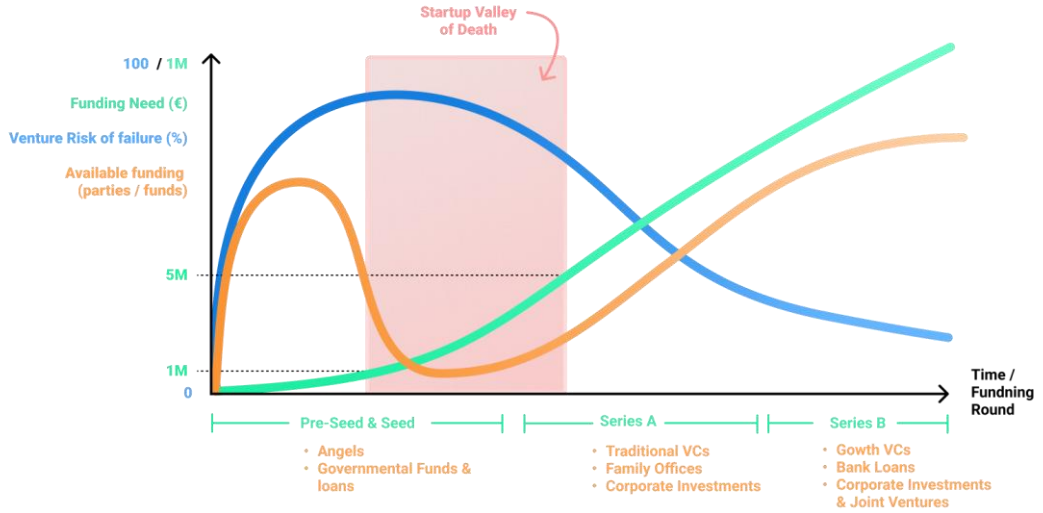

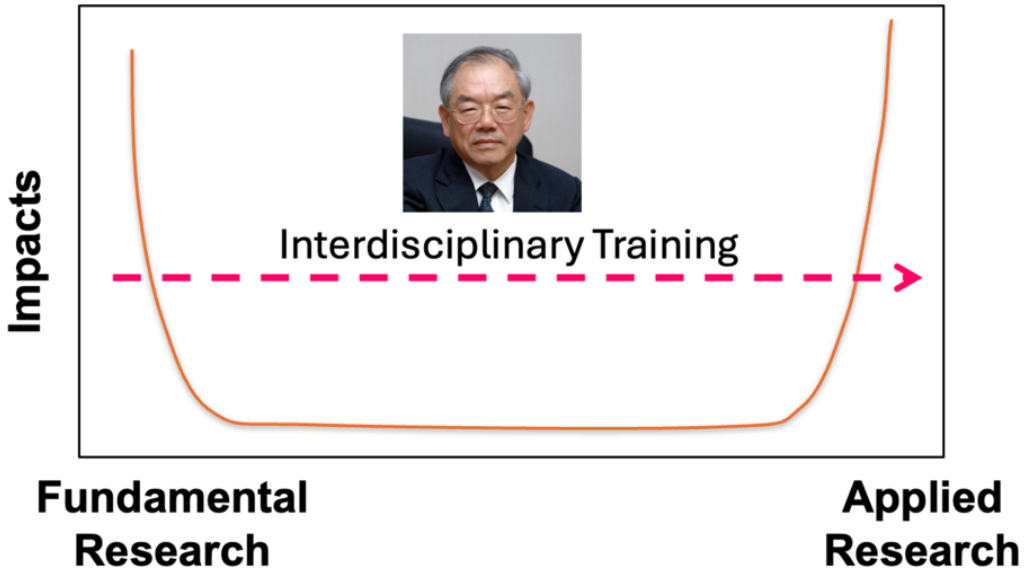

- 跨越壁垒，不同学科之间做翻译和转移
- 建立深度的洞察，从实验到理论或者从理论到实验，从小但具体的问题开始

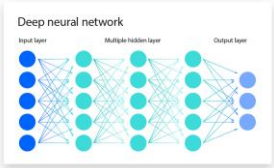

“要有自由的眼光 (free perception)，必须能够同时近观和远看同一课题。”——《爱因斯坦：机遇与眼光 | 杨振宁》

Acknowledgement

US Department of Energy (DOE), Office of Science (SC), Basic Energy Sciences (BES), Award No. DE-SC0020148.

NSF CAREER award grant No. 2042284.

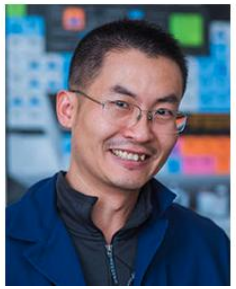

Mingda Li
Class '47 Career Development Professor
Associate Professor of Nuclear Science and Engineering
mingda@mit.edu
24-209A
Lab website

Bi-Cheng Zhou

Associate Professor, Materials Science and Engineering

MSE: Kang Wang(SHJT), Kunyan Zhang(UC Berkeley), Yang Yang (PSU), …
EE: Shengxi Huang (Rice), …
Physics: Mouyang Cheng(MIT), Phum Siriviboon (MIT), Michael Landry (MIT), …
MechE: Gang Chen (MIT), Zhantao Chen (UT Austin), …
NSE: Thanh Nguyen (IBM Research), …
CS: Song Wang (central Florida), Peng Wang (UVA), Zheng Huang (Dartmouth), …

Thank you for your attention!